5-14-2024

Air Quality Assessment on Local and Hyperlocal Scales

Zhiyao Li
Washington University – McKelvey School of Engineering

WASHINGTON UNIVERSITY IN ST. LOUIS

McKelvey School of Engineering

Department of Energy, Environmental and Chemical Engineering

Dissertation Examination Committee:
Jay Turner, Chair
Karen DeMatteo
Randall Martin
Jian Wang
Brent Williams

Air Quality Assessment on Local and Hyperlocal Scales

by
Zhiyao Li

A dissertation presented to
the McKelvey School of Engineering
of Washington University in
partial fulfillment of the
requirements for the degree
of Doctor of Philosophy

May 2024
St. Louis, Missouri

Table of Contents

List of Figures

List of Tables

Acknowledgments

This dissertation is comprised of projects funded by the National Institute of Health through grants to the University of Louisville and the United Nation Children's Fund. I am grateful to all helpful supporters along my PhD journey, I am especially thankful to:

Field technician: Barkhasragchaa Baagii (Mongolia), Rick. L. Strehl (Louisville, KY) and Gregg Shirk (Louisville, KY): for their time and efforts establishing sensor networks and visiting sites for data retrieval which made our projects successful;

Collaborators from Public Lab Mongolia (PLM): for their invaluable time and support throughout the Mongolia air quality monitoring project. Their significant contribution has been instrumental in my development as a researcher. Special thanks to Enkhtungalag Chuluunbaatar, Byambatsetseg Lkhagvasuren, and Erdenetsogt Sumiyasuren for their generous sharing of knowledge and expertise;

Collaborators from United Nations Children's Fund (UNICEF) Mongolia: for their steadfast support and guidance which greatly facilitated the progress of our project. I am particularly grateful to Altantsetseg Sodnomtseren and Khishigjargal Batjantsan for their dedicated efforts and commitment;

Committee members: Drs. Karen DeMatteo, Randall Martin, Brent Williams and Jian Wang, for their time and effort reviewing this work;

My fellow graduate students: for their invaluable assistance during sampling field campaigns, and for fostering a rich environment of knowledge sharing and camaraderie throughout my journey. Special thanks to my lab-mates Dr. Pradeep Prathibha, Dr. Maryssa Loehr, Xuan Liu, Tyler Cargill, Yan He, as well as the numerous rotating students and

undergraduates; your support and friendship have been integral to my experience and success;

My advisor Dr. Jay Turner: for his invaluable guidance, unwavering support, and kindness throughout my PhD Journey, His mentorship has been instrumental in shaping my academic and professional growth;

My parents Chao Shen and Yipin Li: for their unconditional love, unwavering encouragement and endless sacrifices that have made my academic pursuits possible;

My partner Sisi Ren: for all your love, support and understanding throughout my academic endeavors.

Zhiyao Li

Washington University in St. Louis

May 2024

ABSTRACT OF THE DISSERTATION

Air Quality Assessment on Local and Hyperlocal Scales

by

Zhiyao Li

Doctor of Philosophy in Energy, Environmental and Chemical Engineering

Washington University in St. Louis, 2024

Professor Jay Turner, Chair

Air quality monitoring across local and hyperlocal scales has attracted increased attention from both the public and research community. There are several approaches such as passive samplers and low-cost air quality sensors, depending on the pollutant and measurement objectives. Local and hyperlocal air pollutant measurements help to characterize local emission sources such as traffic and industry, including separating these signals from large scale influences (e.g., urban and regional scales), and better understand how land use types and meteorology influence pollutant spatiotemporal patterns.

Low-cost sensors (LCS) are now a popular approach to monitor several criteria pollutants (e.g., particulate matter (PM), ozone, carbon monoxide), complementing the use of relatively expensive regulatory-grade reference monitors. Utilizing LCS networks for local air quality monitoring helps people understand more about air pollutants in their immediate surroundings, raising awareness of the exposures they may encounter. LCS have several advantages compared to the reference grade monitors including cost (typically ~$300 compared to ~$20,000), compactness and ease to deploy, and largely “plug-and-play” data management with many

vendors providing cloud-based services and automated mapping. However, LCS data accuracy and precision typically do not match the reference monitors and protocols are lacking to efficiently detect changes in sensor performance over time. Work is needed to assess LCS utility in harsh environments and determine whether small variations can be accurately detected. With the fast development and utilization of LCS for different air quality related projects, a general guideline for LCS deployment is needed to make sure results generated by LCS can be comparable.

This dissertation includes four major chapters to advance air quality measurement strategies and/or to conduct monitoring studies at local and hyperlocal scales. It begins by meticulously characterizing five different types of low-cost sensors (LCS) under the challenging winter conditions of Mongolia, facilitating the establishment of long-term $PM_{2.5}$ monitoring networks outdoors and within kindergartens. Utilizing indoor network measurements, a novel land use regression model was developed to predict indoor $PM_{2.5}$ concentrations within kindergartens in the absence of physical sensors. The subsequent study focused on the characterization of a popular LCS device based on device siting and varying meteorological conditions, offering valuable insights for the deployment of citizen science-based LCS networks. The final investigation centered on characterizing the impact of traffic-related ultrafine particle (UFP) concentrations by employing a near-road, engineered vegetative buffer within the Green Heart Louisville study area. Stationary monitoring campaigns were conducted to measure UFP number concentrations in the study area both with and without the presence of the vegetative buffer to understand the efficiency of vegetation to modulate ground-level UFP concentrations. These projects collectively yield significant findings that enhance the accuracy of exposure estimates and inform the public about their exposure to particulate matter.

Chapter 1: Introduction

This dissertation contributes to the advancement of knowledge concerning the characterization of low-cost sensor (LCS) devices used for particulate matter (PM) monitoring and their application to local scale air quality monitoring. The research encompasses the implementation of LCS devices under extreme environmental conditions, particularly in regions such as Mongolia, and the evaluation of sensor performance under real-world conditions to ascertain their potential for long-term air quality monitoring. This endeavor addresses the monitoring gaps resulting from the costliness of reference grade monitors. Additionally, this study focuses on enhancing understanding of ultrafine particulate matter (UFP) originating from traffic emissions in urban settings, and seeks to quantify the efficacy of engineered vegetative buffers to mitigate UFP exposures for nearby residents.

This chapter provides a summary of the health-related impacts associated with two major air pollutants, $PM_{2.5}$ and UFP, and outlines the technological advancements in sensor technology for sampling these pollutants. Detailed background information will be presented in subsequent chapters.

1.1 Human Health & Urban air pollutants: $PM_{2.5}$ and UFP

Air pollution, notably particulate matter less than 2.5 micrometers aerodynamic diameter ($PM_{2.5}$), is a significant contributor to global human mortality [1], [2], [3], [4]. These fine particles can penetrate deep into the respiratory system, leading to respiratory issues such as asthma, bronchitis and chronic obstructive pulmonary disease (COPD) [5]. $PM_{2.5}$ exposure is also associated with cardiovascular diseases, including heart attacks and strokes, as well as

neurological disorders, cognitive decline, and adverse birth outcomes[5], [6], [7], [8], [9]. Certain populations, such as children, the elderly, and individuals with pre-existing health conditions, are particularly vulnerable to the health impacts of $PM_{2.5}$ exposure [10], [11], [12].

Unlike $PM_{2.5}$, which has been extensively studied, there is a need for further research to fully understand ultrafine particulate matter (UFP). UFPs, defined as particles with aerodynamic diameters less than 0.1 micrometers, constitute a significant portion of airborne pollutants in urban environments[13]. These particles possess unique characteristics due to their extremely small size, which grants them increased surface area and reactivity[14]. Despite their importance, the generation, distribution, and health impacts of UFPs remain relatively understudied compared to larger particles.

UFPs are generated through a multitude of processes, including combustion engines, industrial activities, and natural sources such as sea spray and wildfires[13]. The combustion of fossil fuels, particularly from vehicular traffic, represents a major source of UFP emissions in urban settings[15], [16]. Industrial processes, such as power generation and manufacturing, also contribute to the release of UFPs into the atmosphere[17]. Due to their small size, UFPs can penetrate deep into the respiratory system, reaching the alveolar region of the lungs[13]. This unique characteristic raises concerns about their potential health impacts, as they can bypass the body's natural defense mechanisms and enter systemic circulation. Epidemiological studies have linked exposure to UFPs with adverse health outcomes, including respiratory and cardiovascular diseases, as well as increased mortality rates even increased risk of Alzheimer’s and Parkinson’s disease[18], [19].

Furthermore, the surface chemistry of UFPs may facilitate the adsorption of toxic pollutants, such as heavy metals and organic compounds, exacerbating their potential health effects[20]. Additionally, UFPs have been implicated in the exacerbation of pre-existing health conditions, such as asthma and COPD, due to their ability to induce inflammation and oxidative stress in the respiratory tract[18], [21].

1.2 Characterizing $PM_{2.5}$ and LCS technology

The reference method for measuring $PM_{2.5}$ typically involves the use of a high-volume sampler (HVS) or a low-volume sampler (LVS) in conjunction with a filter, such as a Teflon or quartz filter, to collect particulate matter from the air[22]. The collected samples are then analyzed using gravimetric analysis (after conditioning the particle laden filters at a specified temperature and relative humidity), where the mass of the collected particles is determined by weighing the filter before and after sampling. This method provides standardized measurements of $PM_{2.5}$ concentrations by capturing particles smaller than 2.5 micrometers in diameter and controlling the water content through the post-sampling equilibration process. Additionally, the reference method often includes quality assurance measures, such as calibration checks and blank filter tests, to ensure the accuracy and reliability of the measurements[23].

In addition to the reference method using high-volume or low-volume samplers, there are also Federal Equivalent Method (FEM) approaches. The FEM is a designation given to instruments and methods that have been demonstrated to provide results comparable to those obtained by the Federal Reference Method (FRM), but may offer advantages such as improved portability, reduced cost, or increased ease of use[24]. FEM instruments undergo rigorous testing and

evaluation by regulatory agencies to ensure their accuracy and reliability in measuring $PM_{2.5}$ concentrations[25].

While FRM sampling and FEM monitoring are renowned for their accuracy in measuring $PM_{2.5}$ levels in ambient air, their widespread adoption is often impeded by the considerable costs involved in both initial procurement and ongoing maintenance. These financial constraints present significant hurdles for individuals and communities striving to effectively monitor their local $PM_{2.5}$ levels. Addressing these challenges necessitates the development and deployment of alternative, more cost-effective monitoring solutions capable of providing reliable $PM_{2.5}$ measurements without sacrificing accuracy[26].

Emerging technologies, such as low-cost sensor (LCS) networks and other portable monitoring devices, offer promising avenues for democratizing access to real-time air quality data at a fraction of the cost of traditional FEM and FRM hardware and operations. Air quality LCS devices have been available on the market for several years, with prices ranging from $200 to $1500 depending on features. Some LCS devices are tailored for indoor air quality measurements, boasting digital real-time displays and user-friendly interfaces (e.g., AirVisual Pro, Laser Egg), while others are ruggedized for outdoor deployment (e.g., PurpleAir)[6], [7], [8], [27]. However, it's crucial to note that LCSs exhibit varying data quality, as evidenced by studies comparing them to regulatory-grade air quality monitors (typically FEMs) [28], [29]. With proper operation and maintenance, LCS-generated air quality data can serve as educational tools for general audiences and be instrumental in research projects[29], [30].

In contrast, regulatory-grade monitors typically cost $20,000 or more, making them financially unfeasible for research studies requiring high temporal and spatial resolutions[31]. For the price

of one regulatory monitor, researchers could deploy a network of LCSs to achieve high spatial resolution results, thereby maximizing research efficiency and data coverage.

By reducing the financial barriers to entry and empowering individuals and communities with access to affordable $PM_{2.5}$ monitoring tools, we can elevate public awareness of air quality issues, bolster evidence-based policymaking, and ultimately, safeguard human health and the environment.

1.3 UFP characterizing inside Green Heart Louisville

Airborne ultrafine particles ($PM_{0.1}$; UFP) pose a health risk as discussed in the previous section. A 2021 World Health Organization (WHO) report [32] presents the good practice statement: "Distinguish between low and high PNC [particle number concentration] to guide decisions on the priorities of UFP source emission control. Low PNC can be considered < 1,000 particles/cm^3 (24-hour mean). High PNC can be considered > 10,000 particles/cm^3 (24-hour mean) or 20,000 particles/cm^3 (1-hour mean)." PNC was often above 20,000 particles/cm^3 based on our observed ground-level rush hour near-highway measurements in the Green Heart Louisville study area and warrants attention.

Green Heart Louisville is an extensive neighborhood greening initiative in a Louisville, Kentucky neighborhood, aiming to explore the relationships between urban greenery and cardiovascular health. Complementing the neighborhood greening efforts, engineered vegetation belts primarily consisting of mature evergreen trees were strategically planted along an interstate highway that intersects the study area. The goal of this intervention was to mitigate urban air pollution, particularly stemming from fresh traffic emissions, and reduce elevated ultrafine particle (UFP) concentrations near the roadway.

While Tong et al. utilized computational fluid dynamics modeling to estimate downwind UFP impacts for vegetation positioned behind noise walls[33], there remains a gap in field assessments regarding the combination effect of dense vegetation planted on the road side of noise barriers. By meticulously examining the effectiveness of engineered vegetation buffers in reducing UFP levels near highways, we aim to establish a baseline for future studies and contribute additional insights to air quality monitoring in urban environments.

1.4 Objectives

Given the significance of both $PM_{2.5}$ and UFPs as major air pollutants for urban environment and their potential health impacts, this dissertation aims to contribute to the body of knowledge in this field by investigating the effectiveness of LCS devices usage in $PM_{2.5}$ monitoring under extreme environment and also assess the impact of urban greenness on reducing UFPs in urban environments.

Chapter 2: *Assess different characteristics of particulate matter low-cost sensor devices in the extreme environmental conditions of Mongolia*

I evaluated five low-cost air quality sensor devices for their suitability in a urban PM-monitoring network based on their performance compared to a reference grade monitor and under extreme cold conditions. Evaluation process include developing adjustment factors using long-term collocated data and local environmental conditions. I hypothesized that with careful adjustments LCS can be used in urban PM monitoring and generate reliable results that can be directly compared to the reference grade monitors.

Chapter 3: *LCS characterizations based on its deployment siting and meteorological conditions*

In collaboration with Tyler Cargill, we conducted long-term collocations of PM LCS devices of the same sensor type at different monitoring stations in US. We evaluated the performance of LCS devices compared to each other and to the reference monitors, taking into consideration local meteorological conditions. I hypothesized that the deployment microenvironment will affect the sensor data quality and will cause complexities in LCS data adjustments and interpretation.

Chapter 4: *Children's $PM_{2.5}$ indoor exposures in Mongolian kindergartens*

Mongolia's population centers experience poor wintertime air quality. A study was conducted to characterize particulate matter LCS devices in the Mongolian cold climate, quantify ambient $PM_{2.5}$ spatiotemporal variability across a small city, and assess children's exposures in kindergartens. I hypothesized that this 25-site indoor network can be used to predict indoor $PM_{2.5}$ exposures for other kindergartens with similar conditions using LUR approaches.

Chapter 5: *The effects of vegetation planted along a highway noise wall barrier on ultrafine particle concentrations*

In collaboration with Maryssa Loehr, we conducted mobile and stationary measurements of ultrafine particulate matter in the Green Heart Study neighborhood near a major highway (I-264). I focused on stationary measurements and vertical pollutant profiles while Maryssa Loehr focused on mobile measurements downwind of the highway and into the neighborhood. We hypothesize that the combination of a vegetation buffer and the noise wall have a complex effect on the dispersion of UFP as compared to an open

fetch with only a noise wall that could potentially modulate ground-level downwind UFP concentrations.

Conclusions and recommended future work for each study is summarized in each chapter to address different topics of interest. Furthermore, Chapter 6 includes key conclusion from this thesis regarding human exposures to particulate matter air pollution.

1.5 References

[1] Y.-F. Xing, Y.-H. Xu, M.-H. Shi, and Y.-X. Lian, “The impact of PM2.5 on the human respiratory system,” Journal of Thoracic Disease, vol. 8, no. 1, 2016.

[2] A. Bhatnagar, “Environmental Determinants of Cardiovascular Disease,” Circ Res, vol. 121, no. 2, pp. 162–180, Jul. 2017, doi: 10.1161/CIRCRESAHA.117.306458.

[3] P. James, R. F. Banay, J. E. Hart, and F. Laden, “A Review of the Health Benefits of Greenness,” Curr Epidemiol Rep, vol. 2, no. 2, pp. 131–142, Jun. 2015, doi: 10.1007/s40471-015-0043-7.

[4] P. Dadvand et al., “Green spaces and General Health: Roles of mental health status, social support, and physical activity,” Environment International, vol. 91, pp. 161–167, May 2016, doi: 10.1016/j.envint.2016.02.029.

[5] S. Vedal, “Ambient Particles and Health: Lines that Divide,” Journal of the Air & Waste Management Association, vol. 47, no. 5, pp. 551–581, May 1997, doi: 10.1080/10473289.1997.10463922.

[6] X. H. H. Huang, Q. Bian, W. M. Ng, Peter. K. K. Louie, and J. Z. Yu, “Characterization of PM2.5 Major Components and Source Investigation in Suburban Hong Kong: A One Year Monitoring Study,” Aerosol Air Qual. Res., vol. 14, no. 1, pp. 237–250, 2014, doi: 10.4209/aaqr.2013.01.0020.

[7] J. M. Samet and S. L. Zeger, “Fine Particulate Air Pollution and Mortality in 20 U.S. Cities, 1987–1994,” The New England Journal of Medicine, 2000.

[8] N. Künzli et al., “Ambient Air Pollution and Atherosclerosis in Los Angeles,” Environ Health Perspect, vol. 113, no. 2, pp. 201–206, Feb. 2005, doi: 10.1289/ehp.7523.

[9] T. D. Nelin, A. M. Joseph, M. W. Gorr, and L. E. Wold, “Direct and indirect effects of particulate matter on the cardiovascular system,” Toxicology Letters, vol. 208, no. 3, pp. 293–299, Feb. 2012, doi: 10.1016/j.toxlet.2011.11.008.

[10] A. Anwar, I. Ullah, M. Younis, and A. Flahault, “Impact of Air Pollution (PM2.5) on Child Mortality: Evidence from Sixteen Asian Countries,” IJERPH, vol. 18, no. 12, p. 6375, Jun. 2021, doi: 10.3390/ijerph18126375.

[11] C. Wang, Y. Tu, Z. Yu, and R. Lu, “PM2.5 and Cardiovascular Diseases in the Elderly: An Overview,” IJERPH, vol. 12, no. 7, pp. 8187–8197, Jul. 2015, doi: 10.3390/ijerph120708187.

[12] A. Mainka and P. Fantke, “Preschool children health impacts from indoor exposure to PM2.5 and metals,” Environment International, vol. 160, p. 107062, Feb. 2022, doi: 10.1016/j.envint.2021.107062.

[13] R. Chen et al., “Beyond PM2.5: The role of ultrafine particles on adverse health effects of air pollution,” Biochimica et Biophysica Acta (BBA) - General Subjects, vol. 1860, no. 12, pp. 2844–2855, Dec. 2016, doi: 10.1016/j.bbagen.2016.03.019.

[14] R. Baldauf et al., “Ultrafine Particle Metrics and Research Considerations: Review of the 2015 UFP Workshop,” IJERPH, vol. 13, no. 11, p. 1054, Oct. 2016, doi: 10.3390/ijerph13111054.

[15] J. Marval and P. Tronville, “Ultrafine particles: A review about their health effects, presence, generation, and measurement in indoor environments,” Building and Environment, vol. 216, p. 108992, May 2022, doi: 10.1016/j.buildenv.2022.108992.

[16] M. Masiol and R. M. Harrison, “Aircraft engine exhaust emissions and other airport-related contributions to ambient air pollution: A review,” Atmospheric Environment, vol. 95, pp. 409–455, Oct. 2014, doi: 10.1016/j.atmosenv.2014.05.070.

[17] C. Sioutas, R. J. Delfino, and M. Singh, “Exposure Assessment for Atmospheric Ultrafine Particles (UFPs) and Implications in Epidemiologic Research,” Environ Health Perspect, vol. 113, no. 8, pp. 947–955, Aug. 2005, doi: 10.1289/ehp.7939.

[18] R. J. Delfino, C. Sioutas, and S. Malik, “Potential Role of Ultrafine Particles in Associations between Airborne Particle Mass and Cardiovascular Health,” Environ Health Perspect, vol. 113, no. 8, pp. 934–946, Aug. 2005, doi: 10.1289/ehp.7938.

[19] D. Cserbik et al., “Fine particulate matter exposure during childhood relates to hemispheric-specific differences in brain structure,” Environment International, vol. 143, p. 105933, Oct. 2020, doi: 10.1016/j.envint.2020.105933.

[20] S. Kumar, M. K. Verma, and A. K. Srivastava, “Ultrafine particles in urban ambient air and their health perspectives,” Reviews on Environmental Health, vol. 28, no. 2–3, Jan. 2013, doi: 10.1515/reveh-2013-0008.

[21] S. Ohlwein, R. Kappeler, M. Kutlar Joss, N. Künzli, and B. Hoffmann, “Health effects of ultrafine particles: a systematic literature review update of epidemiological evidence,” Int J Public Health, vol. 64, no. 4, pp. 547–559, May 2019, doi: 10.1007/s00038-019-01202-7.

[22] P. Patel and S. G. Aggarwal, “On the techniques and standards of particulate matter sampling,” Journal of the Air & Waste Management Association, vol. 72, no. 8, pp. 791–814, Aug. 2022, doi: 10.1080/10962247.2022.2048129.

[23] E. D. Ramiro, B. Artinano, A. Rubio, I. Figuero, M. Barreiro, and J. Fernandez, “Field Assessment of Low-cost Particulate Matter Sensors against Reference Methods,” in 2019 5th Experiment International Conference (exp.at’19), Funchal (Madeira Island), Portugal: IEEE, Jun. 2019, pp. 444–448. doi: 10.1109/EXPAT.2019.8876519.

[24] G. Hagler et al., “Evaluation of two collocated federal equivalent method PM2.5 instruments over a wide range of concentrations in Sarajevo, Bosnia and Herzegovina,” Atmospheric Pollution Research, vol. 13, no. 4, p. 101374, Apr. 2022, doi: 10.1016/j.apr.2022.101374.

[25] W. Mui et al., “Development of a Performance Evaluation Protocol for Air Sensors Deployed on a Google Street View Car,” Environ. Sci. Technol., vol. 55, no. 3, pp. 1477–1486, Feb. 2021, doi: 10.1021/acs.est.0c05955.

[26] J. Bi et al., “Publicly available low-cost sensor measurements for PM2.5 exposure modeling: Guidance for monitor deployment and data selection,” Environment International, vol. 158, p. 106897, Jan. 2022, doi: 10.1016/j.envint.2021.106897.

[27] S. Munir, M. Mayfield, D. Coca, S. A. Jubb, and O. Osammor, “Analysing the performance of low-cost air quality sensors, their drivers, relative benefits and calibration in cities—a case study in Sheffield,” Environ Monit Assess, vol. 191, no. 2, p. 94, Feb. 2019, doi: 10.1007/s10661-019-7231-8.

[28] D. H. Hagan and J. H. Kroll, “Assessing the accuracy of low-cost optical particle sensors using a physics-based approach,” Atmos. Meas. Tech., vol. 13, no. 11, pp. 6343–6355, Nov. 2020, doi: 10.5194/amt-13-6343-2020.

[29] M. Badura, I. Sówka, P. Szymański, and P. Batog, “Assessing the usefulness of dense sensor network for PM2.5 monitoring on an academic campus area,” Science of The Total Environment, vol. 722, p. 137867, Jun. 2020, doi: 10.1016/j.scitotenv.2020.137867.

[30] B. Feenstra et al., “Performance evaluation of twelve low-cost PM2.5 sensors at an ambient air monitoring site,” Atmospheric Environment, vol. 216, p. 116946, Nov. 2019, doi: 10.1016/j.atmosenv.2019.116946.

[31] S. Kim, S. Park, and J. Lee, “Evaluation of Performance of Inexpensive Laser Based PM2.5 Sensor Monitors for Typical Indoor and Outdoor Hotspots of South Korea,” Applied Sciences, vol. 9, no. 9, p. 1947, May 2019, doi: 10.3390/app9091947.

[32] World Health Organization, “WHO global air quality guidelines: particulate matter (PM2.5 and PM10), ozone, nitrogen dioxide, sulfur dioxide and carbon monoxide,” 9789240034228. [Online]. Available: https://iris.who.int/handle/10665/345329

[33] Z. Tong, R. W. Baldauf, V. Isakov, P. Deshmukh, and K. Max Zhang, “Roadside vegetation barrier designs to mitigate near-road air pollution impacts,” Science of The Total Environment, vol. 541, pp. 920–927, Jan. 2016, doi: 10.1016/j.scitotenv.2015.09.067.

Chapter 2: Particulate matter low-cost sensor device performance in a cold climate

This work was funded by UNICEF Mongolia (PD Ref. No. MGLA/2880/2019/002-PC).

2.1 Abstract

Mongolia's population centers experience poor wintertime air quality because the cold climate drives strong ground-level inversions and pervasive solid fuels use for distributed residential space heating. Ulaanbaatar (UB, pop. ~1.5MM) has robust air monitoring but measurements outside of UB are sparse. The use of low-cost particulate matter sensor (LCS) devices enables dense networks to increase the spatial resolution of air quality monitoring. However, LCS device performance and data quality are affected by the environmental and aerosol properties. In this study, five PM LCS device types were deployed for more than one year in a Mongolian secondary city to assess which device(s) would be suitable for network deployments. These LCS devices were collocated with a US EPA-approved Federal Equivalent Method (FEM) monitor. Devices were collocated in triplicate for a wintertime five-week period. $PM_{2.5}$ hourly concentrations were highly correlated across devices of the same type with Pearson correlation coefficient greater than 0.96. During this period, three of the five LCS device types exhibited high data capture and high correlation with the FEM for temperatures as low as -30 ºC and hourly $PM_{2.5}$ ranging ~1 to 1450 μg/m^3. Compared to the FEM these device types were biased high by 25-40% with a discernible temperature-dependent bias that likely is a proxy for changes in aerosol properties in this wintertime environment dominated by residential heating with solid field (especially coal). The seasonal adjustment using multivariable quadratic regression model

removed bias from 30 percent to 0.5 percent with a decrease from RMSE to around half when comparing the raw data.

2.2 Introduction

2.2.1 Mongolia Air quality

Air pollution is one of the major contributors to human mortality caused by environmental factors [1], [2], [3], [4]. Particulate matter less than 2.5 micrometers aerodynamic diameter ($PM_{2.5}$) is classified as one of the major air pollutants globally because of its impact on human health. $PM_{2.5}$ can enter the pulmonary alveoli during the air exchange process and spread through the human body to further damage other areas [1], [5]. $PM_{2.5}$ properties including size distribution shape, and composition can vary based on the emissions source and environmental conditions; examples of fuel combustion include biomass burning, transportation, and residential cooking and heating [6]. Health effects like pulmonary disease, cardiovascular disease, premature death, and increased risk of cancer are related to air pollution and, more specifically, to $PM_{2.5}$ [7], [8], [9].

Mongolia is one of the coldest countries in the world; wintertime temperatures can drop to as low as -40 °C in Ulaanbaatar, the capitol city of Mongolia [10]. $PM_{2.5}$ is a major pollutant in Mongolia, especially in the winter and dust seasons. Most Mongolians live in *gers*, a traditional Mongolian dwelling like a yurt, because of the traditional nomadic lifestyles. In the winter, the traditional heating systems in *gers* (and *ger* area houses) typically use coal as a primary combustion source, which leads to high particulate matter emissions. The Mongolian National Agency for Meteorology and Environment Monitoring (NAMEM) reports that, in the wintertime 2017, the $PM_{2.5}$ mean concentration for the Ulaanbaatar was 80–140 $\mu g/m^3$ depending on

location [11], [12]. The associated health impacts are significant and, in the absence of strict emission controls, are projected to increase as the Ulaanbaatar's population grows [13].

2.2.2 $PM_{2.5}$ Low-Cost Sensor Devices

Air quality low-cost sensor devices have been on the market for several years and the price can vary from $200 to more than $1000 depending on their features. Some of these sensors are specifically designed for indoor air quality measurements with a digital real time display and a user-friendly operating interface (e.g., AirVisual Pro, Laser Egg). Other sensors are designed with a more rugged casing for outdoor deployment (e.g., PurpleAir). Numerous studies have demonstrated dramatic differences in performance for $PM_{2.5}$ concentrations reported by LCS devices and regulatory-grade air quality monitors [6], [7], [8], [14]. However, with proper operation and maintenance, the air quality data generated by these low-cost sensor devices can be educational and indicative for general audiences and can be useful for research projects [15], [16]. In comparison, the cost of regulatory grade monitors is usually $10,000 or more [17]. Studies seeking to assess PM spatiotemporal variability most often resort to LCS devices for cost control.

2.2.3 LCS Devices Performance Evaluation

Numerous studies in the literature demonstrate that LCS devices, like PurpleAir and AirVisual Pro [e.g. 18], can be used for air quality measurements and in some cases result in a near research grade dataset after proper adjustments based on regulatory monitors [8], [19]. Many studies illustrate the influence of ambient humidity and temperature on different LCS device reported $PM_{2.5}$ concentrations compared to the regulatory monitors [17], [20], [21], [22], [23]. In this work, a LCS devices performance evaluation study was conducted in Bayankhongor (BKH),

a secondary city in Mongolia with population ~32,700 in 2023, and UB to assess which device(s) would be suitable for longer-term network deployments in the harsh Mongolian environment.

2.3 Materials and Methods

2.3.1 Performance Evaluation Pilot Study

An LCS device pilot study was conducted in Mongolia during winter 2019-2020 with five objectives:

1. Evaluate LCS devices operating performance outdoors for the extreme conditions of Mongolian wintertime.

2. Compare LCS device $PM_{2.5}$ concentrations to an FEM for outdoor measurements.

3. Evaluate LCS device precision by placing identical devices side-by-side (collocation) both indoors and outdoors.

5. Develop appropriate practices for using LCS devices in full-scale network deployments.

This paper focuses only on the outdoor studies conducted in BKH. The tested devices include: Habitat Map AirBeam2 (AB2); Wicked Device Air Quality Egg (AQE, Outdoor Model); IQAir AirVisual Pro (AVP); Kaiterra Laser Egg (LE); and PurpleAir Model PA-II-SD (PA). Note that some of the devices have switched to different PM sensors after our study.

A Beta Attenuation Monitor (BAM; MetOne Model 1020) $PM_{2.5}$ FEM was installed at a monitoring station in BKH commissioned for this project. Three LCS devices of each type were installed outdoors at this site for the collocation study.

LCS device precision was evaluated using the triplicate devices, and LCS accuracy was evaluated by comparing concentration data to the FEM. All devices were operated with their

default configurations except the AirVisual Pro. This device was a user-selected sampling frequency and was set to highest value (continuous operation) to evaluate performance at high time resolution. As described in the Supplemental Material, this approach led to rapid degradation of device performance. The remaining three devices were operated for another ten months to collect a full year of data.

2.3.3 Data processing and calculations

All LCS devices reported data to the respective manufacturer's server through an Internet connection. Data were downloaded from the manufacturer's data dashboards and imported into RStudio (R language program R.13) for further data analysis. All LCS devices output time series data between 1 to 5 mins depending on the sensor settings. These data were averaged over 1-hour time intervals FEM time base. For the LCS devices, a data completeness criterion of 75% of raw values was required for the hourly average to be deemed valid. Daily (24-hour) averages were also compared because this is relevant for certain reporting such as the US EPA $PM_{2.5}$ Air Quality Index (AQI).

2.3.4 LCS Devices $PM_{2.5}$ Data Adjustments

The primary goal was to develop adjustment factors to render the LCS $PM_{2.5}$ values as close to the FEM data as practicable. One LCS device of each type was chosen for these adjustments by selecting the LCS which most closely matched the central tendency across the three identical devices. An ordinary linear least squares regression against this "comparison" device was used to remove bias between the LCS devices of the same type. Relative humidity (RH) and temperature (T) dependence of the LCS bias compared to the FEM using the regression conducted with a yearlong dataset for three different LCS types. Because of data completeness issues, only

duplicate devices for each device type were included in this data adjustment analysis. Three different scenarios were considered for LCS data adjustments, first after obtaining the yearlong dataset for both LCS and the FEM BAM, a multivariable quadratic regression model was used to adjust the LCS data make it more reference like based on equation 2.1.

$$Adjusted\ LCS\ PM_{2.5}\ reading = a + b * \left(PM_{2.5_{LCS}}\right) + c * (T_{LCS}) + d * (RH_{LCS}) + e\left(PM_{2.5_{LCS}}\right)(T_{LCS}) + f\left(PM_{2.5_{LCS}}\right)(RH_{LCS}) + g(T_{LCS})(RH_{LCS}) + h\left(PA_{2.5_{LCS}}\right)^2 + i(T_{LCS})^2 + j(RH_{LCS})^2 \quad (1)$$

Because of the distinct seasonal differences in Mongolian environmental conditions and aerosol properties, the yearlong dataset was then split into winter season and non-winter seasons. The non-winter seasons data were adjusted using the multivariable linear regression model shown in equation 2.2.

$$Adjusted\ LCS\ PM_{2.5}\ reading = 0 + b * \left(PM_{2.5_{LCS}}\right) + c * (T_{LCS}) + d * (RH_{LCS}) \quad (2)$$

Some authors reported challenges for LCS during dust events [24]. There is a dust season in Mongolia, and we operationally defined dust events as hours meeting the following criteria: (i) LCS/FEM $PM_{2.5} \leq 0.4$; and (ii) FEM $PM_{2.5} > 50\ \mu g/m^3$. Dust event hours were removed from the datasets prior to performing the regressions.

2.3.5 Performance metrics

The performance of each LCS device was evaluated by using specific statistical measures against the FEM listed as follows: bias, mean absolute error (MAE), root mean square error (RMSE), and correlation coefficient (r). The scaled arithmetic difference and scaled relative difference were also used as a measure of bias across $PM_{2.5}$ concentration ranges. The square root of 2 term in the denominator was not included in both formulas because we assumed the FEM is a “gold

standard" and all bias is assigned to the LCS devices. After developing the adjustment factors using a yearlong dataset, these factors were then applied to a new set of data from November to December 2020 for validation purposes.

2.4 Results

This section summarizes the pilot study results. First, the outdoor collocated LCS devices are compared with each other to assess the precision within each LCS type. Second, the quantitative performance of LCS devices is directly compared to the FEM monitor. Finally, the proposed adjustments for all LCS devices based on the FEM are developed and evaluated.

2.4.1 Pilot study reference station measurements

Five types of commercial LCS devices with triplicates of each device were deployed outdoors at the Bayankhongor air motoring station ("BKH/Shelter") commissioned for this project. Measurements started in November 2019. The three collocated Laser Egg monitors failed early in the deployment under the cold temperature. This was expected because they are designed for indoor use and were included in the outdoor study because at that time, they were the only $PM_{2.5}$ LCS device with an in-country distributor. The remaining four device types operated continuously, even at extreme temperatures as low as -30 °C.

Figure 2.1 shows hourly $PM_{2.5}$ scattergrams for all collocated LCS device types for the period November 5 December 15, 2019. At the BKH station, ambient hourly temperature varied between -24 °C to +8 °C and Relative Humidity (RH) varied from 14% to 91% for this six-week period. Overall, the correlations among collocated sensors of the same type were strong (typically $r > 0.95$) with LCSs hourly $PM_{2.5}$ concentrations ranging from 1 $\mu g/m^3$ to 1450 $\mu g/m^3$. **Table 2.2** shows the grand average $PM_{2.5}$ concentrations for all collocated LCS devices at BKH

station for the expanded time period of November 7, 2019, to February 27, 2020. Scaled differences (difference divided by the average) for each device type were PA (26%), AVP (24%), AB2 (20%), and AQE (22%).

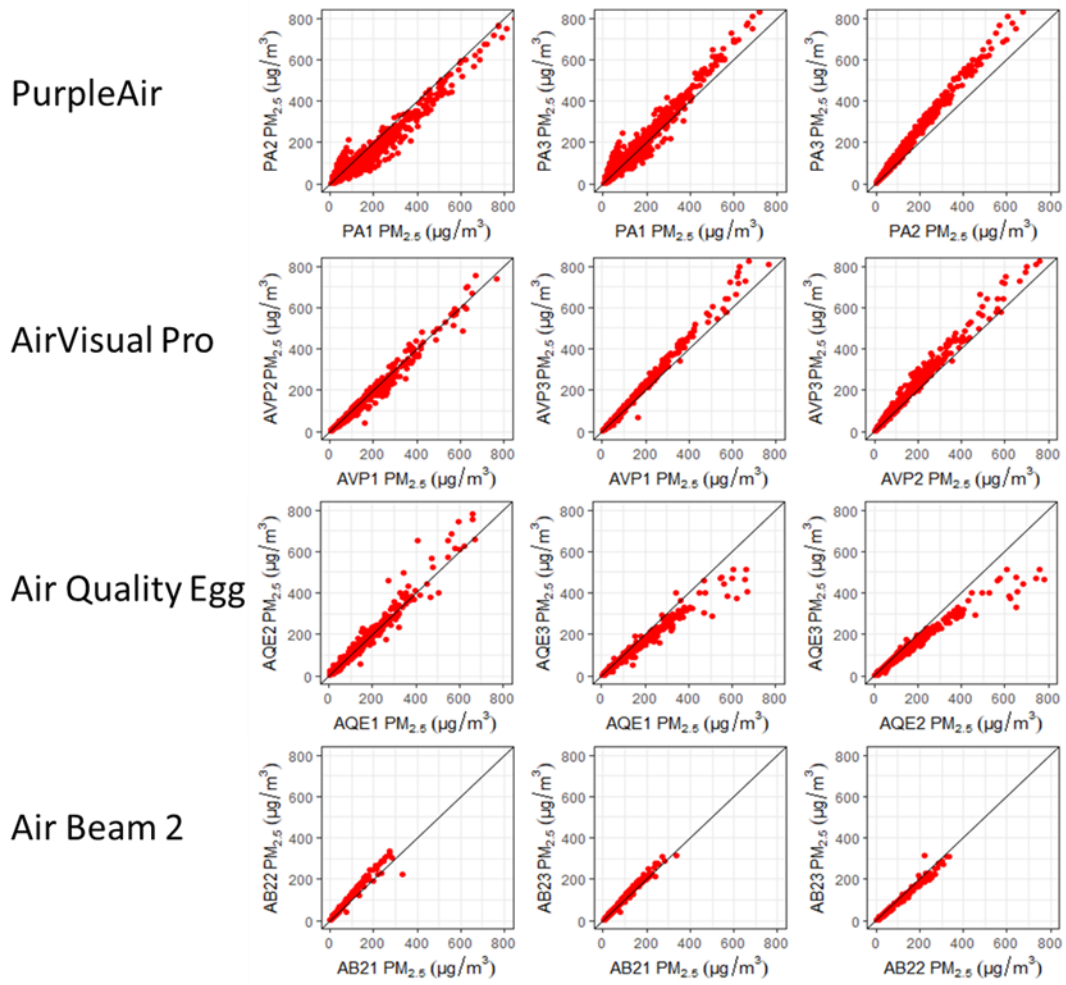

Figure 2.1 Scatter plot for intercomparing LCS collocated data at the Bayankhongor outdoor reference station from 06Nov2019-15Dec2019, each row represents a different LCS type. The solid diagonal line is the 1:1 line.

Table 2.1 $PM_{2.5}$ grand average concentrations (µg/m^3) for triplicate LCS devices outdoors at BKH reference station, 07Nov2019-27Feb2020.

Collocation Device	PA	AVP	AB2	AQE
1	99	79	53	110

2	86	76	65	113
3	112	97	58	91
Mean	**99**	**84**	**59**	**104**

Figure 2.2 shows $PM_{2.5}$ scattergrams for one of each LCS device type against the BAM FEM reference for all hourly data collected from November 7 to December 15, 2019. BAM $PM_{2.5}$ hourly concentrations range from 3 µg/m^3 to 1120 µg/m^3. **Figure 2.3** shows the daily averages for each LCS device type against the BAM FEM for the same time period.

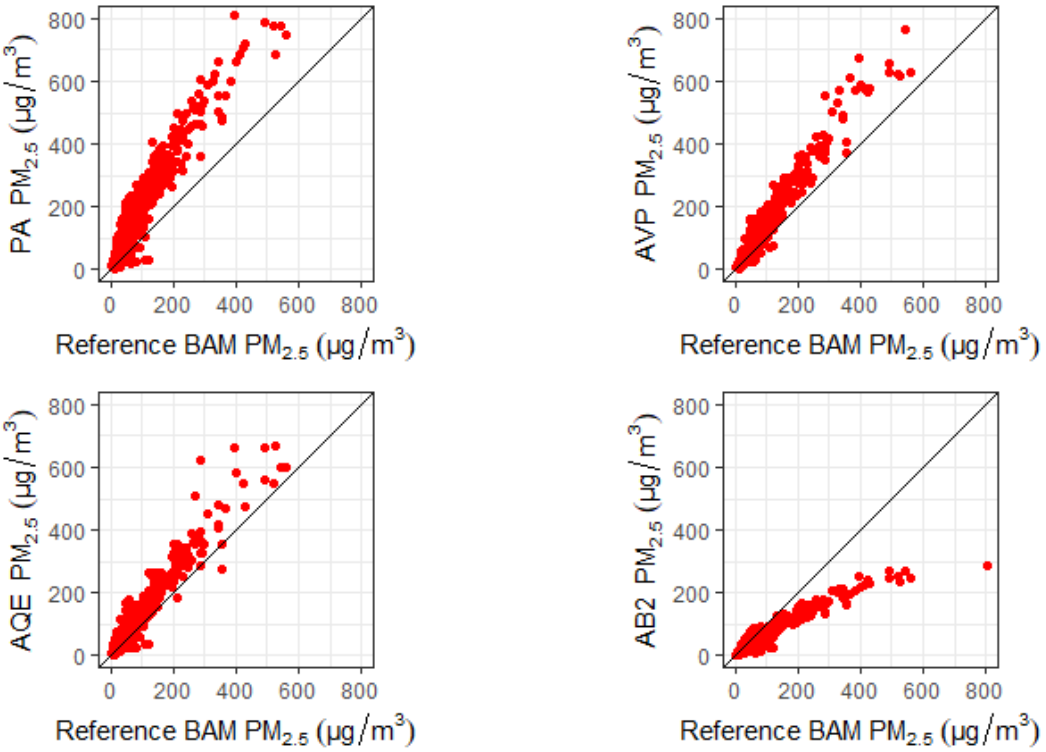

Figure 2.2 Scattergrams for the low-cost sensor devices (one of each type) versus the BAM FEM, Bayankhongor outdoor hourly-average $PM_{2.5}$ concentrations, 06Nov2019-15Dec2019. The solid diagonal line is the 1:1 line.

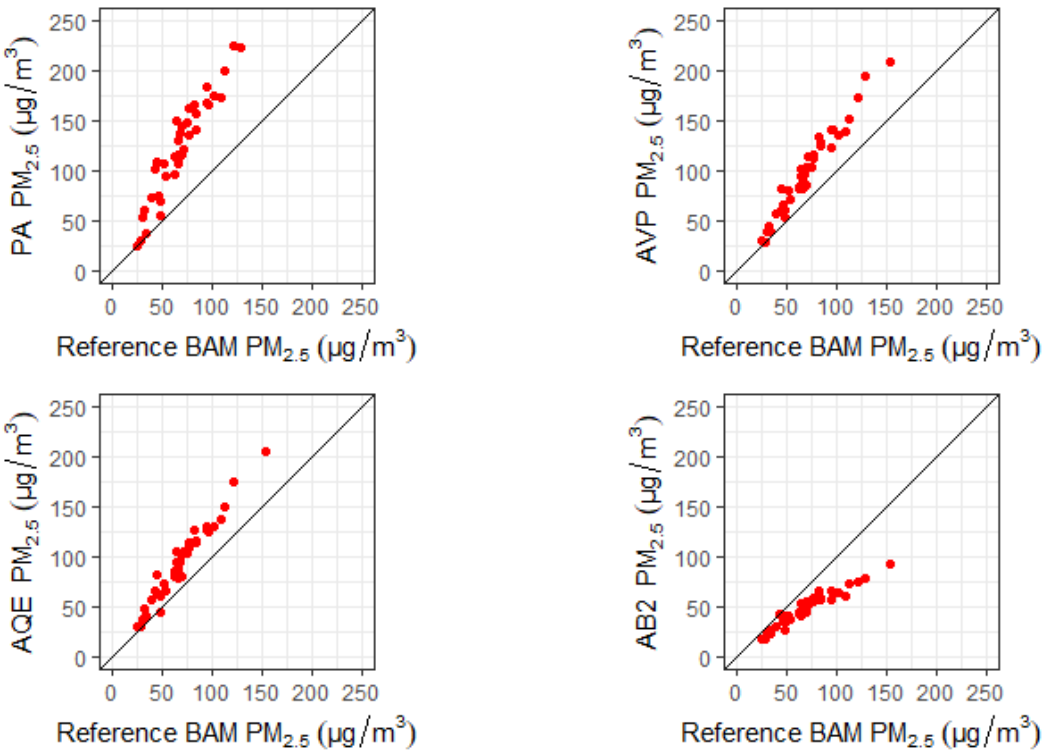

Figure 2.3 Scattergrams for the low-cost sensor devices (one of each type) versus the BAM FEM, Bayankhongor outdoor daily-average $PM_{2.5}$ concentrations, 06Nov2019-015Dec2019. The solid diagonal line is the 1:1 line.

2.4.2 Temperature and RH dependence

The PA-to-BAM relationship was further evaluated by stratifying the hourly and daily average $PM_{2.5}$ data by ambient temperature (**Figure 2.4**) and relative humidity (**Figure 2.5**). For the period from November 7, 2019, to March 21, 2020, the BKH station ambient temperature varied between -30 °C and +11 °C and RH varied from 6% to 91%. At high temperatures the PA bias was relatively higher while at low temperatures the PA bias was relatively lower (**Figure 2.4**, A). The opposite pattern was expected if the wintertime particles have a large semivolatile component that would be measured by the low-cost sensors but at least partially missed by the FEM because of its inlet line heater and the relatively warm temperature inside the shelter housing the BAM. This temperature-dependent bias is not observed in the daily average

concentrations (**Figure 2.4**, B) because of the range of temperatures experienced over a day. The reason for the temperature dependence of the bias is currently unclear. At high RH values (**Figure 2.5**, A) the PA readings was more dispersed compared to RH around 25%, similar RH dependence was also observed for daily data **(Figure 2.5**, B).

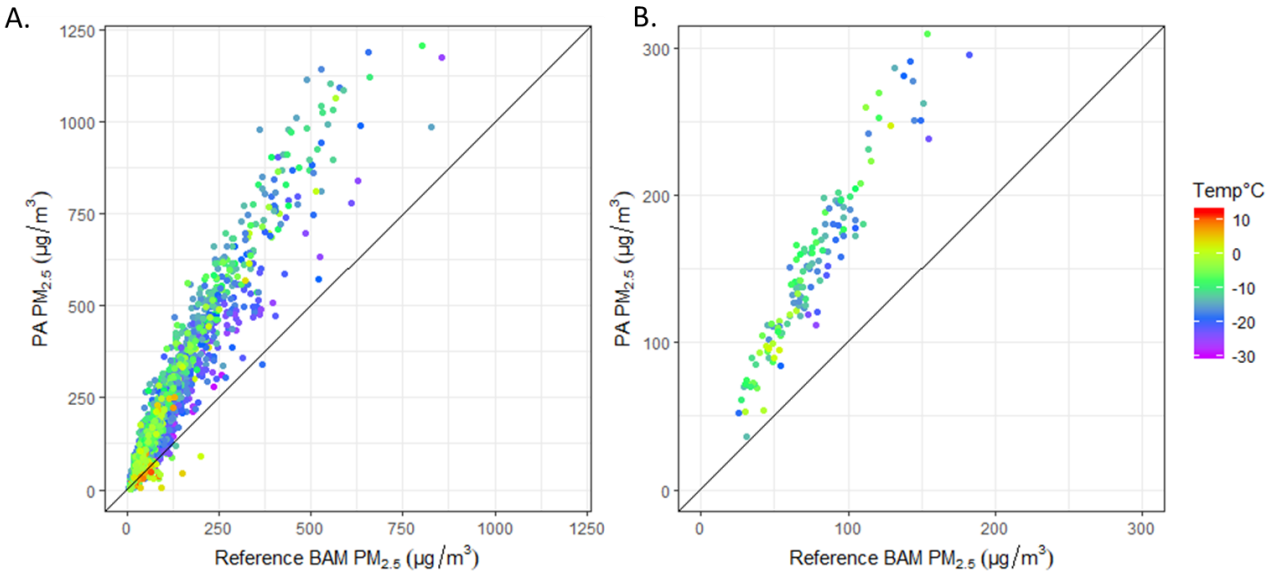

Figure 2.4 Hourly average (A) and daily average (B) $PM_{2.5}$ from the Purple Air (PA) and FEM monitor (BAM) for the period 06Nov2019-20March2020. Data are color-coded by ambient temperature.

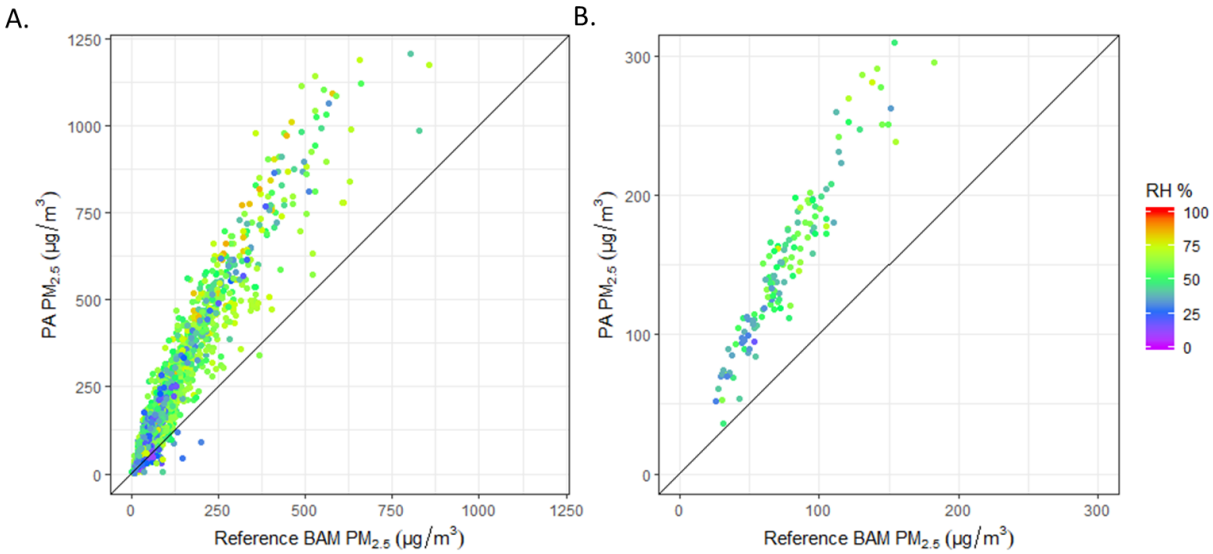

Figure 2.5 Hourly average (A) and daily average (B) $PM_{2.5}$ from the Purple Air (PA) and FEM monitor (BAM) for the period 06Nov2019-20March2020. Data are color-coded by ambient relative humidity.

The AQE-to-BAM temperature and RH dependence was also evaluated with hourly and daily average $PM_{2.5}$ data.

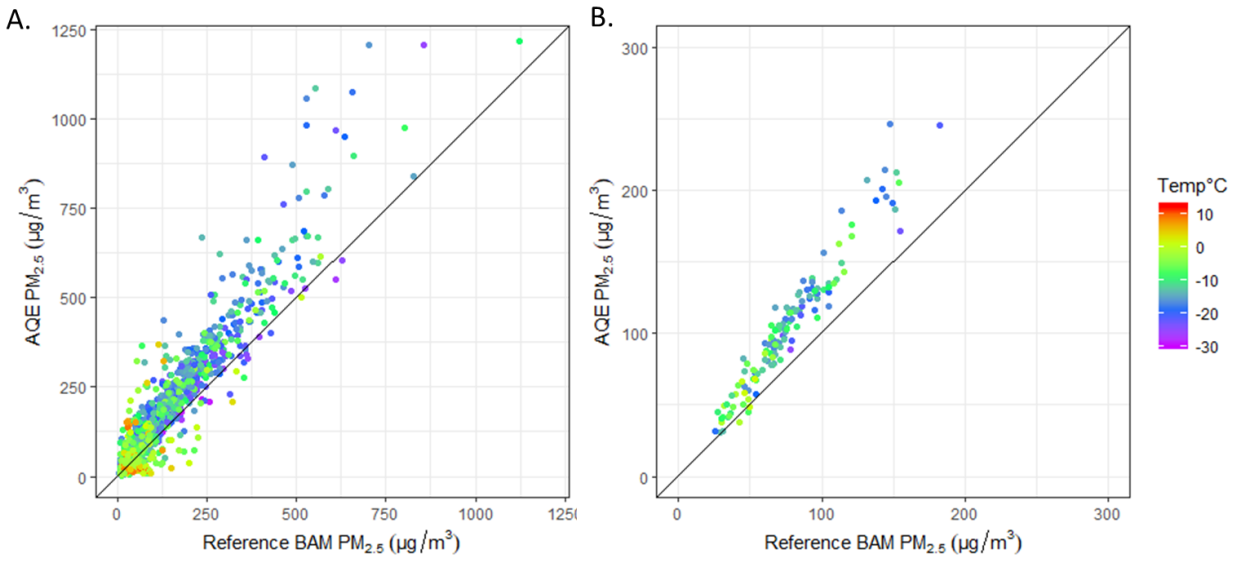

Figure 2.6 Hourly average (A) and daily average (B) $PM_{2.5}$ from the Air Quality Egg (AQE) and FEM monitor (BAM) for the period 06Nov2019-20March2020. Data are color-coded by ambient temperature.

Figure 2.7A shows at higher RH, AQE is biased high compared to the FEM BAM while at lower RH the scatter is largely about the 1:1 line. **Figure 2.7B** more clearly shows the RH dependence of the LCS-to-FEM bias.

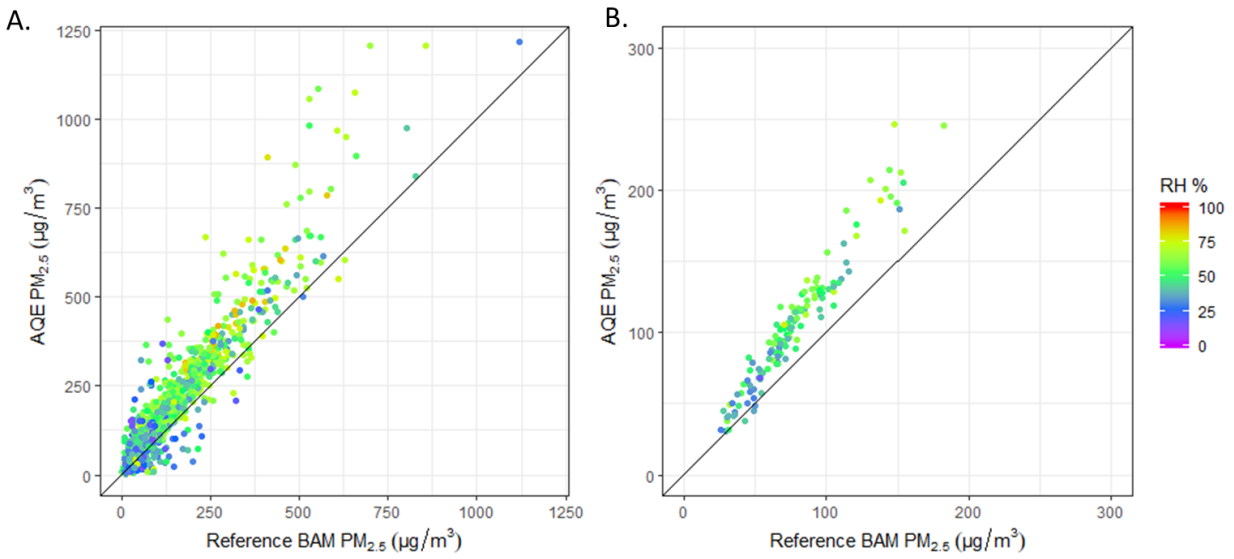

Figure 2.7 Hourly (A) and daily average (B) $PM_{2.5}$ from the Air Quality Egg (AQE) and reference monitor (BAM) for the period 06Nov2019-20March2020. Data are color-coded by ambient relative humidity.

2.4.3 LCS $PM_{2.5}$ adjustments using one year of hourly data (Nov-06-2019~Nov-06-2020)

In this data adjustment analysis, there were only three different LCS device types and each device type was in duplicate instead of triplicate because of data completeness issues. As previously described, an ordinary least squares regression was used to remove the $PM_{2.5}$ bias between LCS devices of the same type. Subsequently, linear and quadratic regression models were used to develop adjustment factors for each device type to better match the FEM. **Table 2.2** presents the quadratic regression coefficients for the winter data (October to March) while **Table 2.3** presents the linear regression coefficients for the non-winter (April to September) data.

Table 2.2 Adjustment factors for the low-cost sensor devices for the winter season.

Adjustment Coefficients	PurpleAir #3	Air Quality Egg #1	Air Beam 2 #1
(Intercept)	7.986	16.6	13.749
LCS $PM_{2.5}$	0.5010	0.6254	1.9079
LCS temp	1.2150	0.3707	0.5807
LCS RH	-0.0815	-0.3107	-0.3152
$(LCS\ PM_{2.5})^2$	0.0001	-0.0001	0.0036
$(LCS\ temp)^2$	0.0593	0.0018	0.0143
$(LCS\ RH)^2$	0.0044	0.0045	0.0045
LCS $PM_{2.5}$*LCS temp	-0.0071	-0.0183	0.0045
LCS $PM_{2.5}$*LCS RH	-0.0046	-0.0035	-0.0166
LCS temp*LCS RH	-0.0021	0.0121	0.0063

Table 2.3 Adjustment factors for the low-cost sensor devices for the non-winter seasons.

Adjustment Coefficient	PurpleAir #3	Air Quality Egg #1	Air Beam #1
LCS $PM_{2.5}$	0.6278	0.4964	2.0489
LCS temp	0.5469	0.5964	0.6561
LCS RH	0.0632	0.0384	0.0589

Table 2.4 presents valued for the performance metrics recommended by U.S. EPA [25]: Pearson correlation coefficient (Corr), Low-cost sensor device to FEM monitor bias (Bias), Mean Absolute Error (MAE), Root Mean Square Error (RMSE), and Normalized Root Mean Square Error (NRMSE).

Table 2.4 Assessment metrics with bias, MAE and RMSE all having units of $\mu g/m^3$, NRMSE is in percentage.

Metric	PA Raw	PA Adjusted	AQE Raw	AQE Adjusted	AB2 Raw	AB2 Adjusted
Corr	0.93	0.95	0.89	0.90	0.91	0.94
Bias	-29	0.5	-17	0.7	23	0.04
MAE	39	11	27	16	23	13
RMSE	79	22	50	30	43	24
NRMSE	179	50	103	61	92	51

2.5 Discussion and conclusions:

Based on the results in section 2.4 all collocated LCS devices of the same type were highly correlated, and the scaled differences within each device type were less than 25%. PA, AVP and AQE were biased high and the AB2 was biased low compared to the BAM FEM. AB2 exhibits a dramatic reduction in response at high concentrations which is a problem if seeking to report hourly data. AQE data were closer to the BAM data, however, AQE have lower data completeness because communications to the Wi-Fi were periodically dropped. In both daily and hourly data comparisons PA, AQE and AB2 exhibit linear relationships; the issue with the AB2 hourly data is damped out upon averaging over the day because of strong within-day $PM_{2.5}$ variations.

The AB2, AQE, LE and PA devices all use low-cost sensors manufactured by Plantower. AQE and PA devices used Plantower version PMS5003, LE used Plantower version PMS3003 and AB2 used Plantower version PMS7003. The reported $PM_{2.5}$ concentrations for all LCS brands were different to some extent and these differences may be caused by the version of Plantower sensors, how the manufacturer packages of the sensors into a device and, perhaps more importantly, how they processes the raw optical attenuation signal from Plantower sensor to estimate $PM_{2.5}$ mass concentration.

While the PA, AQE and AB2 relationships to the BAM were stable though March 20, 2020, the AVP relationship to the BAM drifted over time. Therefore, the collocation analysis was limited to the period November 7–December 5, 2019, which was prior to the onset of drift. *The AVP concentration is biased high for early data and biased low for later data (i.e. after December 15, 2019).* One possible reason might be the sensors were contaminated from exposure to the high

wintertime outdoor PM levels. This should not be an issue for most indoor deployments where the concentrations are much lower. Furthermore, for the purposes of assessing the quality of data generated by the LCS, the sampling mode for all AVP in this study was changed to continuous mode instead of the factory default mode. This continuous sampling greatly accelerated the contamination rate and for settings like Mongolia with high PM concentrations the continuous sampling would, in retrospect, be not recommended.

Overall, the pilot study focused on evaluating $PM_{2.5}$ LCS during the extreme wintertime conditions in Mongolia. Key observations are as follows:

Outdoor Measurements

1. Most LCS devices operated even at extremely low temperatures. An exception was the Laser Egg and it is not designed for outdoor use. This study did not test LCS devices at high temperature/high humidity conditions.

2. $PM_{2.5}$ concentrations for all LCS devices except the AirBeam2 were biased high compared to a US EPA Federal Equivalent Method (FEM) monitor. A correction factor must be applied to make these data "reference like". The bias might depend on environmental conditions (e.g. temperature, humidity) and particulate matter properties (size distribution, composition) and these parameters often vary by season.

3. $PM_{2.5}$ concentrations reported by LCS devices of the same type varied by as much as 20-30%. Therefore, the collocation before each network deployment is essential for understanding the unique characteristics of each sensor.

4. PM sensors can become contaminated when exposed to high concentrations for long time periods.

We also have the following **recommendations** for deployments in general:

A. LCS device selection should consider the study objectives. Real-time reporting requires reliable Wi-Fi. Other applications might place a higher priority on data completeness and in these cases LCS devices with on-board data storage are attractive. Sometimes this is an option (e.g. PA-II-SD, AQE) not included in the standard device configuration.

B. Correction factors to make the LCS device data "reference monitor-like" will depend on environmental conditions and particle characteristics. *Correction factors developed in one setting (e.g. Mongolia) should not be applied to other settings (e.g. hot, humid zones).* For the data collected to date, there is a temperature dependence to the Mongolia data. Studies in other locations have observed a relative humidity dependence. Any project with goals beyond a qualitative tracking of air quality should include steps to periodically compare the LCS devices to a reference monitor and develop and apply correction factors as needed.

2.6 References

[1] Y. Xing, Y. Xu, M. Shi and Y. Lian, "The impact of PM2.5 on the human respiratory system.," *J. Thorac. Dis.,* no. 8, p. 69, 2016.

[2] A. Bhatnagar, "Environmental Cardiology: Pollution and Heart Diease.," *Royal Society of Chemistry.,* 2011.

[3] P. James, R. Banay, J. Hart and F. Laden, "A Review of the Health Benefits of Greenness.," *Curr Epidemiol Rep.,* no. 2, pp. 131-142, 2015.

[4] P. Dadvand, X. Bartoll, X. Basagana, A. Dalmau-Bueno, D. Martinez, A. Ambros, M. Cirach, M. Triguero- Mas, M. Gascon, C. Borrell and M. Nieuwenhuijsen, "Green spaces and General Health: Roles of mental health status, Social support, and physical activity.," *Environ Int.,* no. 91, pp. 161-7, 2016.

[5] S. Vedal, "Ambient particles and health: Lines that divide.," *J. Air Waste Manag. Assoc.,* no. 47, pp. 551-581, 1997.

[6] X. Huang, Q. Bian, W. Ng, P. Louie and J. Yu, "Characterization of PM2.5 Major components and source investigation in suburban Hong Kong: A one-year monitoring study.," *Aerosol Air Qual. Res.,* no. 14, pp. 237-250, 2014.

[7] J. Samet, F. Dominici, F. Curriero, I. Coursac and S. Zeger, " Fine particulate air pollution and mortality in 20 US cities, 1987-1994.," *Engl. J. Med.,* no. 343, pp. 1742-1749, 2000.

[8] N. Künzli, M. Jerrett, W. Mack, B. Beckerman, L. LaBree, F. Gilliland, D. Thomas, J. Peters and H. Hodis, "Ambient air pollution and atherosclerosis in Los Angeles.," *Environ. Health Perspect.,* no. 113, p. 201–206, 2004.

[9] T. Nelin, A. Joseph, M. Gorr and L. Wold, "Direct and indirect effects of particlulate matter on the cardiovascular system.," *Toxicol. Lett.,* no. 208, pp. 293-299, 2012.

[10] "Mongolia: Heating Stove Market Trends in Poor, Peri-Urban ger Areas of Ulaanbaatar and Selected Markets outside Ulaanbaatar: With Generous Support from the Australian Government.," *The World Bank Group: Washington, DC, USA,* p. 87052, 2011.

[11] G. Laragh, G. Maria and K. Kidist, "Air pollution in Mongolia.," *Bull. World Health Organ.,* no. 97, pp. 79-80, 2019.

[12] P. e. a. Barn, "The effect of portable HEPA filter air cleaner use during pregnancy on fetal growth: The UGAAR randomized controlled trial.," *Environment International,* vol. 121, pp. 981-989, 2018.

[13] L. Hill, R. Edwards, T. J.R., Y. Argo, P. Olkhanud and e. al., "Health assessment of future PM2.5 exposures from indoor, outdoor, and secoundhand tobacco smoke concentrations under alternative policy pathways in Ulaanbaatar, Mongolia," *PLOS ONE,* vol. 12, no. 10,

p. e0186834, 2017.

[14] S. Munir, M. Mayfield, D. Coca, S. Jubb and O. Osammor, "Analysing the performance of low-cost air quality sensors, their drivers, relative benefits and calibration in cities--a case study in Sheffield," *Environmental Monitoring and Assessment,* vol. 191, no. 2, p. 94, 2019.

[15] B. Feenstra, V. Papapostolou and S. Hasheminassab, "Performance evaluation of twelve low-cost PM2.5 sensors at an ambient air monitoring site.," pp. 1352-2310, 2019.

[16] M. Badura, I. Sowka, P. Szymanski and P. Batog, "Assessing the usefulness of dense sensor network for PM2.5 monitoring on an academic compus area," *Science of the Total Environment,* vol. 722, p. 137867, 2020.

[17] S. Kim and J. Lee, "Evaluation of Performance of Inexpensive Laser Based PM2.5 Sensors Monitors for Typical Indoor and Outdoor Hotspots of South Korea," *Applied Sciences,* no. 9, p. 1497, 2019.

[18] E. Molina Rueda, E. Carter, C. L'Orange, C. Quinn and J. Volckens, "Size-Resolved Field Performance of Low-Cost Sensors for Particulate Matter Air Pollution," *Environmental Science & Technology Letters,* p. acs.estlett.3c00030, 2023-02-08.

[19] E. Molina Rueda, E. L. C. Carter, C. Quinn and J. Volckens, "Size-Resolved Field Performance of Low-Cost Sensors for Particulate Matter Air Pollution," *Environmental Science & Technology Letters,* p. acs.estlett.3c00030, 2023-02-08.

[20] C. e. a. Malings, "Fine particle mass monitoring with low-cost sensors: Corrections and long-term performance evalucation.," *Aerosol Science and Technology,* no. 54, pp. 160-174, 2019.

[21] M. Zusman and C. e. a. Schumacher, "Calibration of low-cost particulate matter sensors: Model development for a multi-city epidemiological study," *Environment International,* vol. 134, p. 105329, 2020.

[22] J. Tryner, J. Mehaffy, D. Miller-Lionberg and J. Volckens, "Effects of aerosol type and simulated aging on performance of low-cost PM sensors," *Journal of Aerosol Science,* vol. 150, p. 105654, 2020.

[23] Z. Levy, F. Xiong, D. Gentner, B. Kerkez, J. Kohrman-Glaser and K. Koehler, "Field and Laboratory Evaluations of the Low-Cost Plantower Particulate Matter Sensor," *Environmental Science & Technology,* vol. 53, no. 2, pp. 838-849, 2019.

[24] G. Kosmopoulos, V. Salamalikis, S. Pandis, P. Yannopoulos, A. Bloutsos and A. Kazantzidis, "Low-cost sensors for measuring airborne particulate matter: Field evaluation and calibration at a South-Eastern European site.," *Science of The Total Environment,* vol. 748, p. 141396, 2020.

[25] R. Duvall, A. Clements, G. Hagler, A. Kamal, V. Kilaru, L. Goodman, S. Frederick, K. Johnson Barkjon, I. VonWold and D. &. D. T. Greene, "Performance testing protocols, metrics, and target values for fine particulate matter air sensors: Use in ambient, outdoor, fixed site, non-regulatory supplemental and informational monitoring applications: Technical Report," U.S. EPA Office of Research and Development, Washington, D.C., 2021.

Chapter 3: The influence of siting microenvironment on $PM_{2.5}$ low-cost sensor device performance

3.1 Abstract

In recent years, the establishment of air quality low-cost sensor (LCS) monitoring networks has gained significant attention. The affordability of these LCS devices has empowered community groups and civil societies to enhance their understanding of local air quality conditions. However, our research indicates that the interpretation of data for these sensors may be confounded by the microenvironmental siting conditions that affect device performance. This paper provides a summary of our observations during the testing and deployment stages of particulate matter LCS devices. Our objective is to offer the public insights into issues that may arise when deploying these devices and that may lead to measurement bias. By addressing the nuances of LCS device placement, we aim to improve the utility and reliability of the data generated by these networks.

3.2 Introduction

A crucial aspect of ambient air monitoring with non-open path methods is to deliver a representative sample of the ambient air to the monitor's sensing element. Much work has been invested to design and characterize the EPA Louvered PM_{10} inlet [1,2] which can be paired with a downstream cyclone or impactor to achieve a smaller particle size cutoff (e.g., PM_1, $PM_{2.5}$). EPA provides extensive criteria for locating air monitoring stations and for monitor probe (or sampler inlet) placement to minimize obstructions to air flow [3]. For example, PM

samplers/monitors for air standards compliance measurements and operating at 1.67 LPM flow rate are to be placed at least 2m horizontal distance from supporting structures and at least 10 m from trees. Collocated monitors with flow rate < 200 LPM must be within must be within 4 meters of each other and at least 1 meter apart to avoid airflow interference. In contrast, low-cost sensor (LCS) devices typically have simplistic inlets (e.g., a small hole) and very low flow rate (e.g., ~0.1 LPM) and there are no published criteria for device placement other than on the prevailing upwind side of structures [4]. It is typically assumed that LCS devices can be placed within centimeters apart because of the very low flow rates. Indeed, best practices include collocating all PM LCS devices with a reference-grade monitor before deploying the devices as a distributed network [5] and the LCS devices are often tightly grouped for such studies. In this work, collocation studies were conducted with PM LCS devices arranged in different configurations to assess measurement bias that might arise from device placement and not the sensor's actual performance.

3.3 Material and Methods

Collocated PurpleAir SD-II PM LCS devices were deployed in two configurations to assess how obstructions (e.g., a mounting board for the devices, and devices close to each other), might affect air flow and lead to biased $PM_{2.5}$ measurements. These deployments were conducted at State/Local/Tribal (SLT) air monitoring stations with $PM_{2.5}$ Federal Equivalent Method (FEM) monitors and on-site meteorology measurements including wind speed and direction at 10 m.

3.3.1 Blair Street (City of St. Louis) collocation

At the Missouri Department of Natural Resources (MDNR) Blair Street station in the City of St. Louis, ten PurpleAir devices were collocated with a $PM_{2.5}$ FEM (Teledyne Model T640) to

quantify LCS precision and derive LCS-to-FEM adjustment factors. The devices were deployed atop a shelter and mounted on both sides of a wood board suspended by a post ~1.5 m above the shelter roof (**Figure 3.1**). Each side of the board had five devices for the collocation study and one additional long-term device operating at the site year-round. The St. Louis collocation was conducted from January 22 to March 15, 2021. Subsequently, the ten collocation devices were moved to the Louisville Metropolitan Air Pollution Control District (LMAPCD) Canon's Lane station in the City of Louisville (KY) and deployed in the configuration shown in **Figure 3.2**. Again, the devices were mounted on a wood board suspended by a post ~0.5 m above the shelter roof. The Louisville study was conducted from April 13 to June 2, 2021.

Figure 3.1 PurpleAir SA-II device collocation study layout in St. Louis, MO.

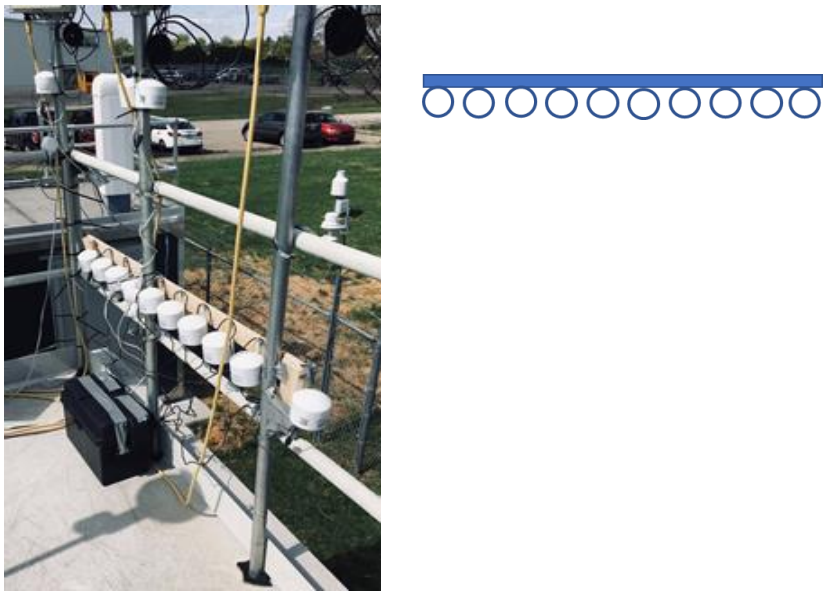

Figure 3.2 PurpleAir SA-II device collocation study layout in Louisville, KY.

PurpleAir raw data is reported at two-minute intervals and was averaged to hourly values. One-hour average winds data for the St. Louis site were provided by MDNR as scalar mean wind speed and vector mean wind direction.

3.4 Results

3.4.1 St. Louis and Louisville Collocation Results

The initial collocation of ten PurpleAir devices at the Blair Street reference site alongside a $PM_{2.5}$ FEM was aimed at developing adjustment factors to better match the LCS devices data to the FEM data. **Figure 3.3** shows $PM_{2.5}$ hourly average scattergrams for the ten PurpleAir devices against the FEM. The panels are organized according to the layout in Figure 3.1.

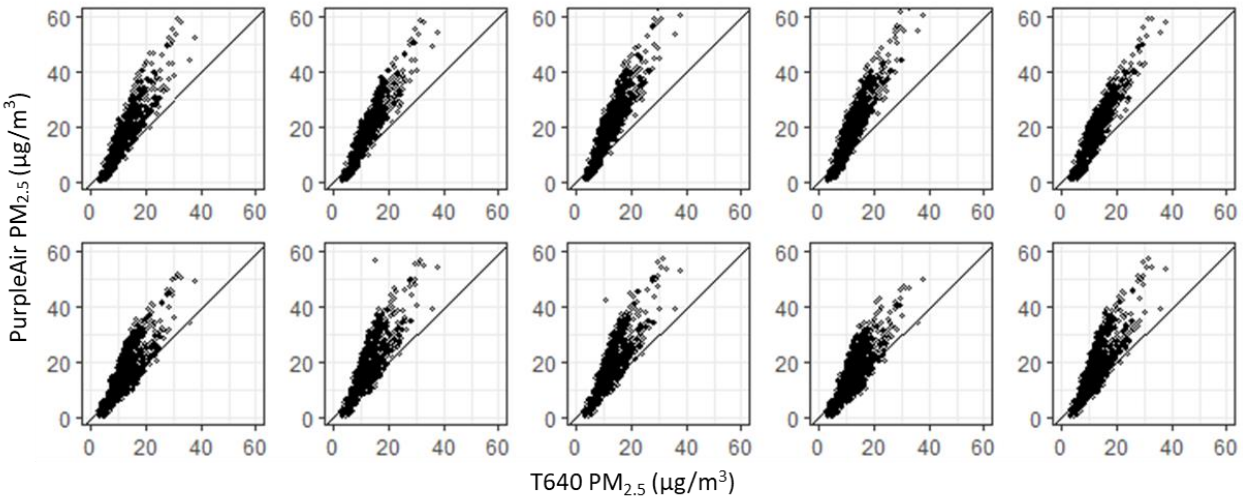

Figure 3.3 PurpleAir vs. Teledyne T640 FEM $PM_{2.5}$ data for the St. Louis collocation study.

Differences in performance metrics, such as the precision of collocated LCS data and slopes for ordinary least squares regression of the LCS on T640 FEM, were observed between sensors deployed on different sides of the wood board. Sensors in Group 1 (top row in Figure 3.1) exhibited generally higher regression slopes in comparison to the FEM, indicating a bias of

approximately 20% higher than Group 2 devices (bottom row in Figure 3.1). Furthermore, Group 1 devices demonstrated greater collocated precision than those in Group 2. These differences were more pronounced than initially anticipated, underscoring the influence of sensor microenvironment on LCS performance.

Figure 3.4 shows hourly $PM_{2.5}$ scattergram matrices for the St. Louis (left) and Louisville (right) deployments. LCS device layout profoundly affects the scatter. The St. Louis data clusters into two groups of five devices with excellent agreement across devices on the same side of the mounting board and large scatter for devices on different sides of the board. In contrast, the Louisville study features all ten devices in a single row and exhibits excellent agreement across all devices. Without a detailed understanding of the drivers for these differences, the scatter in the St. Louis study data might be incorrectly attributed to the LCS devicess. These findings also suggest that similar issues might arise during network deployments depending on the microenvironment around each LCS device.

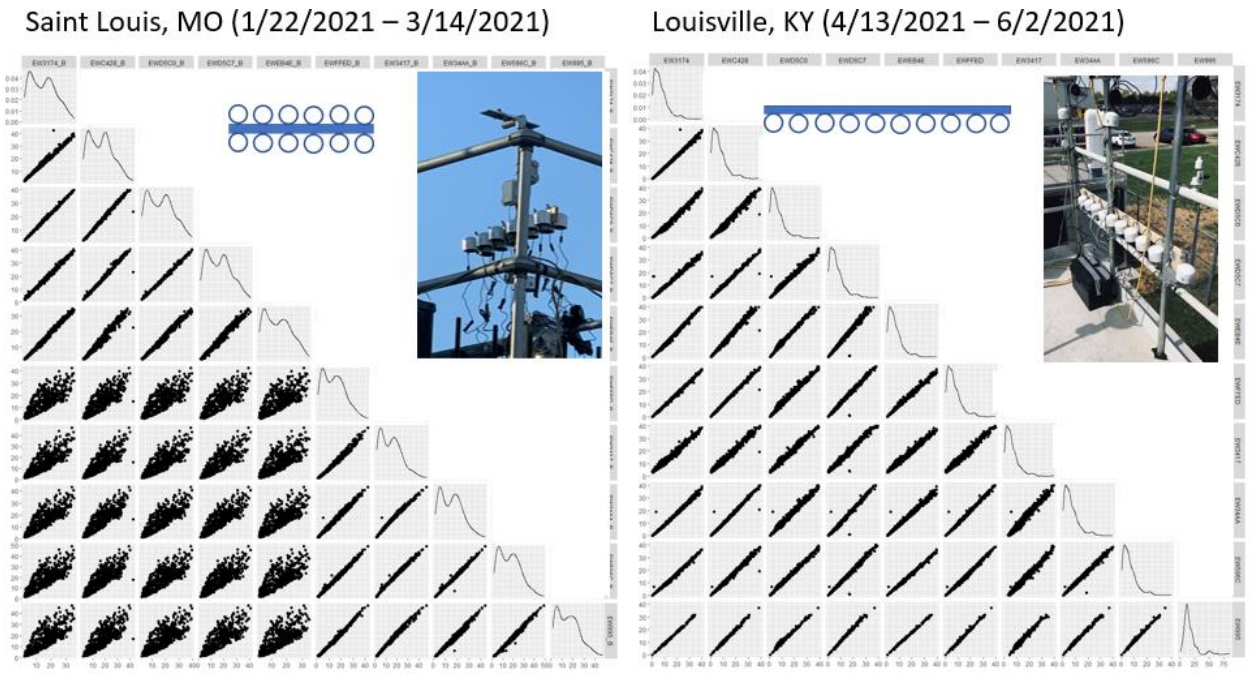

Figure 3.4 PurpleAir 1-hour $PM_{2.5}$ scatterplots for different device deployment layouts at St. Louis and Louisville sites, all axis ranges are 0-40 µg/m^3.

The St. Louis study data were further analyzed by assessing the role of wind speed and wind direction. Hourly mean scalar wind speed data were aggregated into four groups: #1 (0-3 MPH), #2 (3-6 MPH), #3 (6-9 MPH), and #4 (9-12 MPH). Hourly vector mean wind direction was aggregated into two groups: North-South (315°~45° and 135°~225°) and East-West (45°~135° and 225°~315°). The mounting board is nominally oriented in the East-West direction so North-South winds are perpendicular to the board and East-West winds are parallel to the board. One PurpleAir device was selected from each side of the board and hourly $PM_{2.5}$ data were compared. **Figure 3.5** demonstrates the results for all winds direction with color coded wind speed. There is excellent agreement at low winds speeds (blue) and increased bias between the data with increasing wind speed. The data are well distributed about the 1:1 line (i.e. litte overall bias), and this wind speed induced scatter might be incorrectly charcterized as sensor imprecision in the absense of considering the role of wind speed.

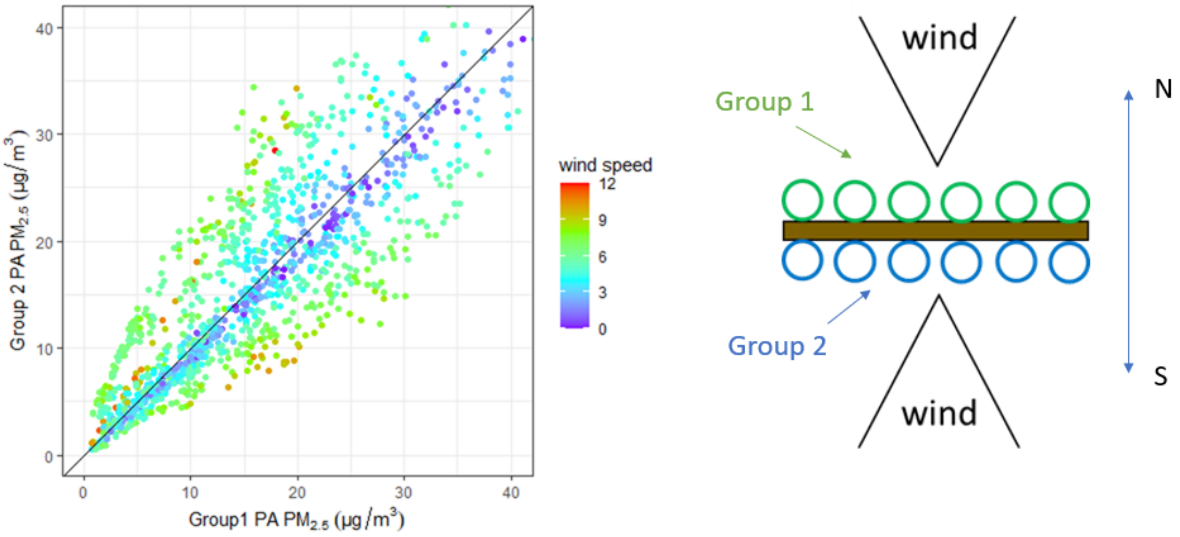

Figure 3.5 (a) Hourly PurpleAir $PM_{2.5}$ data color coded based on wind speed in MPH (left) from selected sensors in each group, (b) top view of PurpleAir sensor deployment and indicated groups based on direction (right).

Figure 3.6 (left) shows the results for data stratified by north versus south wind directions. For winds from the north (red), $PM_{2.5}$ concentrations are biased high for the device on the downwind (south) side of the board. Similarly, for winds from the south (aqua), $PM_{2.5}$ concentrations are biased high for the device on the downwind (north) side of the board. Figure 3.6 (right) exhibits similar patterns east and west winds albeit with less scatter; this likely arises because the board is not perfectly aligned with the cardinal wind direction also might due to the data stratified by east and west wind angle includes a wide range of directions.

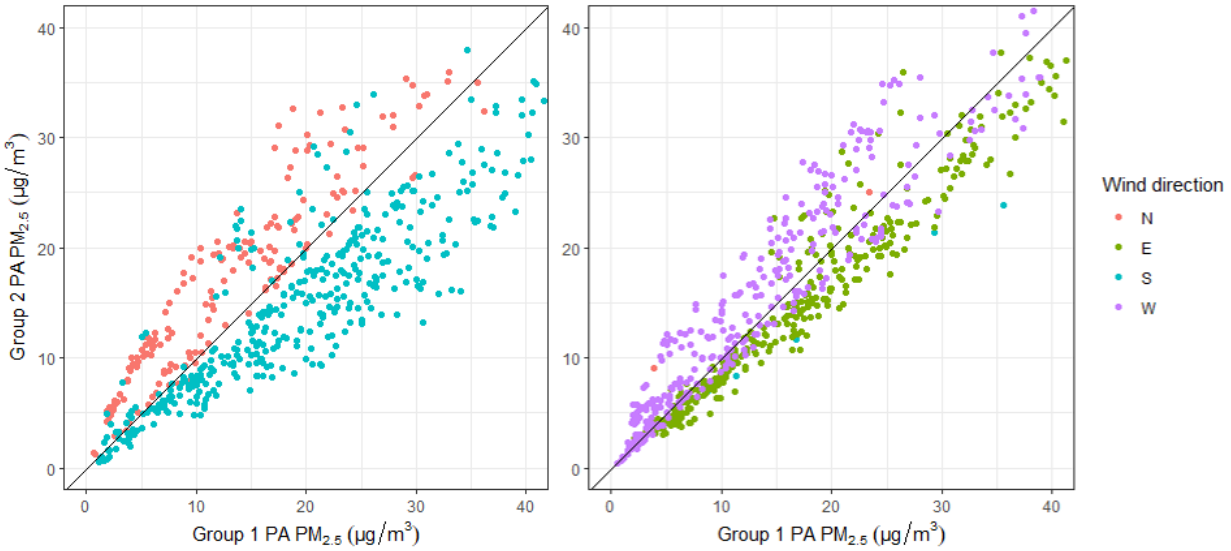

Figure 3.6 Group 1 and 2 sensor $PM_{2.5}$ comparison for data grouped by wind directions: winds nominally perpendicular to the mounting board (left) and winds nominally parallel to the mounting board (right) from 0.1 to 12 mph.

The study further delved into the interplay between wind direction and LCS device performance by examining responses under two distinct wind speed regimes: Wind Speed range #1 (0.2~3 mph) and Wind Speed range #3 (6~9 mph). As illustrated in **Figure 3.7**, within the North-South wind direction subset, LCS devices from both groups exhibited remarkable concordance at lower wind speeds (Wind Speed #1), indicating a high level of agreement in measurements despite differing orientations. This consistency suggests minimal influence of low wind speeds on sensor

discrepancies. Conversely, as wind speeds increased to the Wind Speed #3 category, the data began to reveal distinct divergences in sensor output, manifesting as splits in the measurement slopes that are stratified by wind direction. This divergence highlights the critical need for considering both wind speed and direction in sensor deployment and data interpretation especially in cases when the microenvironment about the device influences airflow.

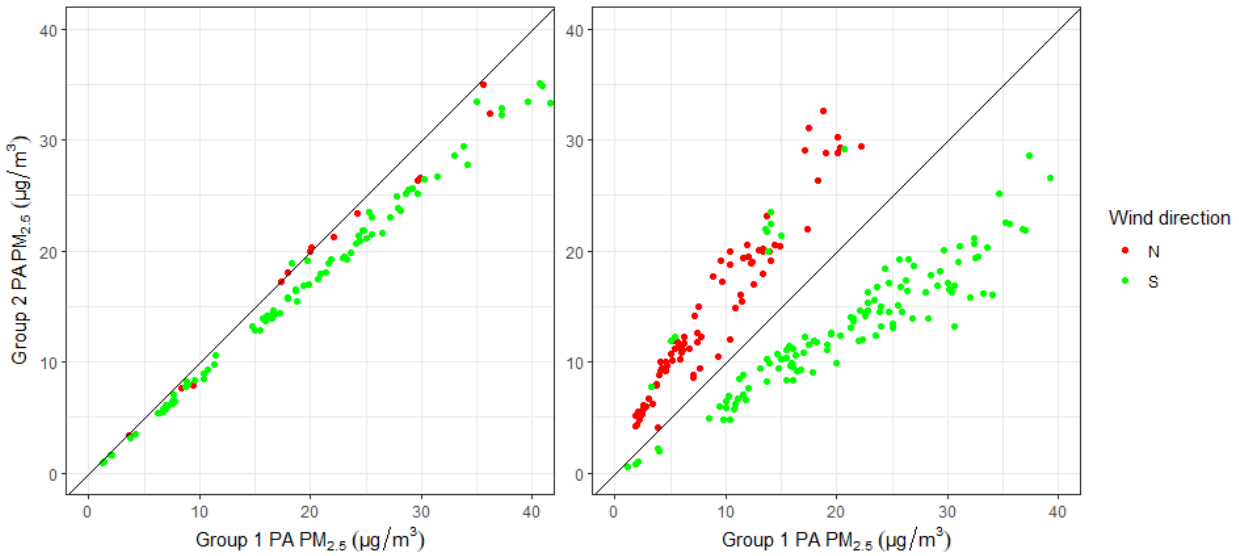

Figure 3.7 Group 1, 2 comparisons under low (0.2~3 mph) (left) and high(6~9mph) (right) wind speed for North and South wind direction only.

For conditions involving crosswinds (North-South), particularly when wind speeds range from 6 to 12 mph, the scattergrams comparing sensors from the two groups begin to diverge, forming distinct slopes. Specifically, under northerly wind conditions, Group 2 sensors exhibit a higher bias compared to Group 1 sensors, whereas under southerly winds, the opposite trend is observed, with Group 1 sensors showing a higher bias compared to Group 2. These disparities highlight significant sensor-to-sensor biases, which pose challenges during the sensor adjustment phases. Conversely, under East-West wind conditions in **Figure 3.8**, calm winds demonstrate a excellent correlation between each sensor group, but as wind speed increases, the data show

slope variations with different wind directions. However, the deviations observed under East-West conditions are not as pronounced as those under North-South wind conditions.

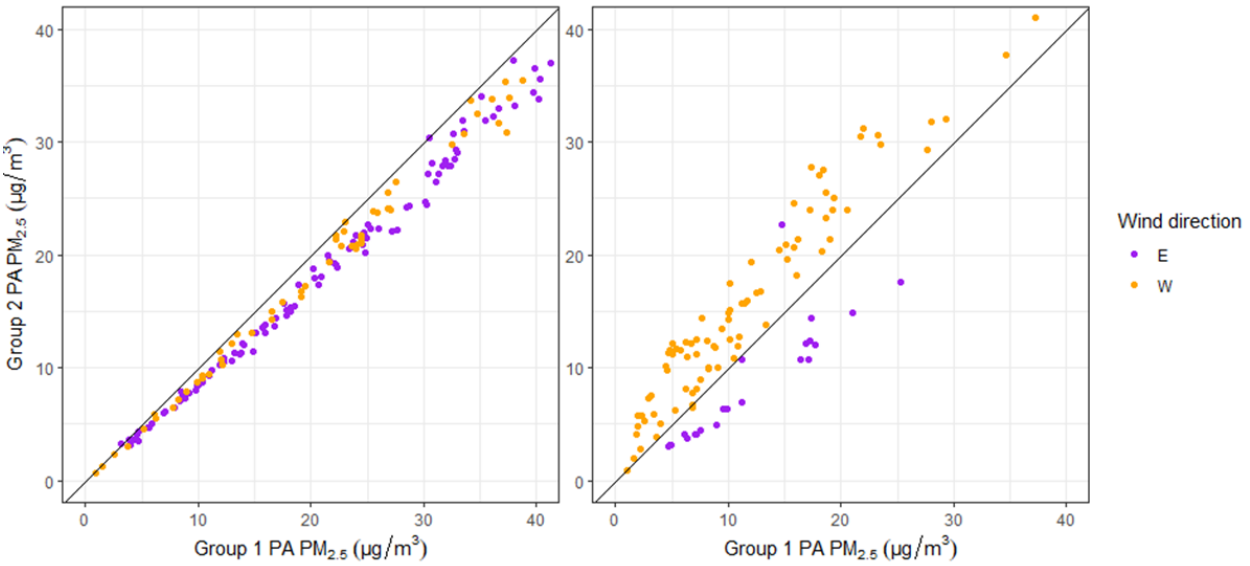

Figure 3.8 Group 1, 2 comparisons under low (0.1~3 mph) (left) and high (6~9 mph) (right) wind speed for East and West wind direction only.

Further analysis of sensor performance, in relation to the reference monitor T640 at the Blair Street reference site, was conducted under varying meteorological conditions. Data from one sensor in Group 1 were plotted against the reference monitor for both North-South and East-West wind directions (F**igure 3.9**), and similarly, data from a Group 2 sensor were plotted (F**igure 3.10**). The Group 2 sensor shows clear wind direction dependance on LCS $PM_{2.5}$ compared to reference monitor for NS wind directions.

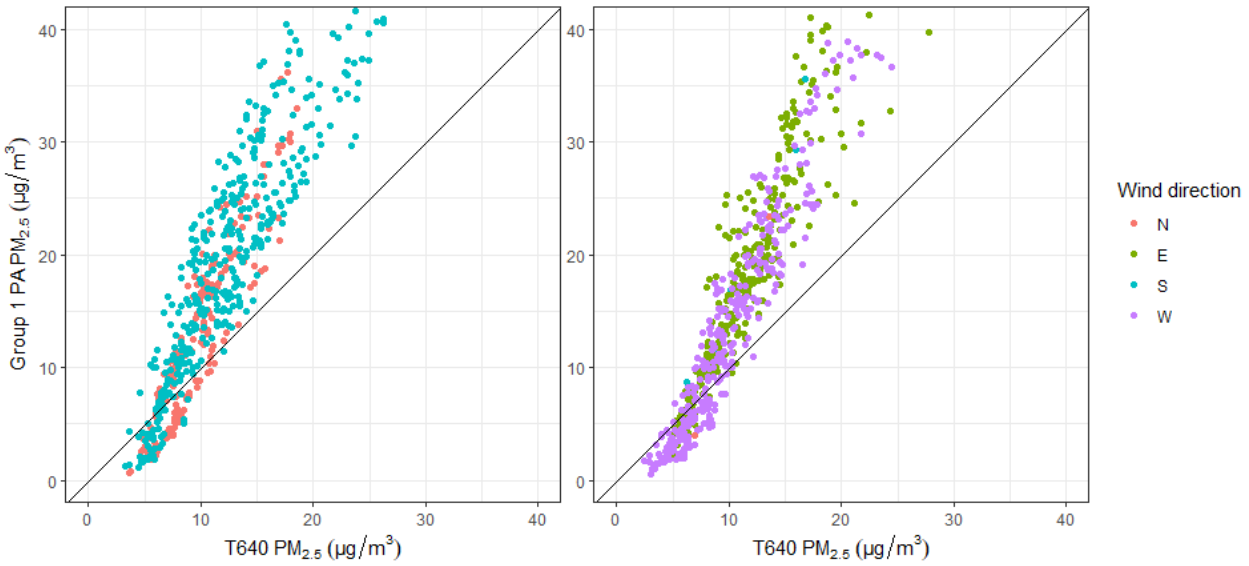

Figure 3.9 Group 1 sensor compared to T640 data color coded based on wind directions.

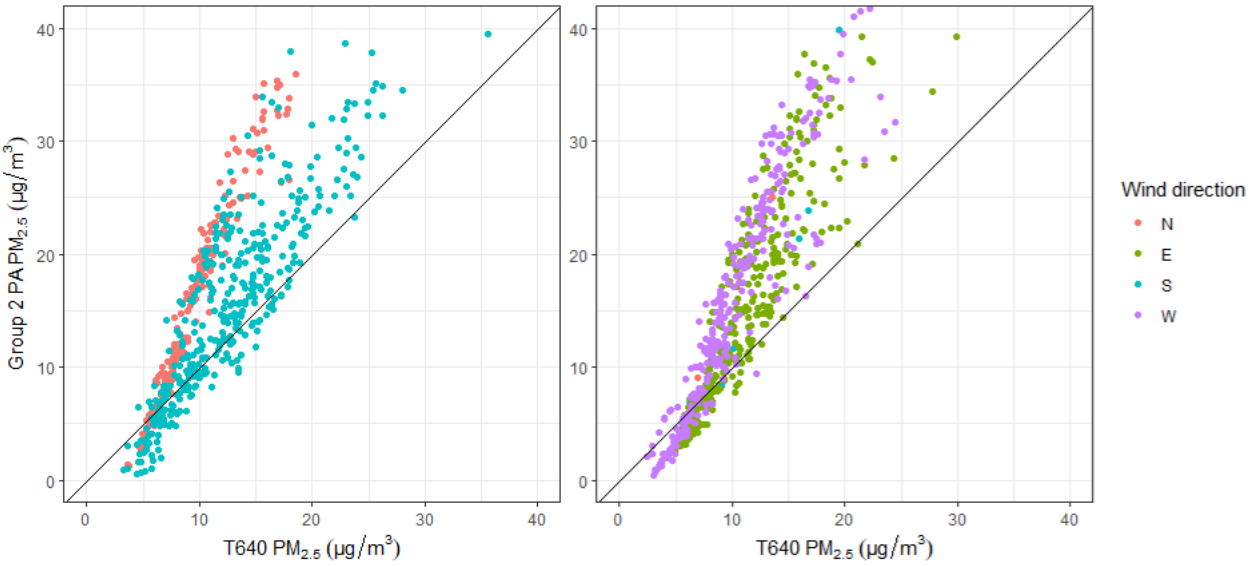

Figure 3.10 Group 2 sensor compared to T640 data color coded based on wind directions.

This detailed examination underscores the critical influence of meteorological conditions, especially wind direction and speed, on the performance and reliability of low-cost air quality devices when the microenvironment affect airflow near the device inlet. These findings suggest that sensor deployment strategies, as well as calibration and adjustment methodologies, must account for microenvironmental effects to enhance the precision and applicability of air quality monitoring efforts.

3.5 Conclusions and discussions

Our investigation into the deployment and performance of PurpleAir LCS devices at multiple sites reveals several key findings:

Siting and Configuration Impact: The performance of LCS devices is significantly influenced by their microenvironment (e.g., layout configuration for collocated devices). This was evident from the variation in data accuracy between sensors deployed on different sides of a wood board at the Blair Street site, as well as the comparison between the St. Louis and Louisville deployment layouts. Such discrepancies highlight the need for standardized siting criteria to minimize biases and improve the comparability of data across different locations.

Meteorological Dependencies: The analysis underscored the dependency of LCS measurements on meteorological conditions, particularly wind speed and direction, when there are microenvironmental siting influences. This dependency manifests in the stratification of PM when comparing across devices, where different wind conditions resulted in divergent sensor readings. The findings demonstrate that the extent of biases induced by LCS device layout depends on the meteorological conditions.

Perceived Sensor-to-Sensor Variability: Despite being of the same model and make, significant sensor-to-sensor imprecision was observed because of microenvironmental influences. The true sensor-to-sensor imprecision was relatively small as observed during calm winds.

The deployment of LCSs for air quality monitoring has democratized access to environmental data, enabling communities to identify and respond to pollution sources with unprecedented granularity. However, this study highlights the critical need for establishing robust guidelines for

sensor siting, configuration, and data interpretation to leverage fully the potential of these technologies. It is imperative for future deployments to consider the effects of microenvironmental siting on sensor performance to ensure data accuracy and reliability.

To mitigate the identified challenges, we recommend the following:

Development of Standardized Siting Criteria: Collaborative efforts between sensor manufacturers, environmental scientists, and regulatory bodies should aim to establish comprehensive guidelines for LCS deployment. These criteria should account for local environmental characteristics, potential sources of air pollution, and meteorological conditions.

Enhanced Sensor Calibration Protocols: Prior to deployment, LCSs should undergo rigorous calibration against reference-grade monitors in conditions that closely mimic their intended deployment environment. Additionally, periodic recalibration should be considered to account for sensor drift and other environmental factors that may affect sensor accuracy over time.

Public Engagement and Education: Engaging with the community and educating the public about the nuances of LCS data interpretation can enhance the impact of community-based air quality monitoring projects. Transparent communication about the strengths and limitations of LCS data can foster informed decision-making and community action on air quality issues.

Looking ahead, the integration of advanced data analytics and machine learning models presents an opportunity to refine LCS data interpretation further, potentially compensating for the effects of variable siting and environmental factors. Continued research and development in sensor technology, alongside efforts to standardize data collection and analysis protocols, will be critical in advancing the field of air quality monitoring.

In conclusion, while low-cost air quality sensors offer a promising tool for community-based environmental monitoring, their effective deployment requires careful consideration of siting, environmental factors, and calibration. By addressing these challenges, we can improve the accuracy and reliability of LCS data, empowering communities to take informed action towards improving air quality and public health.

3.6 References

[1] McFarland, A. R., and C. A. Ortiz. Characterization of Sierra-Andersen PM-10 inlet model 246B. Air quality laboratory report, 4716/02/02/84/ARM, 1984. Texas A&M University System, College Station, TX.

[2] Tolocka, M. P., T. M. Peters, R. W. Vanderpool, F. L. Chen, and R. W. Wiener. On the modification of the low flow-rate PM10 dichotomous sampler inlet. Aerosol Sci. Technol. 34 (5):407–415. 2001. doi: 10.1080/02786820119350.

[3] U.S. Environmental Protection Agency. "40 CFR Part 58 Appendix E – Probe and Monitoring Path Siting Criteria" Code of Federal Regulations. [https://www.ecfr.gov/current/title-40/chapter-I/subchapter-C/part-58#Appendix-E-to-Part-58]

[4] Clements, A., R. Duvall, D. Greene, AND T. Dye. The Enhanced Air Sensor Guidebook. U.S. Environmental Protection Agency, Washington, DC, 2022.

[5] N. Zimmerman, “Tutorial: Guidelines for implementing low-cost sensor networks for aerosol monitoring,” Journal of Aerosol Science, vol. 159, p. 105872, Jan. 2022, doi: 10.1016/j.jaerosci.2021.105872.

Chapter 4: Winter $PM_{2.5}$ indoor levels in Mongolian kindergartens

This work was funded by UNICEF Mongolia (PD Ref. No. MGLA/2880/2019/002-PC).

4.1 Abstract

Mongolia's population centers experience poor wintertime air quality because the cold climate drives strong ground-level inversions and solid carbon fuels are pervasively used for distributed residential space heating. Infiltration of the poor-quality ambient air leads to high indoor $PM_{2.5}$ exposure, especially for those who live or study in or near the "ger" (yurt) neighborhoods that surround Ulaanbaatar's urban core. While the air quality in the core, which has distributed central heating, is relatively poor, it is much worse in the surrounding ger areas, where the dwellings are individually heated by coal burning stoves In a partnership between UNICEF and Washington University in St. Louis, a two-year monitoring study was conducted to quantitatively evaluate Mongolian indoor air quality, with a focus on children's exposure inside kindergartens and hospitals in the Bayanzurkh District of Ulaanbaatar. A 28-site network of air sensors, deployed in February 2020 and operated through spring 2022, included 24 kindergartens and 4 healthcare facilities, where AirVisual Pro low-cost sensing devices (IQAir, Goldach, Switzerland) assessed the indoor $PM_{2.5}$ and CO_2 concentrations. A subset of four sites also had PurpleAir PM devices outdoors (PurpleAir Inc., Draper, Utah). Adjustments factors for the AirVisual Pro and PurpleAir sensor, and others, were developed from a winter 2019/2020

outdoor pilot study in Bayankhongor, Mongolia, that included collocation with a MetOne Model 2010 Beta Attenuation Monitor (BAM).

In the Bayanzurkh District, kindergarten indoor concentrations were highest in and near the ger areas. Across the District, large variations of indoor concentrations were sometimes observed over relatively small spatial scales. Indoor air quality and detailed building characteristics data were paired with land use characteristics to generate an indoor-focused land use regression model that helped predict indoor $PM_{2.5}$ concentrations for kindergartens that did not have a monitoring sensor. Here, we report the measured indoor and outdoor $PM_{2.5}$ spatiotemporal variability results across the networks and discuss their application in the land use regression model for predicting the air quality inside kindergartens without sensors.

4.2 Introduction

4.2.1 Mongolian air quality

Air pollution is a major contributor to human mortality caused by environmental factors[1], [2], [3], [4]. Because of its impact on human health, particulate matter less than 2.5 micrometers in aerodynamic diameter ($PM_{2.5}$) is classified as an especially harmful air pollutant globally. $PM_{2.5}$ can enter the pulmonary alveoli during the air exchange process and spread through the human body to damage other areas[1], [5]. The composition of $PM_{2.5}$ can vary with the emission source and local environmental conditions; some of the major sources include biomass burning, incomplete fuel combustion, transportation, and residential cooking[6]. Health effects such as pulmonary disease, cardiovascular disease, premature death, and increased risk of cancer are related to air pollution and, more specifically, to $PM_{2.5}$[7], [8], [9].

Mongolia is one of the coldest countries in the world: the wintertime temperature can drop to as low as -40 °C in Ulaanbaatar, the capitol city of Mongolia[10]. In Mongolia, pollution by $PM_{2.5}$ is especially high in the winter and the dust season that follows winter. Because most Mongolians have traditional nomadic lifestyles, they live in *gers*, a yurt that is easily relocated several times during the three grazing seasons. In the winter, the heating systems in the individual *gers* in the neighborhoods outside the core of Ulaanbaatar use coal and other solid fuels as a primary combustion source, which creates high particulate matter emissions. The Mongolian National Agency for Meteorology and Environment Monitoring (NAMEM) reports that, in the winter of 2017, the mean concentration of particulate matter in urban centers was between 80–140 $\mu g/m^3$ [11], [12]. The associated health impacts for example respiratory infections and premature death and, in the absence of strict emission controls, are projected to increase as Ulaanbaatar's population grows[13].

4.2.2 The effect of Mongolian indoor air quality on children's health

In September 2019, the United Nations Children's Fund (UNICEF) and Washington University in St. Louis (WUSTL) entered into a Program Cooperation Agreement to support an existing air pollution study administered by UNICEF Mongolia. The specific goals of this project are to develop and operationalize an ambient air quality monitoring network in Bayankhongor (BKH) and to deploy indoor air quality monitoring systems for kindergartens and health care facilities in both BKH and Ulaanbaatar (UB). This study has three broader objectives: to help local government, UNICEF and the public better understand the air pollution problem; to guide researchers in selecting suitable sensors for their studies; and to inform and motivate the public to act to reduce air pollution.

4.2.3 Indoor LCS $PM_{2.5}$ network with land use regression (LUR) prediction

Most current research categorizes indoor $PM_{2.5}$ sources into indoor-generated emissions and outdoor infiltrations[14], [15], [16]. Indoor-generated PM primarily originates from activities such as cooking, cleaning, smoking, and incense burning [15], [16]. Conversely, outdoor air pollution contributes to indoor $PM_{2.5}$ levels through infiltration and ventilation processes, particularly when outdoor concentrations significantly exceed indoor levels, as observed in Mongolia's winter conditions [17].

Using networks of air quality sensors has become a prevalent method for comprehending spatial variations in ambient $PM_{2.5}$ within specific areas [18], [19]. Cheap, laser-based, low-cost sensors facilitate the assessment of hyperlocal $PM_{2.5}$ variability, supplementing city-scale monitoring efforts. Moreover, they provide direct insights into individuals' exposure to indoor PM, particularly in environments such as kindergartens or schools, which typically lack indoor emission sources. In such settings, indoor $PM_{2.5}$ monitoring can be directly correlated with outdoor PM concentrations after accounting for local meteorological conditions and building characteristics.

Land use regression (LUR) modeling is widely recognized as a valuable technique for generating surface air pollution maps, enabling the prediction of pollutant concentrations based on limited ground measurements and surrounding emission sources [18], [20], [21], [22]. As demonstrated by Briggs et al. in their LUR modeling work on predicting air quality, this empirical approach is inherently area-specific, necessitating tailored models to capture the spatial heterogeneity of pollutant distributions [23].

This study presents an innovative approach to estimating indoor PM concentrations within kindergartens lacking indoor monitors. It leverages indoor low-cost sensor measurements collected in similar environments and integrates the LUR methodology with additional building characteristics as predictors. Through this novel approach, the study aims to showcase the efficacy of estimating indoor PM concentrations.

The findings of this study can significantly contribute to the field, aiding researchers in achieving more accurate estimates of indoor exposure to $PM_{2.5}$. Moreover, these insights could enhance epidemiological research by providing a more comprehensive understanding of indoor air quality dynamics and their implications for human health.

4.3 Material and Methods

4.3.1 Study area

Two areas within Mongolia were selected as the focal points of the sensor network investigation: Bayankhongor (BKH), a remote city, and Ulaanbaatar (UB), the capital city. Bayankhongor, situated approximately 650 km southwest of Ulaanbaatar, encompasses an urban area of 64 km^2, with a population of 32,500 as of 2021. In contrast, Ulaanbaatar, the capital, spans an area of 4,700 km^2 and has a population of 1.5 million (source: *https://www.citypopulation.de/en/mongolia/cities/*). Both cities grapple with severe winter air pollution, primarily attributed to the combustion of coal for residential heating and cooking. Ulaanbaatar, a major urban center, exhibits a notably more intricate array of pollution sources than Bayankhongor, yet coal burning is still the predominant contributor to its winter air pollution.

4.3.2 Air quality data sampling

We employed Purple Air and AirVisual Pro sensors for both outdoor and indoor $PM_{2.5}$ monitoring networks deployed in UB and BKH[24], [25], [26], [27], [28]. Both LCSs operate on similar light scattering principles, but differ in their features. Purple Air sensors feature a rigid casing suitable for long-term outdoor deployment under harsh conditions, while AirVisual Pro sensors offer a screen display showing real-time $PM_{2.5}$ and CO_2 concentrations, which is particularly useful for indoor monitoring. Purple Air utilizes two Plantower Particle sensors, PMS5003, capable of measuring ambient $PM_{2.5}$. To identify spatial and temporal variabilities of $PM_{2.5}$ in BKH, a network of outdoor network sensors was deployed in early February of 2020. To quantify UB kindergarten children's exposure to $PM_{2.5}$ and high concentrations of CO_2, as well as measure temperature and relative humidity, network of AirVisual Pro sensors, equipped with a light scattering particle sensor and an IR CO_2 sensor, was also deployed inside classrooms in early February of 2020. Each kindergarten room was assigned a unique identification number, e.g., "KG167", which was the same as the school's government-assigned name.

The last data was retrieved of February 2022, yielding two years of continuous LCS indoor monitoring data inside kindergartens. By this time it had become apparent that the extreme winter cold had damaged the onboard SD data storage cards of the outdoor PurpleAir sensors, and that intermittent wi-fi had compromised the continuity of the data, so we turned our attention to the kindergarten indoor data. Data generated from LCS were utilized to better understand the dynamics of the 24 kindergarten buildings and human activities inside the classrooms. $PM_{2.5}$ measured by LCS served as the dependent variable for the land use regression (LUR) model, which will be discussed in later sections.

To make sure LCS could be intercompared with each other, 10 additional outdoor AVP sensors were collocated with our reference BAM instrument at BKH, and adjustment factors based on linear regressions were generated for each sensor to remove bias between the LCS and the reference monitor. The 10 AVP sensors were then distributed into the UB kindergarten LCS network, where sensor-specific adjustments to the LCSs in the indoor network fine-tuned the accuracy of the collected data.

The average $PM_{2.5}$ indoor concentrations for winter 2021 and 2022 were used as the winter $PM_{2.5}$ average dependent variable for the LUR model. To more accurately estimate children's exposure to indoor $PM_{2.5}$ inside kindergartens, the average data included only 8 to 17 hours, representing school operation hours on weekdays, excluding holidays. Due to outdoor air infiltration, During the winter of 2021, the kindergarten was closed due to COVID-19, so data from that period reflect solely $PM_{2.5}$ from outside infiltrating the room. Winter 2022 data, however, reflected resumed indoor operations post-COVID-19 restrictions, including potential ventilation such as opening doors and windows. KG167 winter 2021 data and KG210 winter 2022 data were excluded due to sensor failure.

4.3.3 Auxiliary databases for the land use regression prediction

To predict indoor $PM_{2.5}$ concentrations, the land use regression model employed in this study relied on the local environmental characteristics of Ulaanbaatar and considered specific building characteristics. This modeling approach assumed that kindergartens lack significant indoor air pollution sources, and thus indoor $PM_{2.5}$ concentrations primarily reflected outdoor $PM_{2.5}$ levels, adjusted for building characteristics to account for infiltration.

Shapefiles for main roads, kindergarten locations for the year 2019, medium-sized heat-only boiler locations, and UB restaurant locations were provided by colleagues from Public Lab Mongolia (PLM). Additionally, the number of gers within the study area in 2022 was manually counted using satellite imagery from Google Earth. Information regarding traffic signals and crossings, gas stations, parking lots, and local roads was obtained from OpenStreetMap (2023) (source: *https://www.openstreetmap.org/*).

For the indoor monitoring location within each kindergarten, ArcGIS Pro 3.0 (ESRI, Redlands, CA) was utilized to calculate proximity variables by determining the distances to main roads, the city center, medium-sized heat-only boiler locations, traffic signals and crossings, UB restaurant locations, and gas stations and parking lots. Cumulative occurrence variables were also computed using ArcGIS Pro by creating buffers ranging from 100 m to 1000 m, with 100-meter increments. Within each buffer zone, these cumulative occurrence variables encompassed counts of gers, medium-sized heat-only boilers, traffic signals and crossings, UB restaurants, the total road length, and the total number of areas with a gas station or a parking lot.

Building characteristic data were collected through a survey conducted by a consulting firm in Mongolia (NEWCON LLC, Mongolia). Based on the survey results, categorical variables were created as predictors for the land use regression model, including building types and heating methods. The combination of proximity and cumulative occurrence variables resulted in a total of 94 independent variables.

4.3.4 Variable selections and model validation

All land use regression analyses, including variable selection, were conducted using R for Windows, version 4.3.0. Because the initial model comprised 94 independent variables and high

collinearity expected among predictors, a Pearson correlation matrix was calculated. Pairs of predictors exhibiting the highest correlation were then removed in a stepwise process. Subsequently, the correlation of each predictor with the dependent variable was assessed, and predictors with lower correlations were systematically removed. This process was iterated until a feasible model, comprising 20 variables, was obtained from the initial set of 94 independent variables.

To determine the final combination of predictors explaining the most variance in $PM_{2.5}$ concentrations, forward stepwise variable selection was employed using the "step ()" function from the stats package in R (source: *https://search.r-project.org/CRAN/refmans/emdi/html/step.html*). The resulting combination of predictors was evaluated based on the adjusted R-squared value.

Two separate land use regression models were constructed for the winters of 2021 and 2022. The final models were validated using the leave-one-out cross-validation (LOOCV) method, considering the limited sample size. For the winter 2021 model, validation was conducted with 21 sites, with KG 167 removed for sensor failure, and for the winter 2022 model, it was performed with 21 sites, with KG 210 removed for sensor failure. Results of the cross-validation process are presented in the Results section.

4.4 Results

4.4.1 Spatial variation $PM_{2.5}$ findings from indoor LCS networks Bayanzurkh (BZD)

Figure 4.1 shows all the indoor monitoring sites, with their specific kindergarten labels.

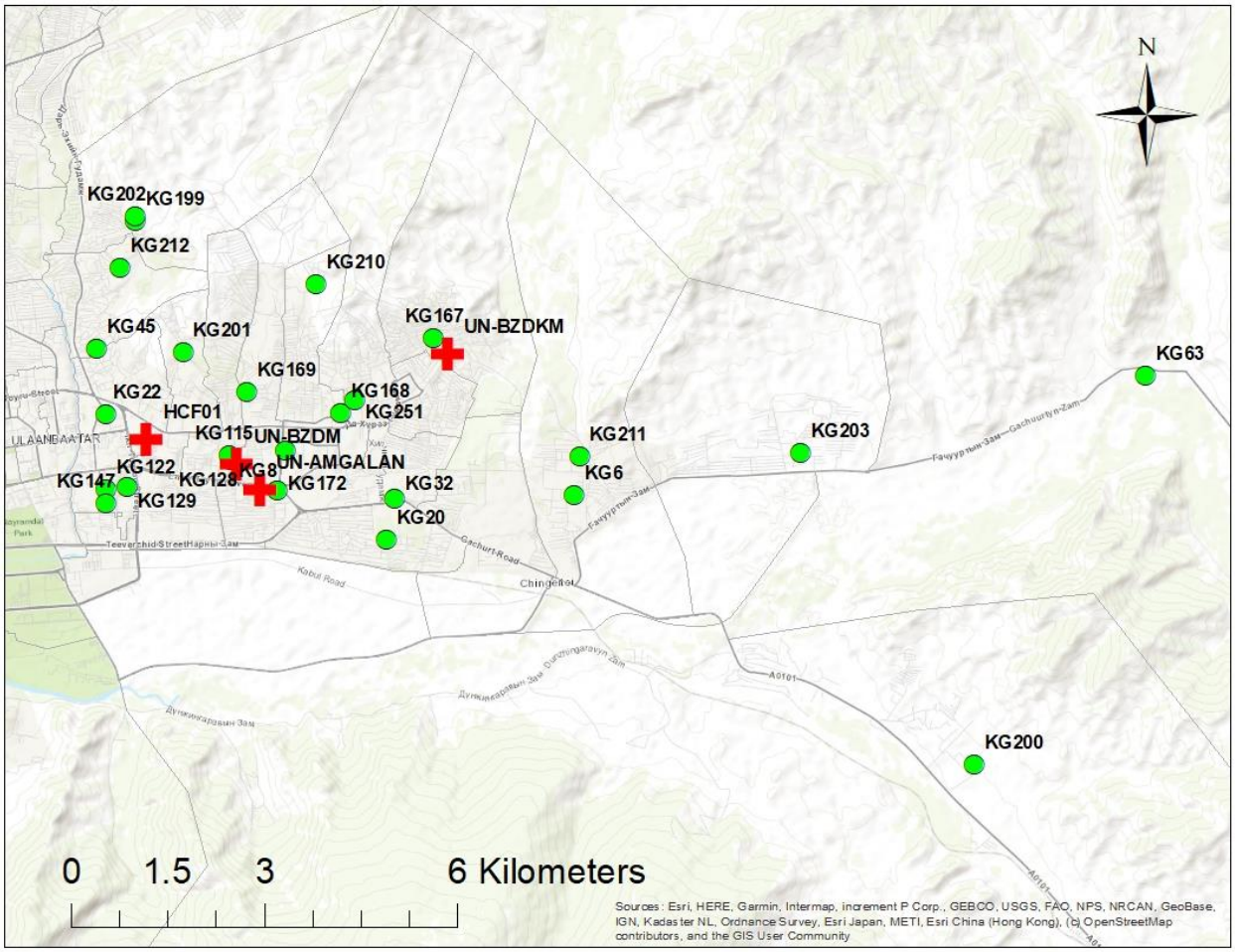

Figure 4.1 BZD: Indoor monitoring sites at 24 kindergartens (and four healthcare facilities not discussed here).

Figure 4.2 shows the winter indoor average $PM_{2.5}$ concentrations for two consecutive winters. Measurement data are from November to February of 2020-21 and 2021-22. Each circle represents a location shown in **Figure 4.1**, and the size of the circle is proportional to the actual $PM_{2.5}$ concentration. The average concentration includes hourly data only from 8 a.m. to 5 p.m.,

the assumed hours of the kindergarten's operation. The circle colors, the same as those used by the US Air Quality Index (US AQI), show similar spatial variations of $PM_{2.5}$ concentration for the two winters.

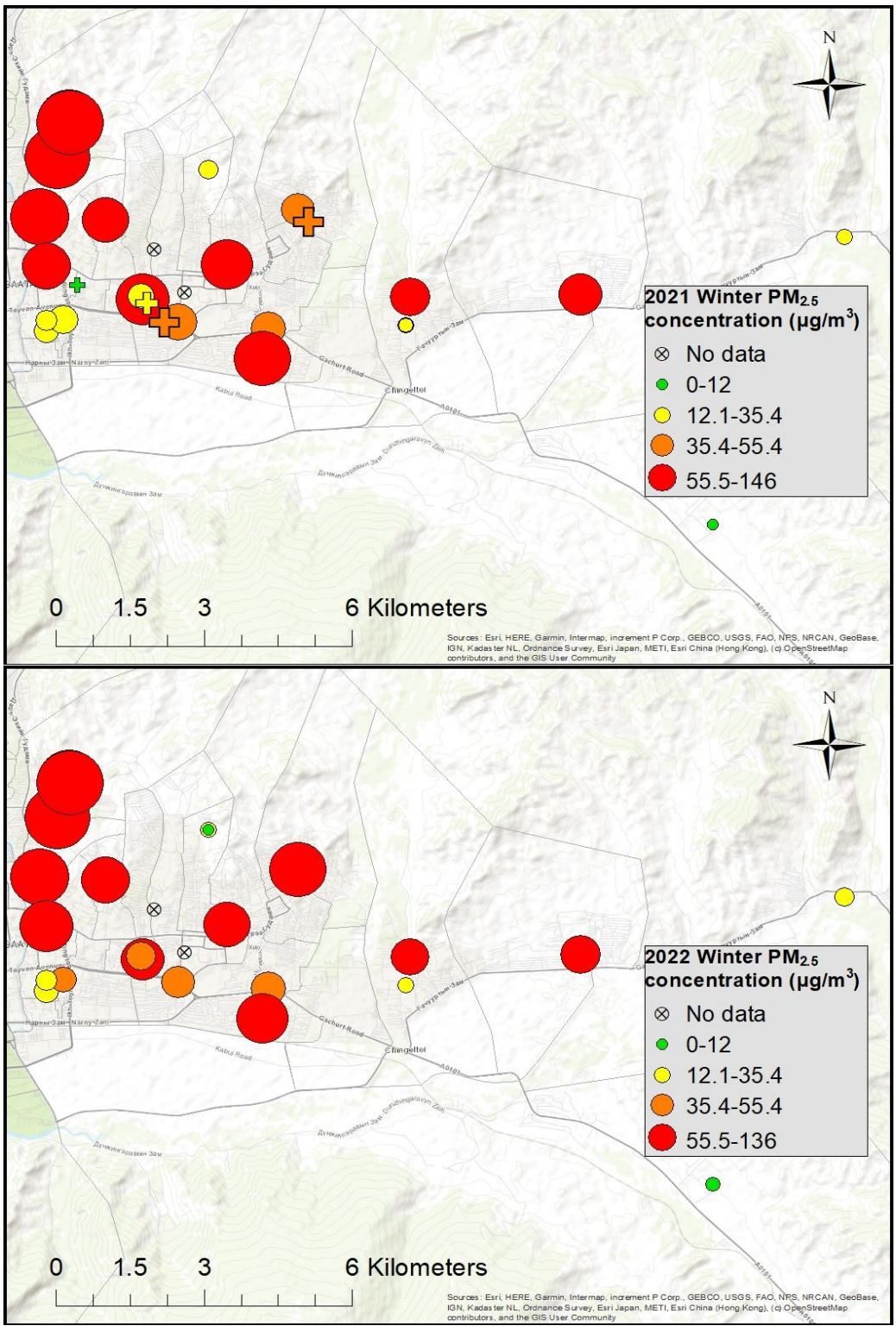

Figure 4.2 Bayanzurkh district (Ulaanbaatar) indoor winter average $PM_{2.5}$ (Nov 2020~Feb 2021 and Nov 2021~Feb 2022)

4.4.2 Land use regression model

The final land use regression (LUR) model for winter 2021 was constructed using forward stepwise selection with the dependent variable (Y) as the winter averaged $PM_{2.5}$ indoor concentration measurements from indoor AirVisual Pro sensors. After selecting the independent variables, the remaining variables are the manual ger counts within a 1000 m buffer, the total distance of road within a 300 m buffer, and inverse of each kindergarten's distance from the nearest mid-sized heat-only boilers.

Table 4.1 shows the detailed coefficients for the model, with the standard error, t-value, p-value (Pr(>|t|)), and variance inflation factor (VIF). The winter 2021 LUR model shows that all remaining coefficients are statistically significant, based on their p-values, and all VIF values are smaller than 5, which shows there is no multicollinearity within the independent variables.

Table 4.1 Winter 2021 LUR, detailed information about independent variables

Independent variables	Name code	Estimate	Std. Error	t value	P value	VIF
Intercept	-	-3.09e+1	2.30e+1	-1.34	0.19	-
Ger counts	Ger1000	3.69e-2	1.11e-2	3.33	<<0.05	1.41
Total distance of road within 300m	Roads300	8.58e-3	3.87e-3	2.22	0.04	1.02
Proximity to HOB	NEAR_HOB	1.19e+3	5.97e+2	1.99	0.06	1.42

Due to COVID restrictions, winter 2021 $PM_{2.5}$ measurements do not reflect activities inside the kindergartens. In contrast, the winter 2022 $PM_{2.5}$ measurements were collected after COVID restrictions were lifted, and they reflect normal kindergarten operations.

The LUR model for winter 2022 was also constructed using forward stepwise selection. Its five independent variables include the manual ger counts within a 900 m buffer, the total road length within a 300 m buffer, the number of medium sized HOBs within a 600 m buffer, the kindergarten's heating method (boiler), and its proximity to the nearest traffic signal or crossing. All predictors are statistically significant based on their p values much small than 0.05 except the inverse distance to the nearest traffic signal or crossing with a p value of 0.058. **Table 4.2** shows the detailed LUR model results, including coefficient values for the winter 2022 model.

Table 4.2 Winter 2022 LUR, detailed information about independent variables

Independent variables	Name code	Estimate	Std. Error	t value	P value	VIF
Intercept	-	-1.22e+1	1.55e+1	-0.79	0.44	-
Ger counts	Ger900	3.61e-2	6.62e-3	5.44	<<0.05	1.16
Total distance of roads within 300m	Roads300	8.86e-3	2.36e-3	3.75	<<0.05	1.09
Medium size HOB counts with 600m	MediumHOB600	7.59	2.56	2.97	<<0.05	1.31
Categorical variable Boiler	boiler	-2.71e+1	8.23	-3.29	<<0.05	1.45
Proximity to the nearest traffic signal	NEAR_traffic_signal_or crossing	-1.11e+3	5.43e+2	-2.05	0.058	1.32

4.4.3 Model performance evaluation and model validation

Each model's performance was evaluated based on statistical metrics that had been previously implemented in other studies for LUR modeling, as discussed in the Introduction. Because of the relatively small dataset, the model validation used leave-one-out-cross-validation (LOOCV). Statistical metrics for performance evaluation included the determination coefficient (R^2), residual standard error (RSE), adjusted R^2, and mean absolute error (MAE). **Table 4.3** gives detailed information about both full model's performances and the LOOCV validation performance. The performance metrics for both LUR models yielded 0.88 and 0.95 as the adjusted R2 values for winter 2021 and 2022 respectively. The winter 2021 validation shows the model is sensitive to the cross validation, based on the lower R^2 value from LOOCV. The winter 2022 LUR model is comparably more robust, based on the LOOCV results. Both models have p-values that are much smaller than 0.05 indicating they are both significant.

Table 4.3 Detailed information for the LUR models and the LOOCV procedure

Winter-based LUR	**LUR Model**				**LOOCV**		
	RSE	R2	Adjusted R2	P-Value	R2	RMSE	MAE
Winter 2021	25.82	0.66	0.60	<<0.05	0.51	27.87	19.42
Winter 2022	14.79	0.84	0.79	<<0.05	0.72	16.76	12.19

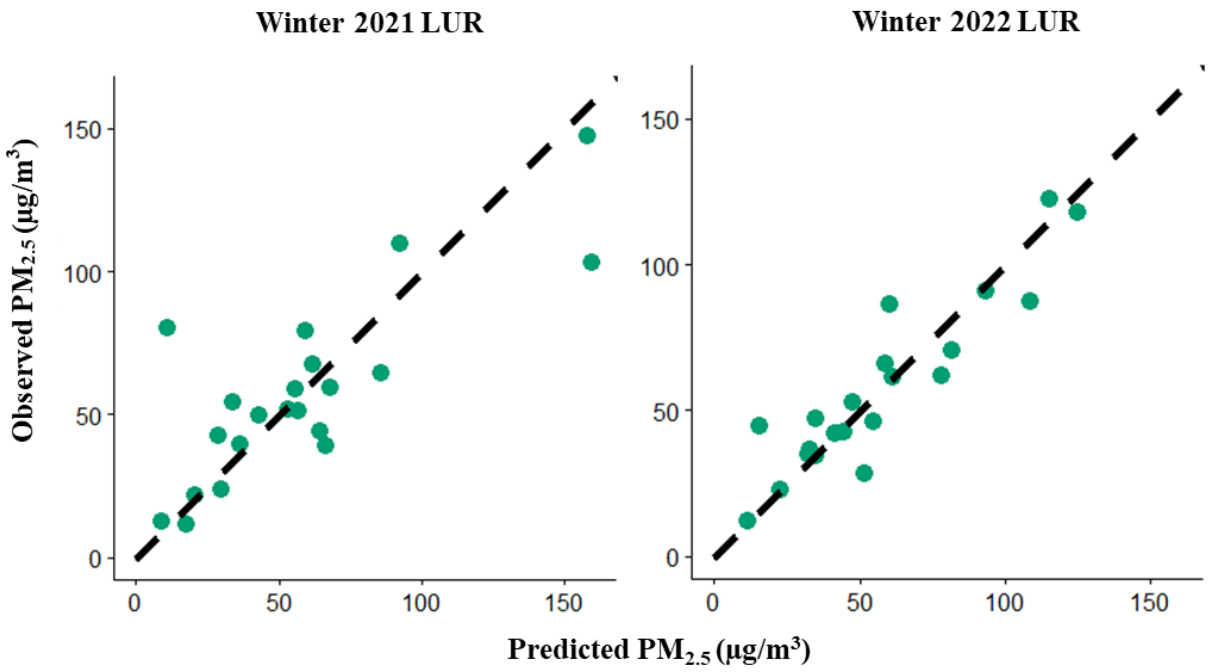

Figure 4.3 Scattergram of indoor $PM_{2.5}$ predictions versus observations using LUR for winter 2021 and winter 2022 $PM_{2.5}$ averaged data.

Figure 4.3 shows observed and predicted values of the LUR models for winter 2021 and winter 2022. Both winter models have similar scattering along the 1:1 line, and, compared to winter 2022, winter 2021 had higher indoor $PM_{2.5}$ concentrations for the extreme values.

4.5 Discussion

The findings of this study underscore the unusual challenges posed by air pollution in Ulaanbaatar, Mongolia, where winter $PM_{2.5}$ concentrations are significantly elevated due to traditional heating practices, predominantly coal combustion in the ger areas. The extreme cold exacerbates the issue by trapping fine particulate matter within the city's shallow mixing layer, prolonging exposure to high $PM_{2.5}$ concentrations, especially in residential areas, where most particles are emitted.

Our study utilized low-cost sensor (LCS) networks to characterize $PM_{2.5}$ concentrations both indoors and outdoors, providing insights into spatial and temporal variations at hyperlocal scales. Additionally, we employed land use regression (LUR) models to predict indoor $PM_{2.5}$ concentrations, particularly in areas where indoor levels are primarily influenced by outdoor infiltrations and air exchange.

A notable aspect of our research is the differences between winters 2021 and 2022, which were caused by COVID-19 restrictions. These restrictions led to changes in building operation, resulting in two distinct LUR models. Based on its model performance and LOOCV method results, the winter 2021 model is more sensitive, reflecting the reduced traffic and other activity changes during the COVID lockdown. Despite this sensitivity, the 2021 model is not suitable for predicting indoor $PM_{2.5}$ level in normal times.

On the other hand, the winter 2022 LUR model is a valuable tool for qualitatively assessing children's exposure to indoor $PM_{2.5}$ in Ulaanbaatar during future winter months. By identifying locations with immediate needs for improved indoor air quality, our research can contribute to providing a healthier environment for future generations.

In conclusion, this study sheds light on the intricate dynamics of air pollution in Ulaanbaatar, emphasizing the need for targeted interventions to mitigate its adverse effects on public health. Moving forward, continued monitoring and assessment efforts are essential for devising effective strategies to improve air quality and safeguard the well-being of the population.

4.6 References

[1] Y.-F. Xing, Y.-H. Xu, M.-H. Shi, and Y.-X. Lian, “The impact of PM2.5 on the human respiratory system,” Journal of Thoracic Disease, vol. 8, no. 1, 2016.

[2] A. Bhatnagar, “Environmental Determinants of Cardiovascular Disease,” Circ Res, vol. 121, no. 2, pp. 162–180, Jul. 2017, doi: 10.1161/CIRCRESAHA.117.306458.

[3] P. James, R. F. Banay, J. E. Hart, and F. Laden, “A Review of the Health Benefits of Greenness,” Curr Epidemiol Rep, vol. 2, no. 2, pp. 131–142, Jun. 2015, doi: 10.1007/s40471-015-0043-7.

[4] P. Dadvand et al., “Green spaces and General Health: Roles of mental health status, social support, and physical activity,” Environment International, vol. 91, pp. 161–167, May 2016, doi: 10.1016/j.envint.2016.02.029.

[5] S. Vedal, “Ambient Particles and Health: Lines that Divide,” Journal of the Air & Waste Management Association, vol. 47, no. 5, pp. 551–581, May 1997, doi: 10.1080/10473289.1997.10463922.

[6] X. H. H. Huang, Q. Bian, W. M. Ng, Peter. K. K. Louie, and J. Z. Yu, “Characterization of PM2.5 Major Components and Source Investigation in Suburban Hong Kong: A One Year Monitoring Study,” Aerosol Air Qual. Res., vol. 14, no. 1, pp. 237–250, 2014, doi: 10.4209/aaqr.2013.01.0020.

[7] J. M. Samet and S. L. Zeger, “Fine Particulate Air Pollution and Mortality in 20 U.S. Cities, 1987–1994,” The New England Journal of Medicine, 2000.

[8] N. Künzli et al., “Ambient Air Pollution and Atherosclerosis in Los Angeles,” Environ Health Perspect, vol. 113, no. 2, pp. 201–206, Feb. 2005, doi: 10.1289/ehp.7523.

[9] T. D. Nelin, A. M. Joseph, M. W. Gorr, and L. E. Wold, “Direct and indirect effects of particulate matter on the cardiovascular system,” Toxicology Letters, vol. 208, no. 3, pp. 293–299, Feb. 2012, doi: 10.1016/j.toxlet.2011.11.008.

[10] World Bank, “Mongolia : Heating Stove Market Trends in Poor, Peri-Urban Ger Areas of Ulaanbaatar and Selected Markets Outside Ulaanbaatar,” 87052, Feb. 2013. [Online]. Available: http://hdl.handle.net/10986/18700 License: CC BY 3.0 IGO.

[11] “Air pollution in Mongolia,” Bull. World Health Organ., vol. 97, no. 2, pp. 79–80, Feb. 2019, doi: 10.2471/BLT.19.020219.

[12] P. Barn et al., “The effect of portable HEPA filter air cleaner use during pregnancy on fetal growth: The UGAAR randomized controlled trial,” Environment International, vol. 121, pp. 981–989, Dec. 2018, doi: 10.1016/j.envint.2018.08.036.

[13] L. D. Hill et al., “Health assessment of future PM2.5 exposures from indoor, outdoor, and secondhand tobacco smoke concentrations under alternative policy pathways in Ulaanbaatar, Mongolia,” PLoS ONE, vol. 12, no. 10, p. e0186834, Oct. 2017, doi: 10.1371/journal.pone.0186834.

[14] S. Künn, J. Palacios, and N. Pestel, “Indoor Air Quality and Strategic Decision Making,” Management Science, vol. 69, no. 9, pp. 5354–5377, Sep. 2023, doi: 10.1287/mnsc.2022.4643.

[15] S. Lung, I. Mao, and L. Liu, “Residents’ particle exposures in six different communities in Taiwan,” Science of The Total Environment, vol. 377, no. 1, pp. 81–92, May 2007, doi: 10.1016/j.scitotenv.2007.01.092.

[16] Z. Li, Q. Wen, and R. Zhang, “Sources, health effects and control strategies of indoor fine particulate matter (PM2.5): A review,” Science of The Total Environment, vol. 586, pp. 610–622, May 2017, doi: 10.1016/j.scitotenv.2017.02.029.

[17] W. Yuchi et al., “A description of methods for deriving air pollution land use regression model predictor variables from remote sensing data in Ulaanbaatar, Mongolia: Derivation of land use regression model predictor variables,” The Canadian Geographer / Le Géographe canadien, vol. 60, no. 3, pp. 333–345, Sep. 2016, doi: 10.1111/cag.12279.

[18] P.-Y. Wong et al., “An alternative approach for estimating large-area indoor PM2.5 concentration – A case study of schools,” Building and Environment, vol. 219, p. 109249, Jul. 2022, doi: 10.1016/j.buildenv.2022.109249.

[19] C. E. Flowerday, P. Lundrigan, C. Kitras, T. Nguyen, and J. C. Hansen, “Utilizing Low-Cost Sensors to Monitor Indoor Air Quality in Mongolian Gers,” Sensors, vol. 23, no. 18, p. 7721, Sep. 2023, doi: 10.3390/s23187721.

[20] A. Yang et al., “Agreement of central site measurements and land use regression modeled oxidative potential of PM2.5 with personal exposure,” Environmental Research, vol. 140, pp. 397–404, Jul. 2015, doi: 10.1016/j.envres.2015.04.015.

[21] D. Gao et al., “Assessment of children’s personal and land use regression model-estimated exposure to NO2 in Springfield, Massachusetts,” Science of The Total Environment, vol. 892, p. 164681, Sep. 2023, doi: 10.1016/j.scitotenv.2023.164681.

[22] O. Enkhjargal, M. Lamchin, J. Chambers, and X.-Y. You, “Linear and Nonlinear Land Use Regression Approach for Modelling PM2.5 Concentration in Ulaanbaatar, Mongolia during Peak Hours,” Remote Sensing, vol. 15, no. 5, p. 1174, Feb. 2023, doi: 10.3390/rs15051174.

[23] D. J. Briggs et al., “Mapping urban air pollution using GIS: a regression-based approach,” International Journal of Geographical Information Science, vol. 11, no. 7, pp. 699–718, Oct. 1997, doi: 10.1080/136588197242158.

[24] B. Feenstra et al., “Performance evaluation of twelve low-cost PM2.5 sensors at an ambient air monitoring site,” Atmospheric Environment, vol. 216, p. 116946, Nov. 2019, doi: 10.1016/j.atmosenv.2019.116946.

[25] K. K. Barkjohn, B. Gantt, and A. L. Clements, “Development and application of a United States-wide correction for PM_{2.5} data collected with the PurpleAir sensor,” Atmos. Meas. Tech., vol. 14, no. 6, pp. 4617–4637, Jun. 2021, doi: 10.5194/amt-14-4617-2021.

[26] R. E. Connolly et al., “Long-term evaluation of a low-cost air sensor network for monitoring indoor and outdoor air quality at the community scale,” Science of The Total Environment, vol. 807, p. 150797, Feb. 2022, doi: 10.1016/j.scitotenv.2021.150797.

[27] L. Wallace and W. Ott, “Long-Term Indoor-Outdoor PM2.5 Measurements Using PurpleAir Sensors: An Improved Method of Calculating Indoor-Generated and Outdoor-Infiltrated Contributions to Potential Indoor Exposure,” Sensors, vol. 23, no. 3, p. 1160, Jan. 2023, doi: 10.3390/s23031160.

[28] Y. Kang, L. Aye, T. D. Ngo, and J. Zhou, “Performance evaluation of low-cost air quality sensors: A review,” Science of The Total Environment, vol. 818, p. 151769, Apr. 2022, doi: 10.1016/j.scitotenv.2021.151769.

Chapter 5: The effects of vegetation planted along highway noise wall barriers on downwind ultrafine particle concentrations

This work was funded by the Green Heart Louisville project (NIH R01 ES029846-01) and the University of Louisville Superfund Research Center (NIH 2P42ES023716). Field measurements were supported by Maryssa Loehr, Tyler Cargill, Yan He and Xuan Liu (Washington University in St. Louis).

5.1 Abstract

Computational fluid dynamics modeling suggests vegetation barriers–alone or in tandem with noise barriers–can reduce ultrafine particle (UFP) concentrations downwind of major roadways. Prior measurement studies provide limited evidence for UFP reductions, and more studies are needed to establish a firmer scientific basis for the design and implementation of engineered vegetation barriers. To examine the relationship between urban vegetation and cardiovascular health, the *Green Heart Louisville* project planted an extensive green belt in a Louisville, KY, neighborhood. Vegetation barrier were installed adjacent to both sides of concrete noise barriers lining a limited access highway bisecting the study area. After about six month, a series of multi-day field campaigns measured ultrafine particle (UFP) number concentrations in the study area, establishing a baseline value for the neighborhood's exposure. Over each multi-day period, typically three vehicles equipped with mixing condensation particle counters (MCPC, a vibration-stabilized version of the Brechtel Model 1720) were used to conduct short-term stationary monitoring on roads just outside the vegetation barriers/noise wall. We operationally

defined the UFP concentration as the total particle number concentration measured by the MCPC. During one period, 3-D wind measurements characterized the airflow recirculation zone on the downwind side of the noise barrier, and the UFP vertical profile was measured 3 meters downwind of the noise barrier. Notably, UFP concentrations immediately above the noise wall were comparable to concentrations near the ground level in the recirculation zone, demonstrating that downwind measurements, even in the relatively static recirculation zone, could effectively characterize the vegetative barrier impacts. Some stretches of the noise walls had no plantings, and under crosswind conditions, there was an average of 10% less UFP immediately downwind of a vegetation barrier/noise wall combination compared to an adjacent unplanted section. However, due to the complexity of the built-up environment, this difference was not statistically significant. As the vegetative buffer grows, we will periodically repeat these measurements to assess its impacts on downwind UFP levels.

5.2 Introduction

Urban air pollution, exacerbated by highway traffic-related emissions, has been identified as a concern in numerous studies[1], [2], [3], [4], [5]. Exposure to toxic and potentially carcinogenic compounds, particularly ultrafine particles (UFP), poses a growing risk in urban areas, where a much of the population spends considerable time immersed in this microenvironment. The increase in cardiovascular disease cases linked to traffic emissions underscores the pressing need for effective mitigation strategies [3].

One promising approach to mitigating air pollution in heavily trafficked urban areas involves increasing urban green spaces [6]. This strategy enhances particle deposition on leaves, reducing

airborne particle concentrations [7]. However, whether roadside vegetative barriers significantly attenuate pollution remains a topic of debate, with conflicting evidence [8], [9], [10], [11].

Moreover, the health benefits of green infrastructure extend beyond pollution attenuation. Reported positive outcomes include reduced stress, reduced psychiatric morbidity, and a decrease in cardiovascular disease (CVD) rates, ultimately contributing to lower all-cause mortality [12].

The combination of constructed noise barriers and engineered vegetation buffers offers a focal point for assessing near-road air pollution. Research has extensively investigated the influence of solid noise barriers on air quality in proximity to roadways using dispersion modeling[13], [14], [15]. However, these studies exhibit variations in their focus: some exclusively consider solid barriers[13], [16], [17], [18], [19], [20], [21], while others examine combinations of vegetation and solid barriers[10], [22]. Furthermore, fieldwork assessments differ depending on the local layout of barriers, with some studies evaluating only solid barriers[13], [23], others focusing solely on vegetation barriers[11], [24], and still others examining solid barriers with a sparse layer of vegetation[25], [26], [27], [28], [29]. Nevertheless, there is a scarcity of studies that closely resemble our scenarios, which involve engineered vegetation interspersed between the highway and solid noise barriers, within similar local environments. The lack of well-structured longitudinal studies further limits our understanding of the long-term growth of vegetation within these built environments.

This study aims to bridge these gaps by providing a comprehensive examination of the combination effects of built-in noise walls and engineered vegetation buffers on near-road air pollution. Through rigorous fieldwork assessments and a longitudinal approach, we seek to

enhance our understanding of the dynamic interplay between urban infrastructure, vegetation, and air quality, contributing valuable insights to the development of sustainable and effective urban planning strategies.

5.3 Material and Methods

5.3.1 Study layout

To optimize particle attenuation, the engineered vegetation barrier was strategically positioned along the interstate highway, forming a green barrier between the highway traffic and the pre-existing noise wall. This particular stretch of I-264 is a 6-lane highway carrying an average daily traffic of approximately 96,600 vehicles in 2020 (Kentucky Department of Transportation https://maps.kytc.ky.gov/trafficcounts/). Notably, 15-foot-high noise walls had been previously installed on both sides of the highway.

Figure 5.1 is an annotated aerial photograph of the buffer sections along the highway, along with the designated unplanted location for conducting Buffer and NoBuffer comparisons. Unlike most near-road studies of UFP, which typically occur in well-controlled suburban settings featuring open land adjacent to the highway, our investigation took place within a built-up residential environment characterized by more complex topography.

Within the study area, the primary locations for collecting stationary samples are two local parallel roads on the residential side of the barrier walls, which allowed collecting samples downwind of the highway in either direction. The central study zone, an approximate area of 400m by 800m, contains around 300 mostly single-family residences. Compared to previous near-road UFP studies, this setting introduces the additional dynamic complexities of a residential environment and varied elevations.

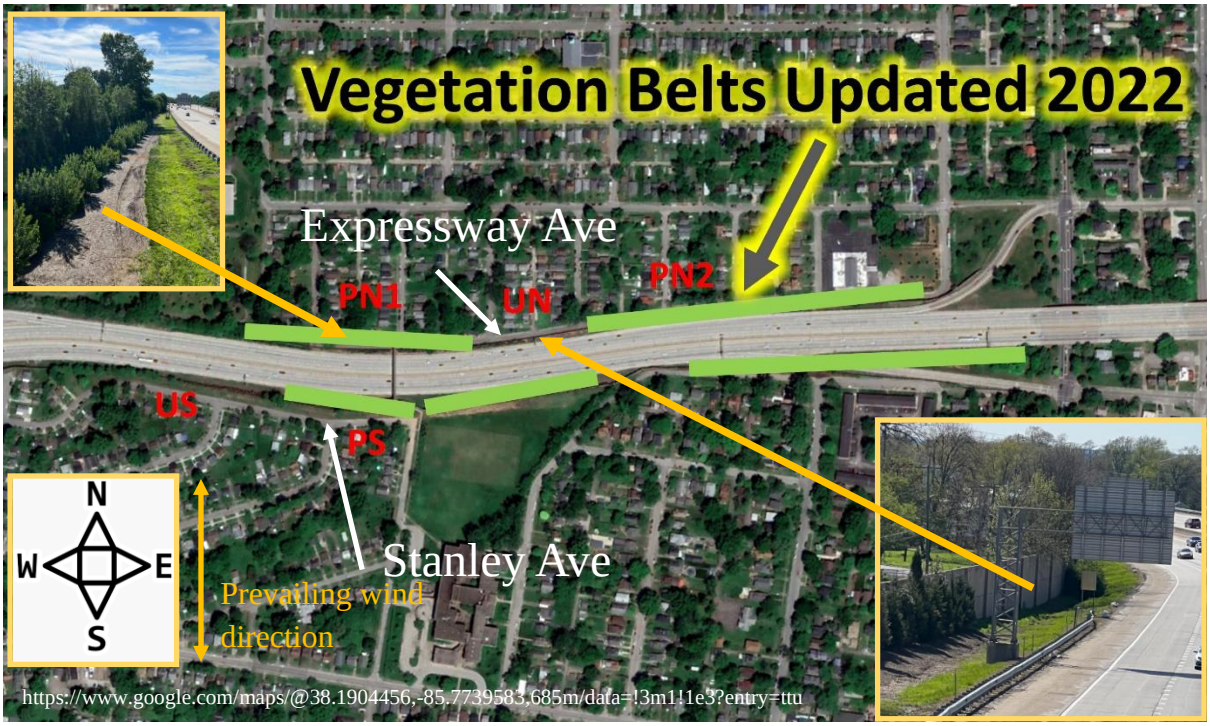

Figure 5.1 Planted vegetation barriers along the Waterson expressway, with the north buffer next to Expressway Ave (PN1,UN,PN2) and the south buffer next to Stanley Ave (US,PS). P= planted, U=unplanted, N = north, S=south. Satellite image obtained from Google Earth.

Stationary measurements were carried out on local roadways and alleyways on both the northern and southern sides of I-264, a six-lane highway. The primary measurement locations, on Expressway Ave and Stanley Ave, are labeled with red letters in **Figure 5.1**. Throughout the sampling periods, two, or at times three, parked instrumented vehicles and initiated sample collection simultaneously. The sampling runs were timed to capture both morning and evening rush hour periods during persistent southerly or northerly winds. By comparing the UFP counts downwind of areas with and without a vegetation barriers, this approach aimed to assess the effects of an engineered vegetative buffer.

5.3.2 Instrumentations

Multi-day field campaigns were conducted from 2021 to 2023 to measure the number concentration of ultrafine particles. Mixing condensation particle counters (MCPCs) with a particle size range of 8-2000 nm (η = 50% at 8 nm) were employed at a high temporal resolution of 1 second. The specific MCPC used in this study was the Brechtel model 1720 (Hayward, California).

To ensure accurate measurements, a sample inlet was installed on the vehicle carrying the MCPC, connecting a 1.0 µm cut cyclone to the downstream MCPC via a 1-meter-long anti-static conductive tubing. Prior to each run, the sample flowrate was verified with a digital flow meter, and the sampling line was tested for air infiltration by placing a high-efficiency particulate air (HEPA) filter at the cyclone inlet and checking for a nearly zero particle count. Up to three instrumented vehicles were utilized, and any variations between individual instrument setups were corrected through collocation data comparisons conducted throughout each sampling campaign. This rigorous approach ensured the reliability and consistency of the collected data.

The wind data utilized in this study were collected from the Automated Surface Observing System (ASOS) monitoring station at Louisville Muhammad Ali International Airport (IATA code, SDF), approximately 3 kilometers east of the study area. Hourly averages of both wind speed and direction served to categorize each 10- to 20-minute stationary run into distinct wind direction sectors. To achieve a more refined local wind resolution, an RM Young model 810003-D anemometer from was employed. This device provided wind data with a 1-second resolution, crucial for analyzing and characterizing the recirculation zone situated downwind of the noise wall.

The vertical profile of the UFP concentration was established using a vertical scissor-type man lift capable of reaching a height of 32 feet, placed adjacent to the noise wall on Expressway Ave. A MCPC instrument was installed atop the lift platform, while a corresponding MCPC was positioned at ground level directly beneath the lift. UFP concentrations downwind of the highway were simultaneously measured by the lift monitor at various heights and the stationary ground-level monitor. The resulting ratio of UFP concentrations is discussed further in the Results section.

5.4 Results

5.4.1 The combined effects of the vegetation barrier and the noise wall on UFP concentration counts, based on stationary measurements

The stationary measurement runs for this baseline study are summarized in Table 1, which lists the maximum and minimum UFP number concentrations for runs within each stationary measurement day. The median UFP counts during a given measurement run, spanning 10 to 20 minutes, surpass 60,000 #/cc. Local meteorological conditions contribute to variations, with concentrations reaching as low as 2,000 #/cc. Upwind UFP concentrations are considered as the background reference, and range from 3,000 to 30,000 #/cc across different measurement days.

The 2021 World Health Organization (WHO) Global Air Quality Guidelines [30] distinguish between low and high (>10,000) particle number concentrations (PNCs), and our stationary measurements during multiple periods consistently indicated levels above 10,000 #/cc near the highway within the residential neighborhood.

A subset of these stationary runs, detailed in **Table 5.1**, focuses on UFP measurements at planted (P) and unplanted (U) zones (see **Figure 5.1**). These measurements form the basis for evaluating the vegetation buffer's effects on UFP concentrations.

Wind direction data from the nearby airport was categorized into two groups, as shown in based on **Figure 5.2**. For winds from the North or South (Group 1), blowing perpendicular to the highway and the barrier wall, the data reveal an approximate 10 percent decrease in UFP mean concentrations for sections of the noise wall with an engineered vegetation buffer area compared to the UFP mean concentrations in zones equipped with only a noise wall. This finding accords with earlier reports on black carbon concentrations downstream of vegetation, which demonstrated a 12% reduction [11].

However, for stationary runs in the subset with group 2 (East or West) wind directions, blowing parallel to the wall and the highway, there is no discernible difference in UFP concentrations between areas with a buffer versus those without.

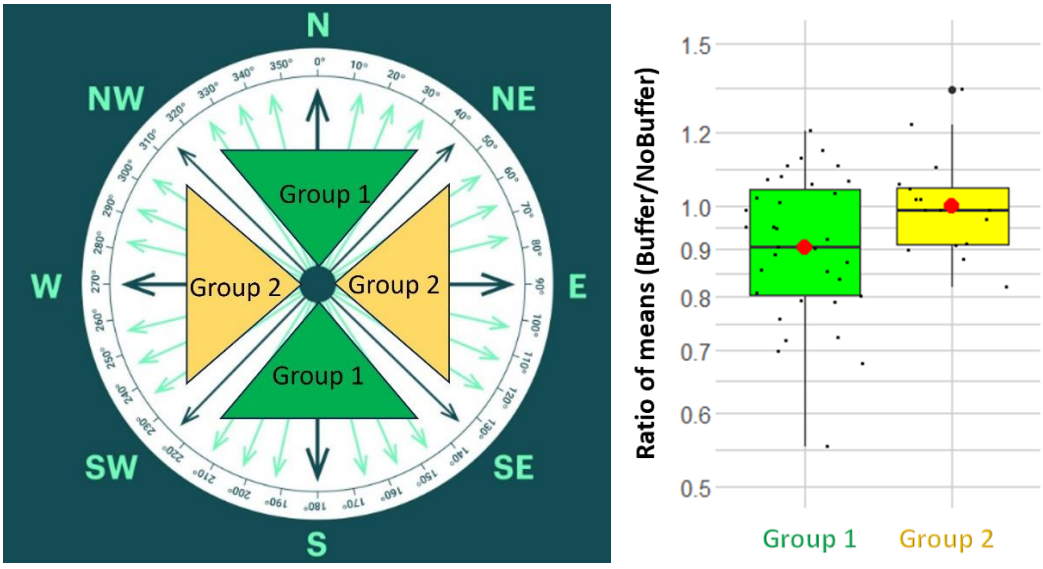

Figure 5.2 UFP stationary data groups based on wind direction (left figure) and box plots for the distribution of run-specific ratios stratified by wind direction relative to the highway.

All stationary measurement series were categorized by wind direction into two groups, illustrated in **Figure 5.2**, with a boxplot depicting the ratio of the means of the UFP concentrations, with and without buffers. Group 1, representing NS winds across the roadway, shows a significant 10

percent reduction in UFP concentration behind buffered zones. Conversely, Group 2, characterized by EW winds (parallel to the roadway), shows no substantial difference in UFP concentrations, regardless of buffering. Since downwind stationary measurements were conducted on both sides of the highway at both buffered and non-buffered locations, **Figure 5.3** separates the measurements made on the south side of the highway from those on the north side. For Group 1 wind directions, both sides demonstrate a consistent 10 percent reduction in UFP concentrations behind buffered areas, whereas Group 2 wind directions showed no notable differences. These findings highlight the impact of wind direction on UFP concentrations and also demonstrate the spatial variability introduced by buffers. **Figures 5.2** and **5.3** visually capture these stratified results: the intricate relationship between wind direction, buffer presence or absence, and UFP concentrations across different locations.

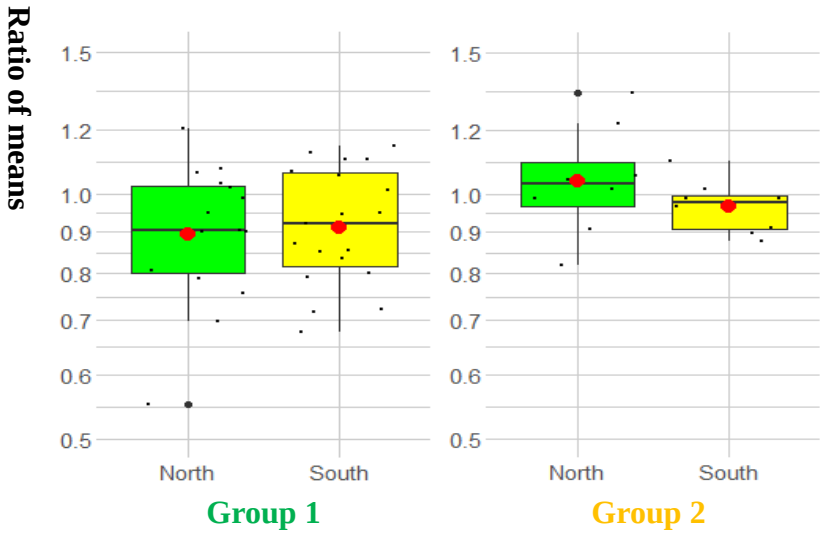

Figure 5.3 Distribution of run-specific Buffer vs. NoBuffer ratios stratified by wind direction relative to the highway and sampling locations on South side and North side of the highway.

Table 5.1 UFP concentrations captured at near noise wall locations for all stationary measurements. The highest medians of each measurement campaign day are in bold, the lowest are in bold italic and, with upwind measurement as the reference for the background UFP concentrations.

Measurement ID	Date	Time of Day	Number of Runs	Max Stationary Series Median(#/cc)	Min Stationary Series Median(#/cc)	Upwind of Highway Median (#/cc)
1	3/29/2021	Morning & Evening	4	35,231	15,116	-
2	3/30/2021	Morning & Evening	3	50,697	8,053	-
3	3/31/2021	Morning & Evening	4	11,287	7,557	-
4	4/1/2021	Morning & Evening	4	23,686	13,446	-
5	4/2/2021	Morning	3	60,970	26,818	-
6	6/1/2021	Morning & Evening	3	22,065	9,098	-
7	6/3/2021	Morning & Evening	3	18,850	17,703	6,929
8	6/4/2021	Morning & Evening	5	26,083	11,487	-
9	10/12/2021	Morning & Evening	7	21,418	8,160	4,052
10	10/13/2021	Morning & Evening	8	13,858	10,016	4,566
11	10/14/2021	Morning & Evening	6	**61,868**	26,952	14,255
12	10/15/2021	Morning	2	17,351	16,219	4,803
13	4/19/2022	Morning & Evening	6	16,662	10,482	-
14	4/20/2022	Morning & Evening	8	60,744	19,139	15,276
15	4/21/2022	Evening	5	17,504	9,343	3,230
16	4/22/2022	Morning	3	49,413	37,716	29,455
17	8/9/2022	Morning & Evening	5	18,727	5,330	-
18	8/10/2022	Morning	4	8,224	***2,320***	-
19	8/11/2022	Morning	4	16,133	6,046	-
20	8/12/2022	Morning & Evening	9	18,657	12,882	-
21	8/15/2022	Morning & Evening	8	15,634	7,099	-
22	8/16/2022	Morning & Evening	6	15,641	14,131	-
23	8/17/2022	Morning & Evening	6	16,828	10,680	-
24	8/18/2022	Morning & Evening	8	20,383	11,029	-

5.4.2 Special Study 1: Downwind vertical UFP profile, with buffer and noise wall

This special study assessed the vertical UFP profile behind the noise wall, using a lift equipped with MCPC and 2D wind sensors, positioned in conjunction with ground level UFP measurements. As shown in Figure 6, the UFP concentrations increase with height and then decrease when the lift reaches the height of the noise wall. Fluid dynamics suggest that solid noise barriers have the potential to induce the formation of a recirculation zone downstream of the barrier, leading to the establishment of a mixing zone. This phenomenon may contribute to the observed increase in ultrafine particle (UFP) concentrations at lift heights ranging from 10 to 15 feet, as illustrated in **Figure 5.4**. [9].

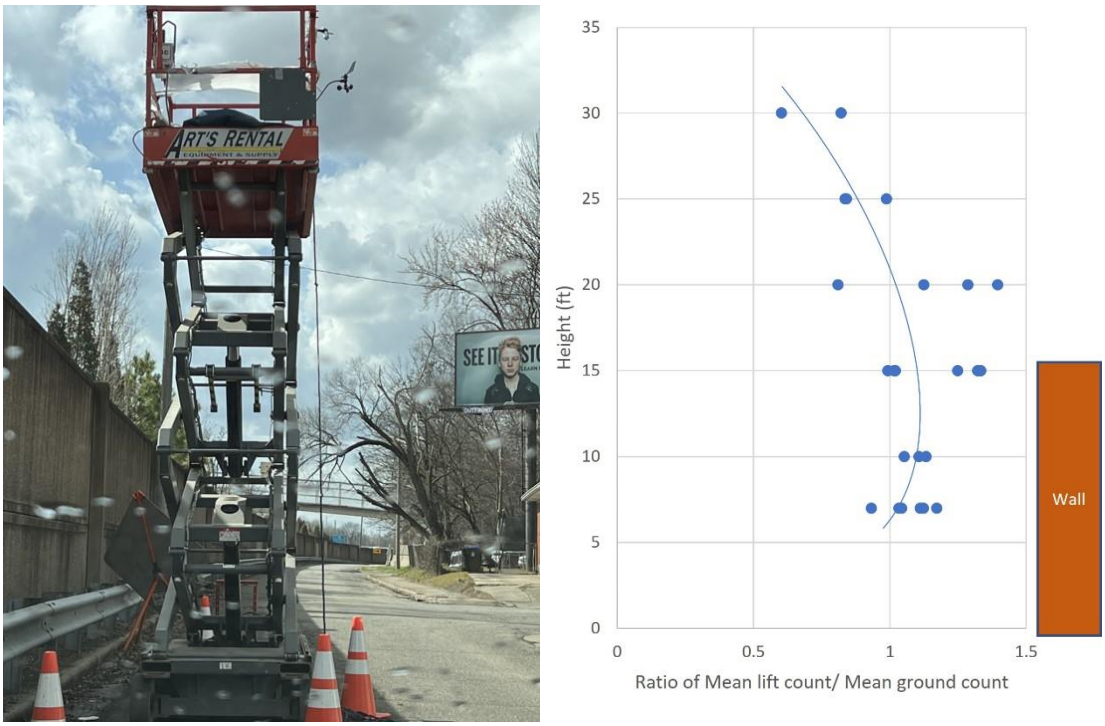

Figure 5.4 Vertical profile measurement setup, with ratios of the lift and ground level UFP concentration mean values versus height. Blue curve shows power law curve fit.

5.4.3 Special Study 2: Recirculation zone characterization

Our stationary measurements were performed adjacent to the highway behind a noise wall, potentially situated within the recirculation zone that created by the wind when downwind of a noise wall, which varies with the wind speed. In order to better characterize the size of this zone, we used a 3D sonic anemometer to analyze variations in the vertical wind component at varying distances from the noise wall. The outcomes for a specific measurement period are depicted in **Figure 5.5**.

The 3D anemometer displays the vertical wind direction, as presented on the secondary Y-axis in **Figure 5.5**. A positive wind angle (indicating wind from below) was observed when the sensor was positioned 5 feet away from the noise wall. After the sensor had been moved to 25 feet from the noise wall, the wind angle had reversed to negative values (indicating wind from above). This vertical wind component was maintained until the sensor reached 45 feet away from the wall and further, where the wind angle stabilized at 0 degrees. This pattern suggests that the recirculation zone for this particular wind direction lies within the 0 to 25 foot range.

Our stationary measurements in the main study were conducted at 20 feet from the noise wall, placing them within the recirculation zone. The effect of the recirculation zone introduces uncertainties into our Buffer to NoBuffer comparisons. However, upon comparing our vertical profile measurements with the ground level measurements, although a substantial majority of our measurements were made within the recirculation zone, the UFP concentrations right above the noise wall are strongly correlated with ground level concentrations. This finding instills confidence in our ability to compare the directional aspects of our measurements with those from the stationary measurement series reported in the main body of this study.

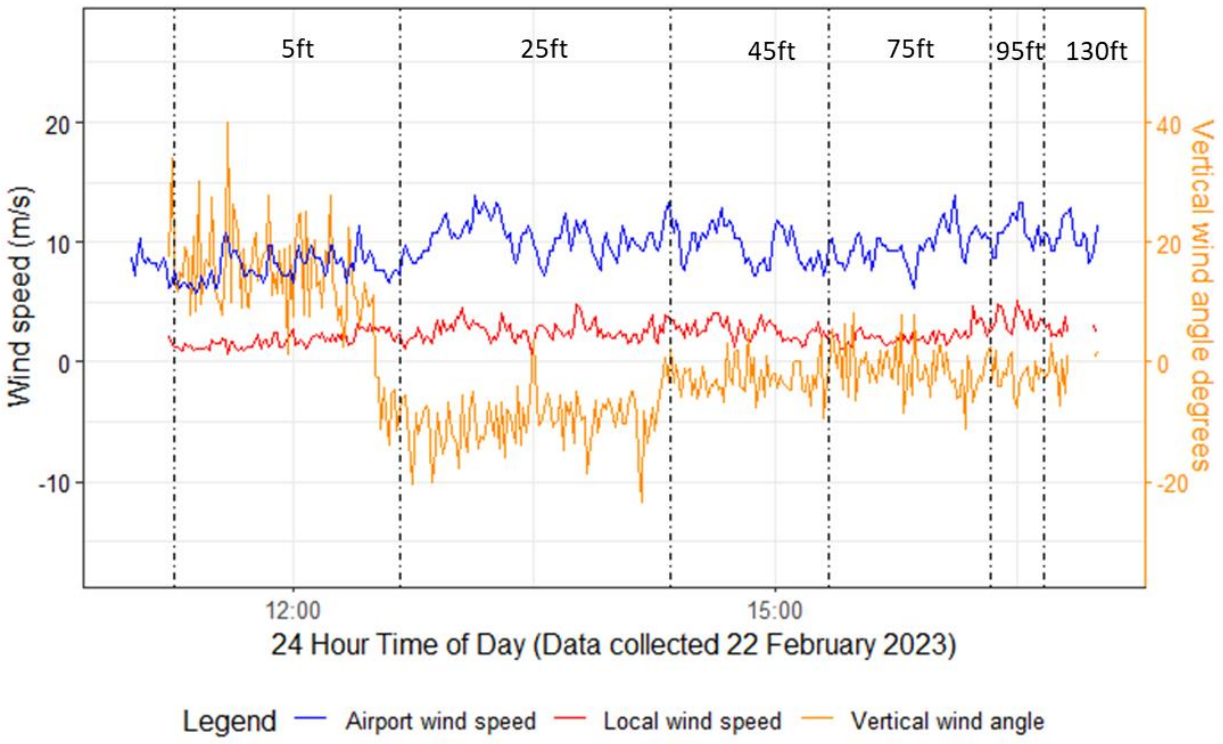

Figure 5.5 Time series for wind speed and angles at various distances from noise wall. Left Y-axis gives wind speeds, and right Y-axis shows vertical wind angle from 3D anemometer.

5.5 Discussion and conclusions

The near-road measurement results in this manuscript highlight the UFP concentrations within a built residential environment downwind of a major highway with a sound barrier and an extensive, but not complete, vegetation buffer. This work helps to assess the impact of vegetation barriers on the UFP exposure of the nearby residents and complements a chronic health study, conducted by the University of Louisville, linking urban greenness and cardiovascular disease. This work also considers the additional factor of a near-road solid noise wall adjacent to the vegetation barriers. Preliminary stationary measurements suggest up to an ~10 % reduction in UFP immediately behind the noise wall and buffer, compared to a noise wall only.

The air recirculation zone behind the noise wall (on the residential side) was assessed using a 3D sonic anemometer, validating that our stationary measurements fell within this zone. Nevertheless, UFP measurements at ground level and above the noise wall indicated that UFP concentrations in the recirculation zone on the residential side continued to reflect the impact of highway UFP concentrations. In future work, dispersion modeling can assess UFP levels downwind of the noise wall, and a steady-state Gaussian model will help understand the environment better.

As expected, our measurements found a strong UFP gradient away from the highway for crosswinds and relatively homogeneous UFP concentrations for winds nominally parallel to the roadway. Although the combination of a noise wall and adjacent vegetation barriers did not dramatically alter the gradients, as the buffer strip trees continue to grow and fill out, longitudinal measurements may find a greater impact.

5.6 Acknowledgements

This project was supported by the Green Heart Louisville project (NIH R01ES029846-01). Mr. Rick Strehl (University of Louisville) and Dr. Pradeep Prathibha (formerly of Washington University in St. Louis) designed the initial versions of the measurement platforms. Mr. Tyler Cargill, Ms. Xuan Liu, and Ms. Yan He (Washington University in St. Louis) assisted with the field measurements.

5.7 References

[1] L. Zhu, D. Ranasinghe, M. Chamecki, M. J. Brown, and S. E. Paulson, “Clean air in cities: Impact of the layout of buildings in urban areas on pedestrian exposure to ultrafine particles from traffic,” Atmospheric Environment, vol. 252, p. 118267, May 2021, doi: 10.1016/j.atmosenv.2021.118267.

[2] S. Ohlwein, R. Kappeler, M. Kutlar Joss, N. Künzli, and B. Hoffmann, “Health effects of ultrafine particles: a systematic literature review update of epidemiological evidence,” Int J Public Health, vol. 64, no. 4, pp. 547–559, May 2019, doi: 10.1007/s00038-019-01202-7.

[3] G. Oberdörster, E. Oberdörster, and J. Oberdörster, “Nanotoxicology: An Emerging Discipline Evolving from Studies of Ultrafine Particles,” Environ Health Perspect, vol. 113, no. 7, pp. 823–839, Jul. 2005, doi: 10.1289/ehp.7339.

[4] D. Brugge, J. L. Durant, and C. Rioux, “Near-highway pollutants in motor vehicle exhaust: A review of epidemiologic evidence of cardiac and pulmonary health risks,” Environ Health, vol. 6, no. 1, p. 23, Dec. 2007, doi: 10.1186/1476-069X-6-23.

[5] “Ultrafine particles (UFP) and health effects. Dangerous. Like no other PM? Review and analysis,” Global NEST Journal, vol. 10, no. 3, pp. 439–452, Apr. 2013, doi: 10.30955/gnj.000579.

[6] V. Viippola, V. Yli-Pelkonen, L. Järvi, M. Kulmala, and H. Setälä, “Effects of forests on particle number concentrations in near-road environments across three geographic regions,” Environmental Pollution, vol. 266, p. 115294, Nov. 2020, doi: 10.1016/j.envpol.2020.115294.

[7] K. Van Ryswyk, N. Prince, M. Ahmed, E. Brisson, J. D. Miller, and P. J. Villeneuve, “Does urban vegetation reduce temperature and air pollution concentrations? Findings from an environmental monitoring study of the Central Experimental Farm in Ottawa, Canada,” Atmospheric Environment, vol. 218, p. 116886, Dec. 2019, doi: 10.1016/j.atmosenv.2019.116886.

[8] G. E. Bowker, R. Baldauf, V. Isakov, A. Khlystov, and W. Petersen, “The effects of roadside structures on the transport and dispersion of ultrafine particles from highways,” Atmospheric Environment, vol. 41, no. 37, pp. 8128–8139, Dec. 2007, doi: 10.1016/j.atmosenv.2007.06.064.

[9] M. Ghasemian, S. Amini, and M. Princevac, “The influence of roadside solid and vegetation barriers on near-road air quality,” Atmospheric Environment, vol. 170, pp. 108–117, Dec. 2017, doi: 10.1016/j.atmosenv.2017.09.028.

[10] Z. Tong, R. W. Baldauf, V. Isakov, P. Deshmukh, and K. Max Zhang, “Roadside vegetation barrier designs to mitigate near-road air pollution impacts,” Science of The Total Environment, vol. 541, pp. 920–927, Jan. 2016, doi: 10.1016/j.scitotenv.2015.09.067.

[11] H. L. Brantley, G. S. W. Hagler, P. J. Deshmukh, and R. W. Baldauf, “Field assessment of the effects of roadside vegetation on near-road black carbon and particulate matter,” Science

of The Total Environment, vol. 468–469, pp. 120–129, Jan. 2014, doi: 10.1016/j.scitotenv.2013.08.001.

[12] P. James, R. F. Banay, J. E. Hart, and F. Laden, “A Review of the Health Benefits of Greenness,” Curr Epidemiol Rep, vol. 2, no. 2, pp. 131–142, Jun. 2015, doi: 10.1007/s40471-015-0043-7.

[13] A. Venkatram, V. Isakov, P. Deshmukh, and R. Baldauf, “Modeling the impact of solid noise barriers on near road air quality,” Atmospheric Environment, vol. 141, pp. 462–469, Sep. 2016, doi: 10.1016/j.atmosenv.2016.07.005.

[14] Y. J. Wang et al., “Modeling multi-scale aerosol dynamics and micro-environmental air quality near a large highway intersection using the CTAG model,” Science of The Total Environment, vol. 443, pp. 375–386, Jan. 2013, doi: 10.1016/j.scitotenv.2012.10.102.

[15] L. Huang et al., “Aerosol–computational fluid dynamics modeling of ultrafine and black carbon particle emission, dilution, and growth near roadways,” Atmos. Chem. Phys., vol. 14, no. 23, pp. 12631–12648, Dec. 2014, doi: 10.5194/acp-14-12631-2014.

[16] F. Enayati Ahangar, D. Heist, S. Perry, and A. Venkatram, “Reduction of air pollution levels downwind of a road with an upwind noise barrier,” Atmospheric Environment, vol. 155, pp. 1–10, Apr. 2017, doi: 10.1016/j.atmosenv.2017.02.001.

[17] D. K. Heist, S. G. Perry, and L. A. Brixey, “A wind tunnel study of the effect of roadway configurations on the dispersion of traffic-related pollution,” Atmospheric Environment, vol. 43, no. 32, pp. 5101–5111, Oct. 2009, doi: 10.1016/j.atmosenv.2009.06.034.

[18] G. S. W. Hagler, W. Tang, M. J. Freeman, D. K. Heist, S. G. Perry, and A. F. Vette, “Model evaluation of roadside barrier impact on near-road air pollution,” Atmospheric Environment, vol. 45, no. 15, pp. 2522–2530, May 2011, doi: 10.1016/j.atmosenv.2011.02.030.

[19] S. Wang and X. Wang, “Modeling and Analysis of the Effects of Noise Barrier Shape and Inflow Conditions on Highway Automobiles Emission Dispersion,” Fluids, vol. 4, no. 3, p. 151, Aug. 2019, doi: 10.3390/fluids4030151.

[20] J. T. Steffens, D. K. Heist, S. G. Perry, and K. M. Zhang, “Modeling the effects of a solid barrier on pollutant dispersion under various atmospheric stability conditions,” Atmospheric Environment, vol. 69, pp. 76–85, Apr. 2013, doi: 10.1016/j.atmosenv.2012.11.051.

[21] X. Jin, L. Yang, X. Du, and Y. Yang, “Particle transport characteristics in the micro-environment near the roadway,” Building and Environment, vol. 102, pp. 138–158, Jun. 2016, doi: 10.1016/j.buildenv.2016.03.023.

[22] T. E. Morakinyo and Y. F. Lam, “Simulation study of dispersion and removal of particulate matter from traffic by road-side vegetation barrier,” Environ Sci Pollut Res, vol. 23, no. 7, pp. 6709–6722, Apr. 2016, doi: 10.1007/s11356-015-5839-y.

[23] M. N. Tezel-Oguz, M. Marasli, D. Sari, N. Ozkurt, and S. S. Keskin, “Investigation of simultaneous effects of noise barriers on near-road noise and air pollutants,” Science of The Total Environment, vol. 892, p. 164754, Sep. 2023, doi: 10.1016/j.scitotenv.2023.164754.

[24] R. W. Baldauf, V. Isakov, P. Deshmukh, A. Venkatram, B. Yang, and K. M. Zhang, “Influence of solid noise barriers on near-road and on-road air quality,” Atmospheric Environment, vol. 129, pp. 265–276, Mar. 2016, doi: 10.1016/j.atmosenv.2016.01.025.

[25] G. S. W. Hagler et al., “Field investigation of roadside vegetative and structural barrier impact on near-road ultrafine particle concentrations under a variety of wind conditions,” Science of The Total Environment, vol. 419, pp. 7–15, Mar. 2012, doi: 10.1016/j.scitotenv.2011.12.002.

[26] D. Ranasinghe et al., “Effectiveness of vegetation and sound wall-vegetation combination barriers on pollution dispersion from freeways under early morning conditions,” Science of The Total Environment, vol. 658, pp. 1549–1558, Mar. 2019, doi: 10.1016/j.scitotenv.2018.12.159.

[27] E. S. Lee et al., “Field evaluation of vegetation and noise barriers for mitigation of near-freeway air pollution under variable wind conditions,” Atmospheric Environment, vol. 175, pp. 92–99, Feb. 2018, doi: 10.1016/j.atmosenv.2017.11.060.

[28] R. Baldauf et al., “Impacts of noise barriers on near-road air quality,” Atmospheric Environment, vol. 42, no. 32, pp. 7502–7507, Oct. 2008, doi: 10.1016/j.atmosenv.2008.05.051.

[29] R. Baldauf, N. Watkins, D. Heist, C. Bailey, P. Rowley, and R. Shores, “Near-road air quality monitoring: Factors affecting network design and interpretation of data,” Air Qual Atmos Health, vol. 2, no. 1, pp. 1–9, Mar. 2009, doi: 10.1007/s11869-009-0028-0.

[30] World Health Organization, “WHO global air quality guidelines: particulate matter (PM2.5 and PM10), ozone, nitrogen dioxide, sulfur dioxide and carbon monoxide,” 9789240034228. [Online]. Available: https://iris.who.int/handle/10665/345329

Chapter 6: Conclusions

This dissertation contributes the advancement of air quality monitoring use low-cost air quality sensor devices and research grade instruments and human exposure estimates to urban air pollution on local and hyperlocal scales.

Each chapter from 2 to 5 have their dedicated conclusions and discussions section, this chapter summarizes the main contributions to the thesis research.

Chapter 2: Particulate matter low-cost sensor device performance in a cold climate

> The growing adoption of Low-Cost Sensors (LCS) for air quality monitoring, coupled with the dedicated efforts of researchers and citizen scientists to enhance the accuracy of LCS-generated data through adjustment factors and machine learning algorithms, underscores the vast opportunity to leverage LCS technology to address air pollution challenges. This study highlights the potential of LCS in monitoring air quality in severely polluted areas, particularly under extreme winter conditions. By developing area-specific adjustment factors, this research opens avenues for broader engagement of research and community groups in LCS initiatives, facilitating the utilization of more cost-effective technologies to monitor air pollution exposure. Furthermore, the adjustment factors derived in this study provide valuable guidance for future LCS network deployments, offering insights into optimizing sensor placement and data interpretation. Overall, this work contributes to advancing the accessibility and effectiveness of air quality monitoring efforts, with implications for both research and public health initiatives.

Chapter 3: LCS characterizations based on its deployment siting and meteorological conditions

As Low-Cost Sensors become increasingly affordable and readily available in the market, researchers are turning to LCS-enabled networks to assess air quality variations at small spatial and temporal scales. However, the diverse designs of sensor brands can influence data reliability, particularly concerning sensor placement. In this study, we identified potential impacts on LCS data quality resulting from sensor siting, a factor that warrants careful consideration during sensor collocation studies and network deployments. Biases arising from microenvironmental airflow obstructions were very sensitive to meteorological conditions. For future LCS endeavors, especially network deployments targeting fine-scale spatial analysis to discern subtle concentration variations, it is essential to not only evaluate the sensor data quality compared to reference-grade monitors but also assess data performance based on various deployment siting criteria. This recommendation underscores the importance of comprehensive evaluation protocols to ensure the accuracy and reliability of LCS-generated data in air quality assessments.

Chapter 4: Winter $PM_{2.5}$ indoor levels in Mongolian kindergartens

Land Use Regression models are frequently employed to create pollution surface maps for various air pollutants across large geographical areas. In this study, we leveraged Low-Cost Sensor technologies to establish an indoor $PM_{2.5}$ sensor network within kindergartens in Mongolia. Through this initiative, we developed a novel LUR model aimed at estimating winter average $PM_{2.5}$ exposure for children inside kindergartens in Mongolia. Our research demonstrates the effectiveness of utilizing indoor $PM_{2.5}$ data in conjunction with nearby land use features and building characteristics to accurately

predict indoor PM levels at locations where physical sensors are not present. This approach showcases the potential of integrating LCS technologies with sophisticated modeling techniques to enhance our understanding of indoor air quality dynamics and better protect vulnerable populations such as young children in educational settings.

Chapter 5: The effects of vegetation planted along highway noise wall barriers on downwind ultrafine particle concentrations

The evidence regarding the ability of roadside vegetation to mitigate air pollution remains limited and, at times, contradictory. This study addresses this gap by assessing the effectiveness of an engineered vegetative buffer installed alongside a solid noise barrier in attenuating ultrafine particles (UFPs) near roadsides. Field sampling events were conducted to compare UFP levels with and without the vegetative buffer adjacent to the noise wall along the highway, providing valuable insights into the reduction of traffic-related pollutants. Additionally, these assessments establish baseline measurements for a longitudinal study, with periodic monitoring of UFP levels as the trees within the buffer zone mature over the coming years. By investigating the effectiveness of engineered vegetative buffers in mitigating roadside air pollution, this research contributes to our understanding of sustainable strategies for improving air quality in urban environments.

The air quality sampling datasets discussed in Chapters 2 and 4 provide high time resolution data for air quality monitoring in Mongolia. With the collection of higher quality land features in Mongolia in the future, the potential exists to develop a more sophisticated land use regression model. Such a model could greatly enhance our understanding of children's exposure to air pollution and support ongoing clinical studies in Mongolia.

Furthermore, while air pollution is often studied on a regional and large scale, this work emphasizes finer spatial scales. By focusing on these scales and utilizing ground measurements, this research contributes to more accurate exposure estimates in the field. This emphasis on finer spatial scales underscores the importance of localized data in understanding and mitigating the impacts of air pollution on public health.

Appendix A. Data summary for Mongolia $PM_{2.5}$ Networks Bayankhongor (BKH)

Reference monitoring BAM site:

Reference monitor MetOne Beta Attenuation Mass Monitor 1020 (BAM):

Continuous monitoring from Nov-06-2019 to Jan-12-2023 and still on going, data over three consecutive years. The data completeness shows total of 1120 (96.3%) valid days and 97% valid hours.

Outdoor PurpleAir Network:

Two different versions of outdoor PurpleAir network were installed, the first network have seven sites (Innovation center, KG6, KG16, Reference BAM Site, KG5, Airport, Children's Hospital), because of the Wi-Fi connection issues the outdoor network was only operated for several month from the beginning of the deployment during 2020, the network was reinstalled using different PurpleAir sensors in February 2022 for six sites (Innovation center, KG6, KG16, Reference BAM Site, KG5, Background).

Table A.1 BKH first PurpleAir network sensor ID and data collection period.

Site Name	Sensor Type & SN	Beginning	Ending
KG5	PA(E39C)	2020-02-07	2020-07-21
KG6	PA(5C4B)	2020-02-07	2020-07-21
KG16	PA(5CA1)	2020-02-07	2020-07-21

Reference BAM Site	PA(167,DAE4,F2D9)	2020-02-07	
Airport	PA(457)	2020-02-07	2020-07-21
Innovation Center	PA(6ADF)	2020-02-07	2020-06-19
Children's Hospital	PA(E53)	2020-05-05	2020-07-21

The utility of LCS devices to evaluate air pollutant spatially variability is demonstrated by the BKH outdoor network. **Figure A.1** and the associated tables show the spatial patterns in outdoor $PM_{2.5}$ across the BKH. The first column of $PM_{2.5}$ values are from the device output, and the second column are estimated "reference monitor-like" values calculate by adjusting the raw data using the PA-to-BAM relationship showed in early reports. Concentration values for the February data better represent winter conditions but the trends across sites are similar for both time periods. Concentrations are highest at the Innovation Center, followed by KG6 and KG16. These three sites are either within or on

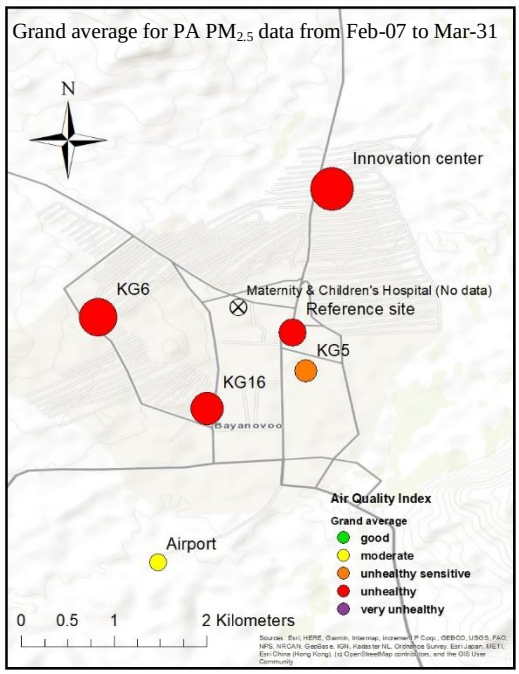

Data from 2-07-2020 to 2-26-2020

Sites	$PM_{2.5}$ grand average ($\mu g/m^3$)	$PM_{2.5}$ grand average ($\mu g/m^3$) adjust
Reference site BAM	87	---
Reference site PA	103	87
Innovation Center	184	155
KG6	144	122
KG5	77	65
KG16	121	103
Airport	52	44

Data from 2-07-2020 to 3-31-2020

Sites	$PM_{2.5}$ grand average ($\mu g/m^3$)	$PM_{2.5}$ grand average ($\mu g/m^3$) adjust
Reference site BAM	62	---
Reference site PA	71	62
Innovation Center	115	98
KG6	98	83
KG5	56	48
KG16	92	78
Airport	35	30

Figure A.1 Outdoor $PM_{2.5}$ average concentrations across BKH, February 7 to March 31, 2020. Air quality levels in the figure are color coded using the US EPA Air Quality Index (AQI) classifications.

the border of large ger areas, consistent with residential coal combustion being a major-and perhaps the dominant-source of $PM_{2.5}$. Intermediate concentrations are observed at KG6 and the reference site which are in the commercial/downtown zone. The lowest concentrations are at the airport, consistent with the land use around it being less developed.

This analysis demonstrates the importance of having network measurements and not just reference site data. There are dramatic differences in concentrations across BKH on scale of less than one kilometer, and thus outdoor exposures-and indoor exposures to the extent they are coupled to outdoor concentrations-will also dramatically vary. The WashU team is working to make the network data available in real time and will coordinate with UNICEF to design a public-friendly Mongolian language website displaying the real-time data across BKH.

While the reference station does not capture the highest concentrations, *$PM_{2.5}$ patterns across the monitoring sites are well-correlated* [not shown] and thus it should be possible to develop equations to predict the concentrations at other LCS monitoring locations and possibly estimate concentrations at locations without monitors using methods such as land use regression modeling (LUR).

Figure A.2 shows diel (time of day) profiles for the outdoor network sites. The patterns are more similar than different. $PM_{2.5}$ concentrations are highest in the morning (~8-9am) at the two sites centrally located within ger areas (Innovation Centre and KG6). This morning peak is present but relatively smaller at the other sites. At all sites, concentrations are relatively high

during the nighttime which is

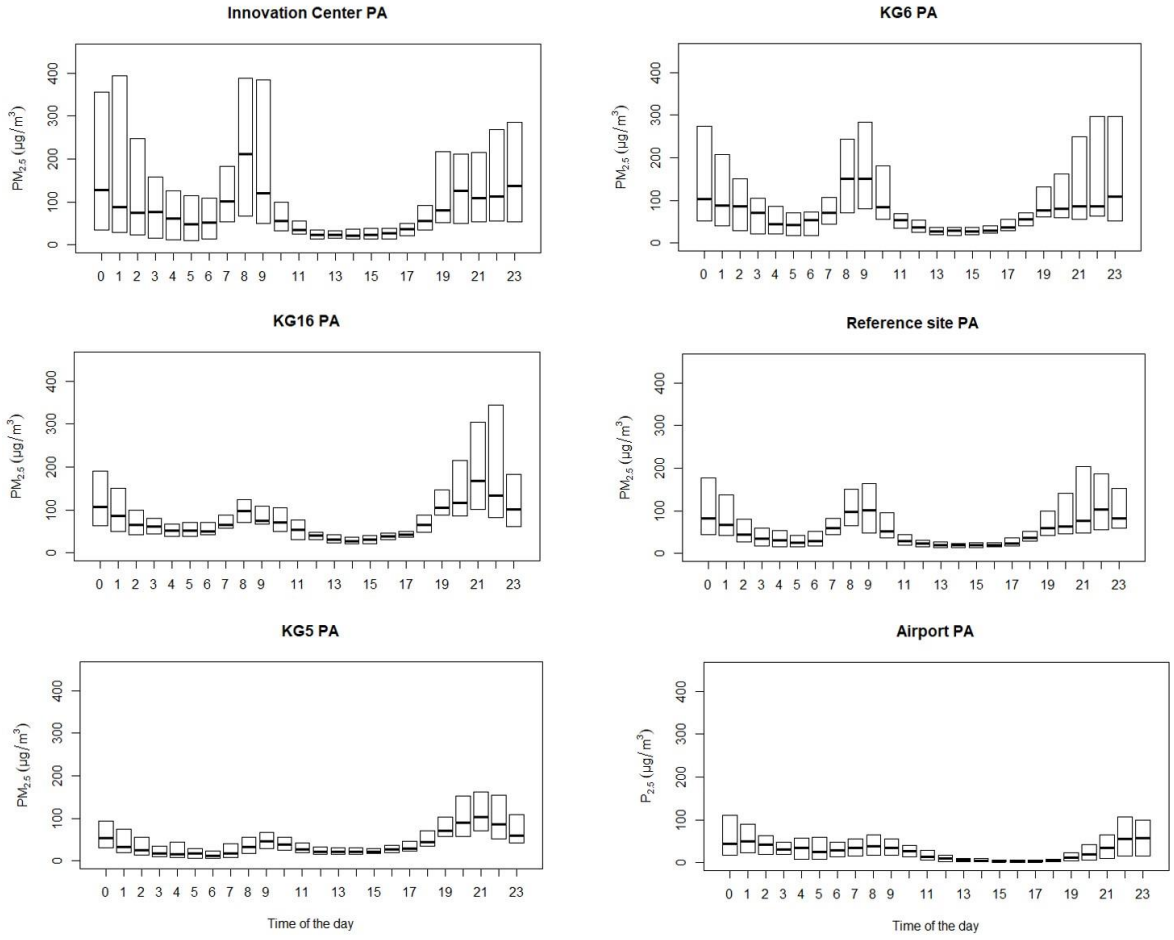

Figure A.2 Outdoor $PM_{2.5}$ diel (time of day) profiles across BKH, February 7 to March 31, 2020.

consistent with residential space heating emissions compounded by the shallow atmospheric mixing layer depth at night. These patterns have important implications to exposures.

Table A.2 BKH Second PurpleAir Network sensor ID and data collection period.

Site Name	Sensor Type & SN	Beginning	Ending
KG5	PA()	2022-02-19	2022-03-19
KG6	PA(2137)	2022-02-19	2022-03-19

KG16	PA()	2022-02-19	2022-03-19
Reference BAM Site	PA(5e9)	2022-02-19	2022-03-19
Background	PA()	2022-02-25	2022-03-03
Innovation Center	PA(3575)	2022-02-19	2022-03-15

Table A.2 shows the data range for the second round PurpleAir Network, due to the cellular network expiring early, the data collection only lasted a month, it is feasible to re-connect this network with updated internet connections. The results from this network [not shown] shows the same trend compared to the previous network, and the conclusion still the same based on the network performance[not shown].

Indoor AirVisual Pro (AVP) Network:

Indoor AVP network was setup from the beginning of the deployment at KG5, Children's Hospital, Maternity ward, KG6, KG16 and BAM site (Outdoor). **Table A.3** listed all the sensors at each indoor BKH site and their time window with collected $PM_{2.5}$ and CO_2 data.

Table A.3 BKH indoor network sensor ID and data collection period.

Site Name	Sensor Type & SN	Beginning	Ending
KG5	AVP(PPRGCGS)	2019-12-17	2022-02-16
KG6	AVP(76UWMHU)	2020-02-05	2022-02-15
KG16	AVP(T67Y7VW)	2020-02-05	2020-11-10
Children's Hospital	AVP(66V6RYU)	2019-12-18	2022-02-15
Maternity Hospital	AVP(KGYMWWS)	2020-02-05	2020-12-22

Table A.4 Indoor network $PM_{2.5}$ and CO_2 concentrations based on all season and winter only.

Site Name	Mean $PM_{2.5}$ $\mu g/m^3$ with room occupied	75 percentile of CO_2 concentration in PPM with room occupied	2022 Winter $PM_{2.5}$ only with room occupied	75 percentile of CO_2 concentration for 2022 winter with room occupied
KG5	43	1072	51	943
KG6	43	1138	62	1033
KG16	21	1178	45*	1316*
Children's Hospital	37	1225	32	1441
Maternity Hospital	66	1079	108*	1065*

*Calculated same value for 2021 instead of 2022 because data missing for 2022

Table A.4 shows the summary results for BKH indoor AVP network, from the summary data CO_2 concentration is higher in winter for KG16 and Children's Hospital, and $PM_{2.5}$ concentration is higher in the winter for all sites except Children's Hospital.

Based on the onsite observation from field work, Children's Hospital is a room on the second floor and the room is more airtight than other locations this could cause similar $PM_{2.5}$ concentration all season vs. winter while CO_2 concentration is higher in winter due to less frequent air ventilation.

Bayanzurkh (BZD)

Kindergarten Network:

UB kindergarten indoor air quality monitoring network consist of 24 sites. All indoor monitoring was conducted using AVP devices. Ten AVP sensors were collocated at BKH BAM reference

site and then collocated at each kindergarten network site to remove the sensor-to-sensor biases between each AVP devices and low cost to reference biases between AVP and BAM. All results for the following analyses for network performance and building characteristics were conducted with all biases removed. **Figure A.3** shows the detailed location of all indoor monitoring sites with specific kindergarten labels. **Figure A.4** show winter averaged $PM_{2.5}$ concentration for two consecutive winter, winter 2021 uses indoor measurement data from Nov-2020 to Feb-2021 and winter 2022 uses data from Nov-2021 to Feb-2022. Each circles represent the location shown in **Figure A.3**, and the size of the circle is proportional to the actual $PM_{2.5}$ concentration. The average concentration included hourly data from 8 a.m. to 5 p.m. which gives the true $PM_{2.5}$ concentration children were exposed to during those heating seasons by assuming school hour is 8 to 5. Each circle was color coded based on the US Air Quality Index (US AQI) and as we can see the spatial variations of $PM_{2.5}$ concentration are similar for two winters.

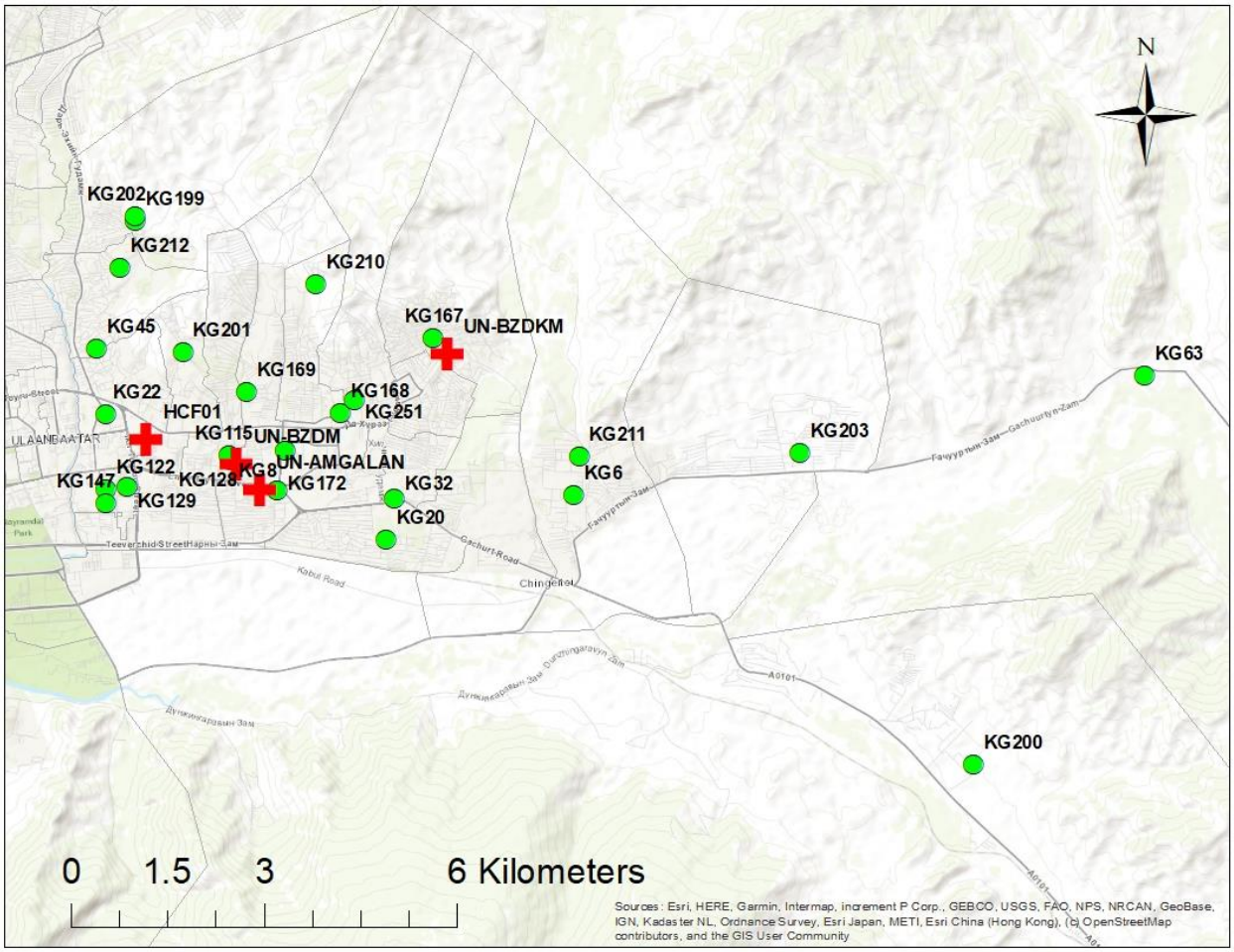

Figure A.3 BZD 24 Kindergartens and 4 Healthcare Facilities Indoor Monitoring site.

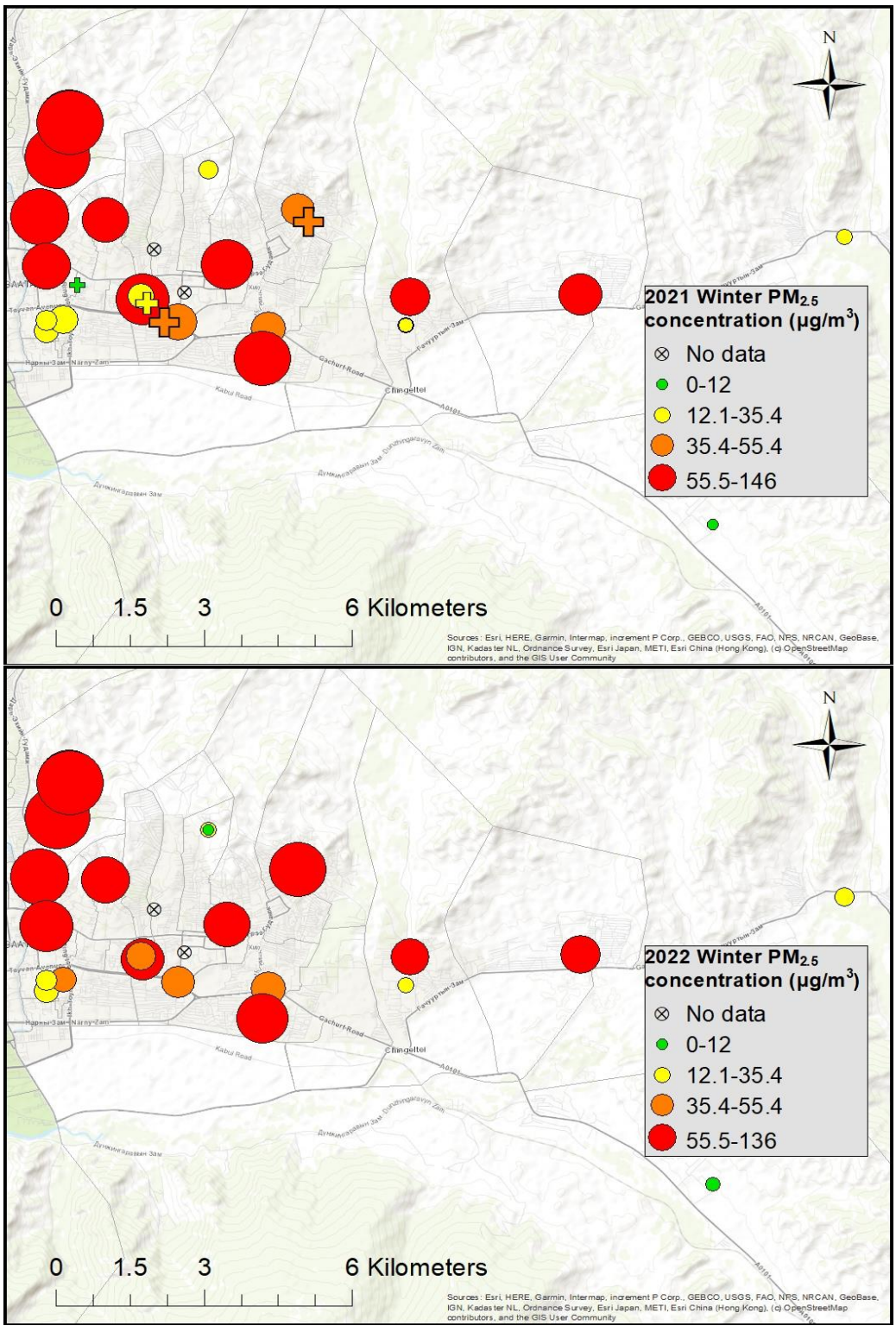

Figure A.4 Bayanzurkh district (Ulaanbaatar) indoor winter averaged $PM_{2.5}$ (Nov2020~Feb2021 and Nov2021~Feb2022)

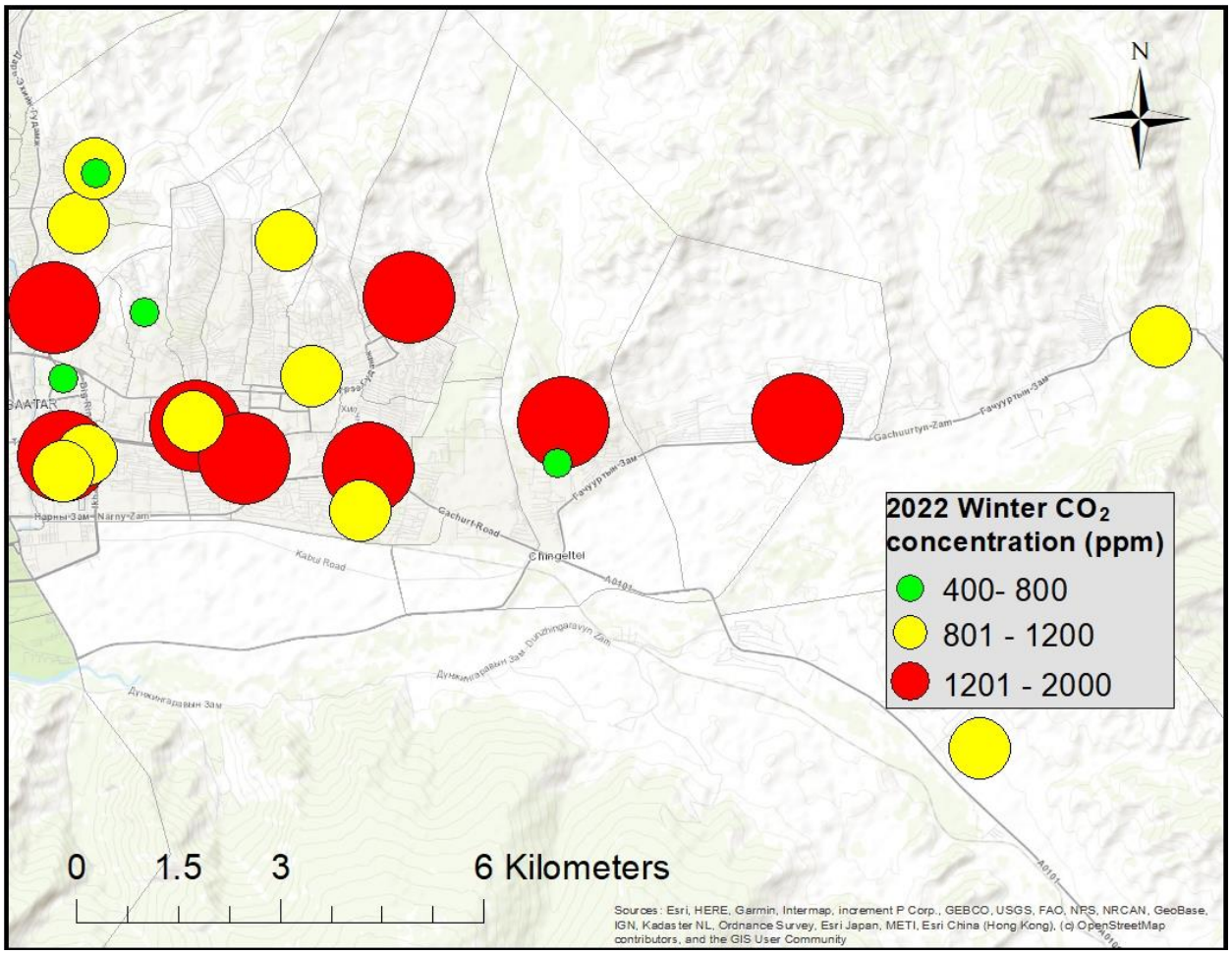

Figure A.5 Bayanzurkh district (Ulaanbaatar) indoor winter average CO_2 (Nov2021~Feb2022)

Figure A.5 shows the 75-percentile value of CO_2 concentration for each site during the same winter period. Indoor CO_2 as expected is not correlated with the indoor $PM_{2.5}$, based on this map we can identify the sites need ventilation to lower the indoor CO_2 concentrations.

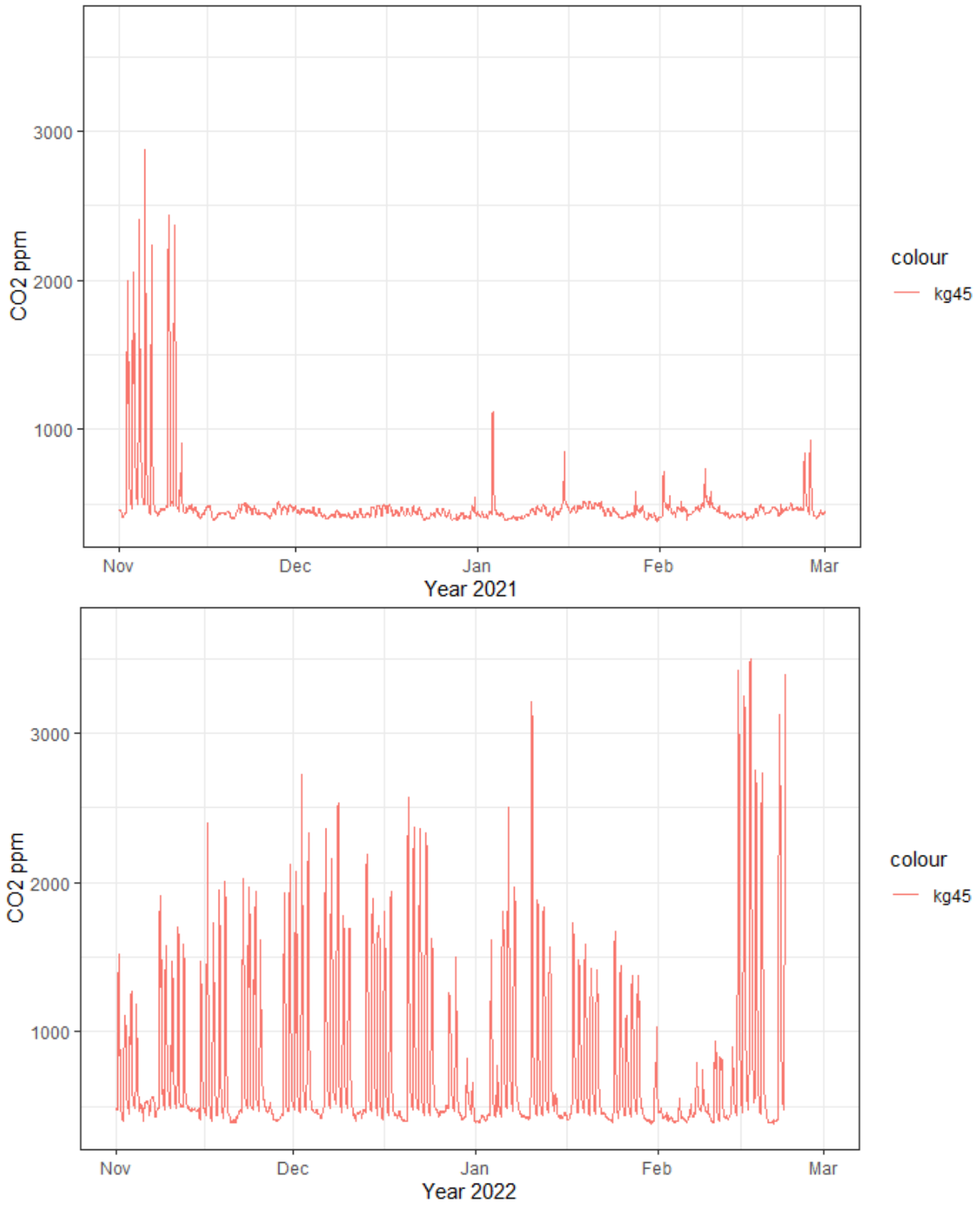

Figure A.6 Time series plot for KG45 CO2 during the winter season from 2020 to 2022

Historical data for the kindergarten network were collected from March 2020 to February 2022, due to the coronavirus situation 2021 winter indoor data were collected when children were not

in school most of the time. Carbon dioxide can be a indicator of indoor human activities, and **Figure A.6** shows the hourly carbon dioxide concentration profile for kindergarten 45 between November to March for both year of 2021 and 2022. Based on the CO_2 concentration profile, it was clear that for the most part of year 2021 winter, this school have no activities due to coronavirus situation.

In order to prioritize the kindergartens which need the most attention for interventions, we looked at both $PM_{2.5}$ concentration and CO_2 concentration for the school based on school activities and different time of the year. The results shows the indoor $PM_{2.5}$ are high during

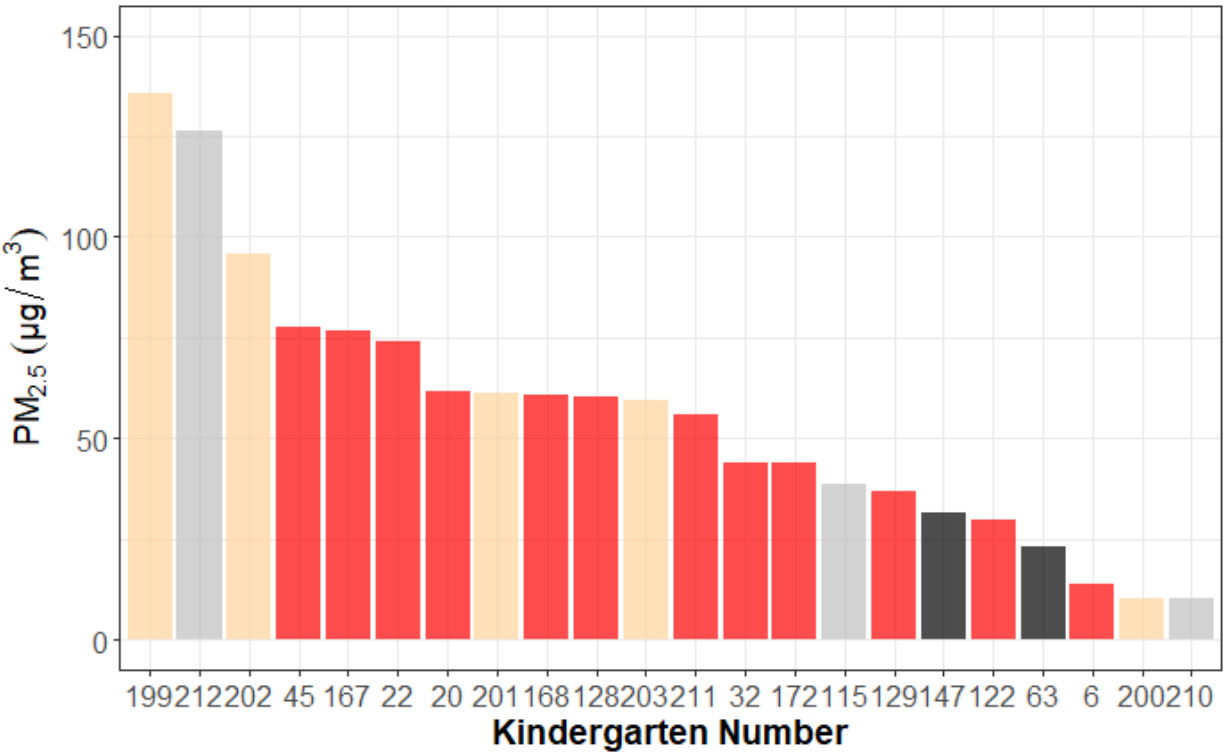

Figure A.7 Indoor $PM_{2.5}$ winter (Nov-2021~Feb-2022) heating season mean school hour concentration, color code based on building type: masonry(red), concrete(grey), wood(light brown), not available(black).

winter heating season due to the high outdoor PM concentration penatrate indoor, and CO_2

concentration are high during the school hours with human activities and depending on the room size and ventilation CO_2 indoor concentration are different.

Figure A.7 shows the mean indoor $PM_{2.5}$ concentration for winter Nov-2021 to Feb-2022, average values were calculated using a subset of hourly data by only considering the school hours from 8 a.m. to 5 p.m. The x-axis gives the rank of kindergartens that need the most attention regarding to indoor $PM_{2.5}$ concentration. All kindergartens were color coded based on its building structure. According to US AQI any concentration above 55.5 $\mu g/m^3$ are considered unhealthy and **figure A.7** shows more than half of the kindergartens considered unhealthy for their indoor $PM_{2.5}$ level. KG199, KG212 and KG202 were among the top three kindergartens need most attention for interventions.

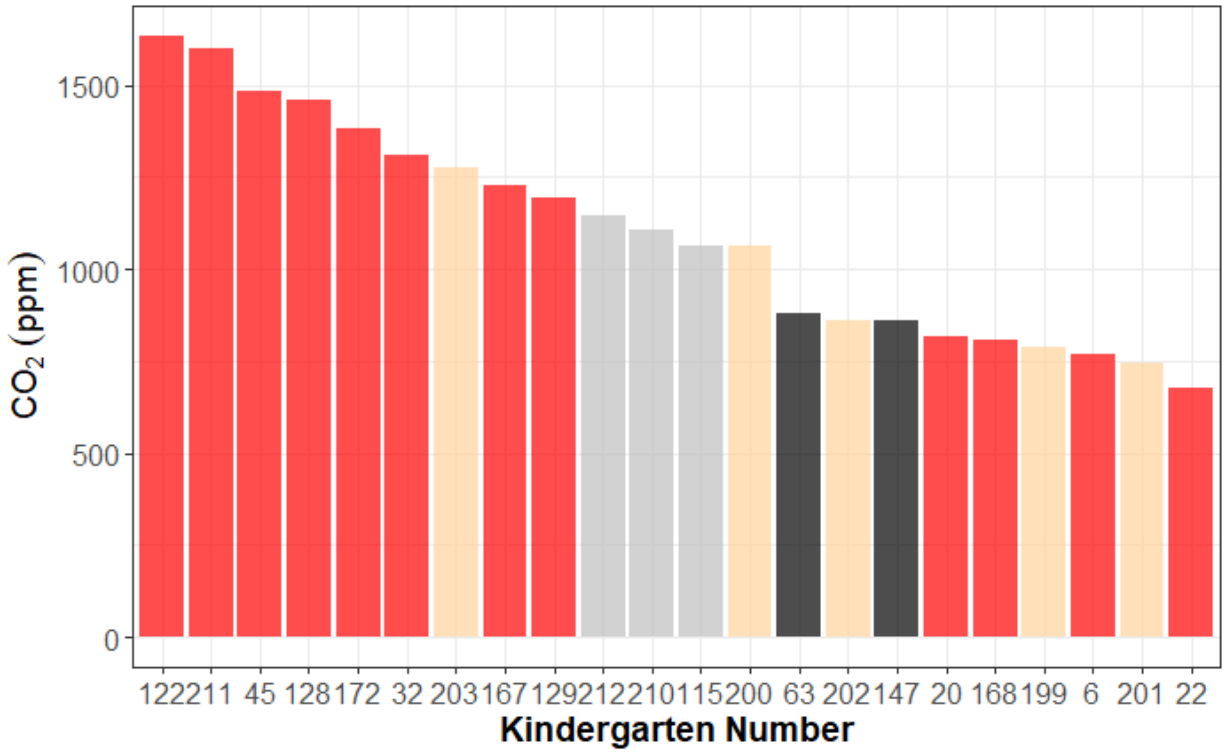

Figure A.8 Indoor CO_2 (Nov-2021~Feb-2022) heating season 75 percentile value school hour concentration, color code based on building type: masonry(red), concrete(grey), wood(light brown), not available(black)

Figure A.8 shows the 75-percentile of CO_2 indoor concentration in all kindergartens ranked from high to low, the concentration here is not extremely high but do note this measurement period is after coronavirus situation, based on the teacher survey most of these schools have a 30 to 50 percent decrease in attendance before and after covid, which means under normal operation indoor CO_2 concentration will be higher. **Figure A.8** is color coded based on the building type, and we can see most masonry structures have higher indoor CO_2 concentrations. This helps prioritize which schools need to install the mechanical ventilation and reduce the room capacity. Different building characteristics were investigated including the building structure (shown above), building Age, building capacity, over capacity number, heating type, and building area.

Healthcare Facility Network:

During the first deployment in March 2020, four health care facilities were selected and after Feb-2022 all AirVisual pro from healthcare facilities were retrieved because no maintenance and Wi-Fi connection issues. Four sites including HCF#1, Bayanzurkh Children Hospital, Central Hospital, Amgalan Birth Hospital. Due to low maintenance and no Wi-Fi connections for most of the time, the data completeness for the Healthcare Facility network is low.

Appendix B. Mongolia kindergarten special studies activities that affect indoor air quality

Two indoor special studies were conducted to further understand the relationship between indoor activities and indoor air quality for both summer and winter seasons. The first special study was conducted September 2021 and focus on the indoor air quality in late summer month. The second special study was conducted February 2022 to demonstrate to what extent the outdoor high $PM_{2.5}$ concentration affect indoor and what people should do indoor to improve the indoor air quality.

KG Late summer special study from PLM (Public Lab Mongolia) Sept 2021:

A special kindergarten indoor air quality study was conducted with the help of PLM colleagues to investigate the correlation between indoor human activities and indoor air quality. All AirVisual pro sensors used in this study were collocated side-by-side at PLM office to develop correction factors to make all sensors intercomparable.

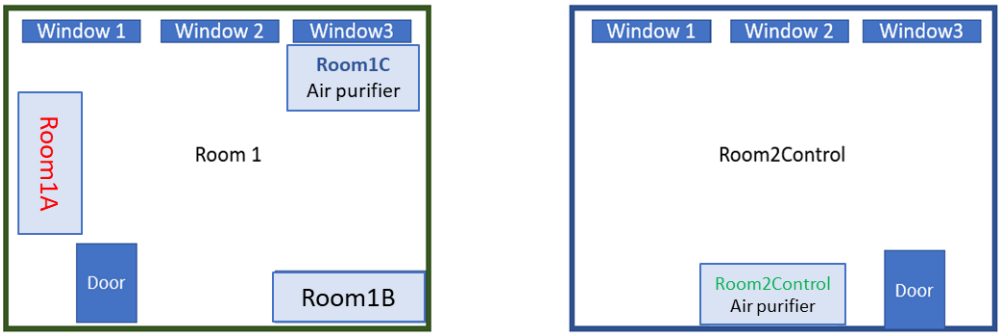

Figure B.1 Sensor arrangement inside two rooms in KG212 Room 1 is the intervention room while room conditions were changed winter open versus close and air purifier on versus off.

Room 2 is the control room where conditions remain the same throughout the study period.

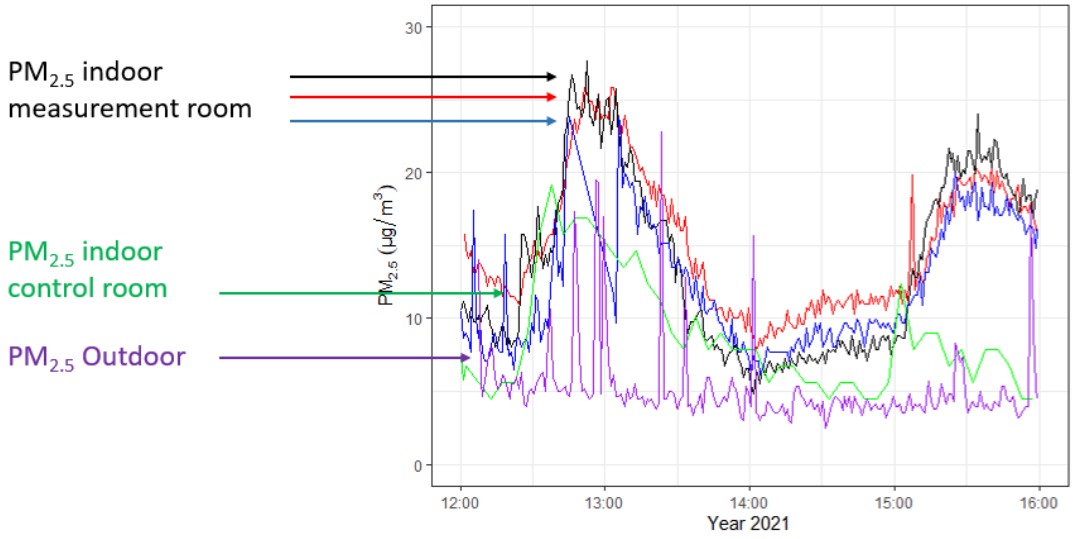

Figure B.2 Thursday September 2 school day (1200~1600 hours)

Figure B.2 shows the timeseries plot from 1200 hour to 1600 hour for September 2 the first day of the special study, each line color corresponds to the sensor color showed in **figure B.1.** The outdoor $PM_{2.5}$ is lower than indoor $PM_{2.5}$ on this summertime day indicates the $PM_{2.5}$ level in the summer was from human activities indoor.

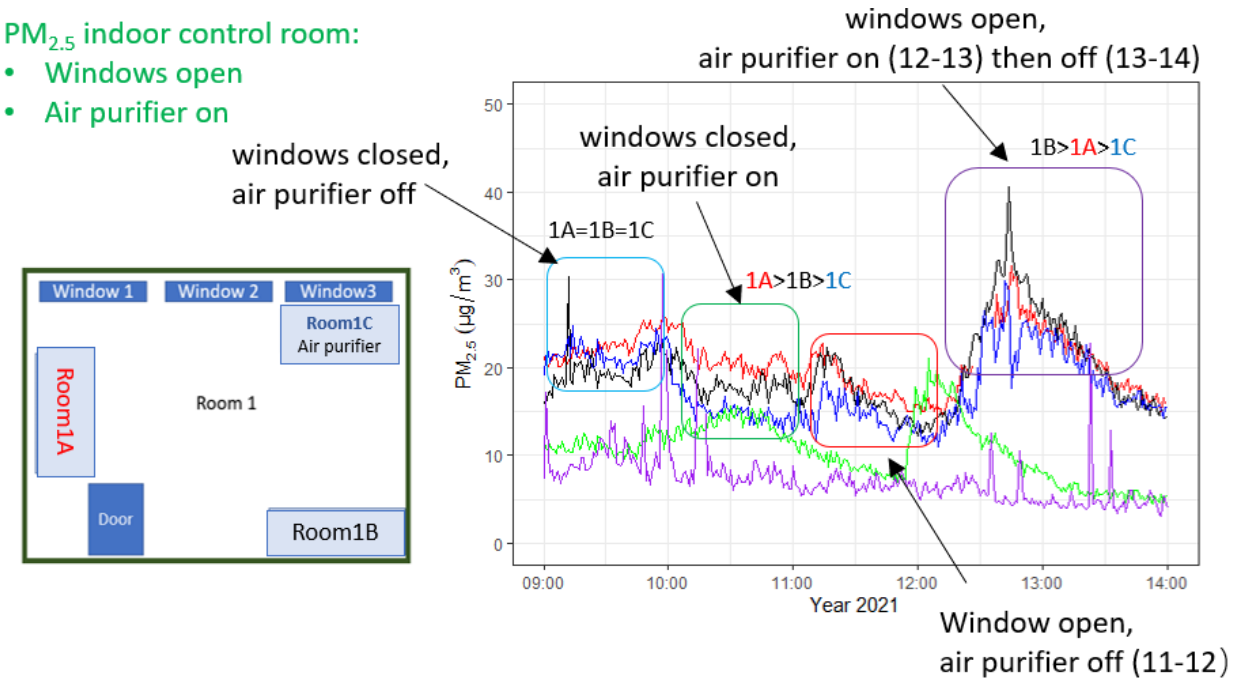

Figure B.3 Friday September 3 school day (0900~1400 hour)

Figure B.3 shows for a school day indoor activities will impact the indoor air quality. The intervention room 1 shows similar sensor concentration from 0900 to 1000 when all windows were closed and air purifier off. The next hour only turned on the indoor air purifier and three sensor reading starts to separate with 1C the lowest (nearest to the air purifier) and 1A the highest (furthest to the air purifier). After window opening from 1100 to 1200, the overall indoor $PM_{2.5}$ concentration decreases because outdoor concentration is lower than indoor and opening window helps lower the indoor concentration. The big jump of indoor $PM_{2.5}$ from 1200 to 1300 was due to the room activity when furniture was moved and prepare for children's nap time at noon.

In summary, this brief study under summertime conditions was helpful to demonstrate window opening and closing affects indoor $PM_{2.5}$ and when outdoor air quality is less polluted opening window helps lower the indoor $PM_{2.5}$ concentration. Air purifier is helpful reducing the $PM_{2.5}$ but due to poor air circulation in the room the effect may be limited to mostly near the device. Indoor activities like vacuuming and preparing the room for children to sleep increases the indoor $PM_{2.5}$ this effect might disappear when the overall background outdoor concentration is much higher in the winter heating season.

Kindergarten Special Study Winter:

KG special study was conducted from February 23rd 2022 to February 28th 2022 in the late winter month. The primary focus was to test out the effectiveness of clean indoor $PM_{2.5}$ using Corsi-Rosenthal DIY box (**figure B.4**). CR box is a do-it-yourself method for indoor particle filteration assembled using 5 MERV 13 filters with a box fan on top of the box.

Figure B.4 C-R box filtration system in KG45

Two kindergartens were selected in this special study KG45 and KG122. KG45 is located inside the residential ger area in contrast KG122 located in the city center near a business district with central heating apartments, a strong indicator is the ger counts inside 1km radius of KG45 and KG122 are 1203 and 36 respectively.

The building structure is also different between two kindergartens, KG45 is masonry structured building and KG122 is concrete reinforced structure. KG45 is heated by a local boiler and

KG122 is connected to the central steam heating. The room size between each kindergarten is quite different KG122 is 2-3 times larger than the classroom in KG45.

KG45 is a two-story building with total of four classrooms and two on each side of the building, with the front gate facing west, the room 1 at the first floor located at the south corner of building was used as the primary intervention room with changes to the room conditions opening and closing windows and turn on and off CR box filter. The other rooms with no operations also had one air quality sensor to distinguish room to room indoor air quality differences.

Outdoor sensor was installed at both locations paired with indoor measurements starting 25Feb2022 based on the time series plot showed in **Figure B.5**, the outdoor concentration at both locations was significantly higher than indoor paired measurements, and the weekend indoor concentrations looks a lot smoother with slow raising and decaying concentrations, the weekday indoor concentrations is more complicated due to room operation and people entering and exiting the room.

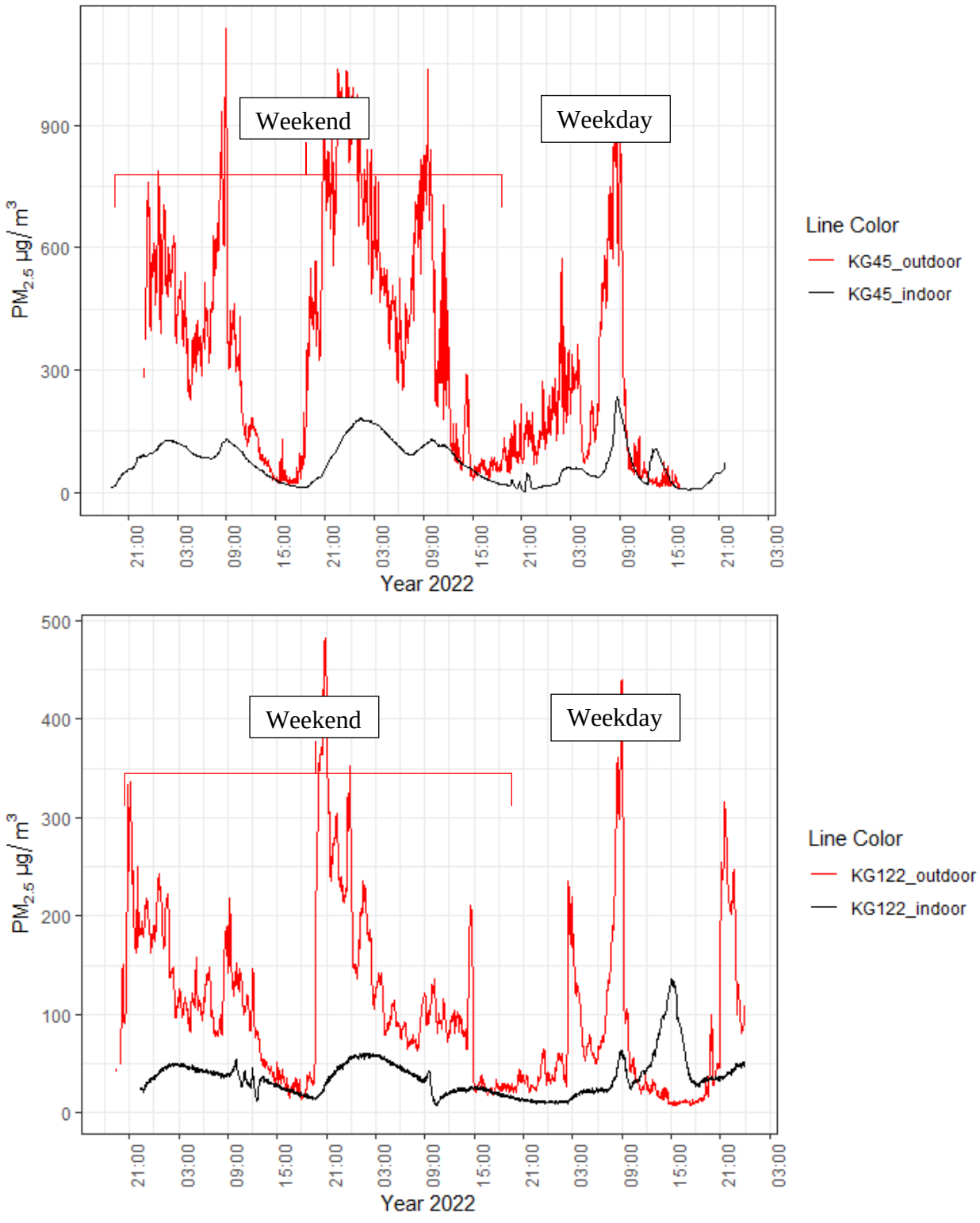

Figure B.5 Outdoor Indoor paired measurements at both KG45 and KG122.

Figure B.6 shows an example of night study at KG45 with CR box on and off in room 1 and at the same time opening and closing windows as outdoor $PM_{2.5}$ is higher than indoor during winter heating season. The room was sealed up with window closed and CR box fan off from 2000 to 2030 hour, all three sensor show similar concentrations for 30 minutes. CR box filter was then setup at low speed for 30 minutes from 2030 to 2100, the indoor concentration decreased from over 100 to less than 50 $\mu g/m^3$ the sensor away from the CR box fan has higher concentration due to poor room mixing. The CR box was then turned off with window still closed from 2100 to 2115, the indoor $PM_{2.5}$ concentration slowly goes up due to outdoor polluted air infiltrate the building. Window was then opened for 15 minutes from 2115 to 2130, the indoor air quality jumps to 300 $\mu g/m^3$ in just this short amount of time. The room window was then closed, and filter fan was turned on high speed for 30 mins to clean the room from 300 to 25 $\mu g/m^3$.

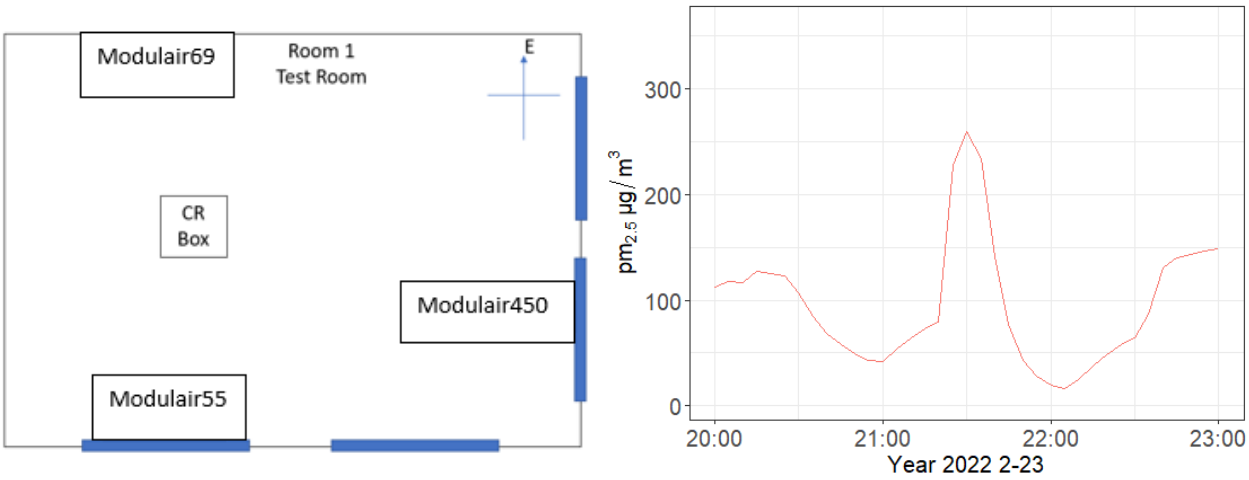

Figure B.6 Room 1 testing layout and nighttime room operation for KG45

This quick study demonstrates how fast the outdoor polluted air can mix indoor and the CR box fan can clearly improve the indoor air quality if running them continuously.

Figure B.7 shows the room arragement for kindergarten 122, the class room is separated into two parts with activity room and sleeping room, kids stays inside the activity room during the day and sleeping room is used for lunch break and nap time.

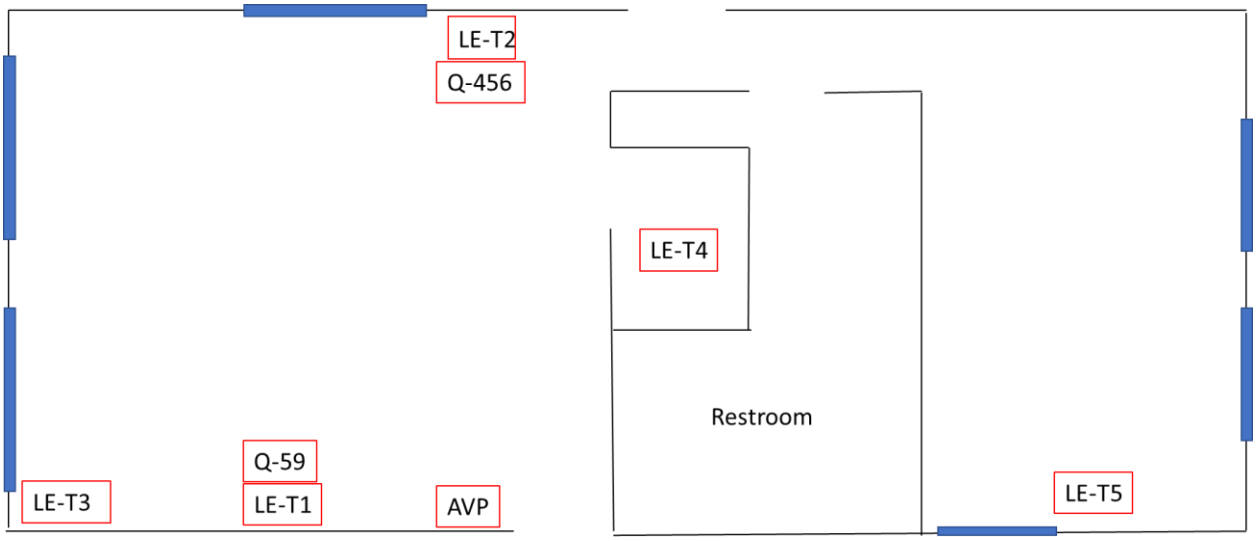

Figure B.7 Room arrangement and sensor layout for KG122 activity room on the left and sleeping room on the right.

The classroom was equipped with an air purifier, and we tested out the effectiveness of improving the indoor air quality inside the main activity room at night with controlled environment and no kids inside. **Figure B.8** shows the result for the time series plot from Feb23 1900 to 2300. As you can see **test1** shows the room air purifier setting was at high mode at 2000 and low mode at 2130, the higher purifier speed seems cleanup the room faster, however under both situation it takes the air purifier about one hour to lower the indoor $PM_{2.5}$ concentration level to under 25 $\mu g/m^3$. The room windows were opened between 1930 to 2000 and 2100 to 2130 to let the outdoor pollution in, meanwhile the sleeping room window was opened from 1930 to 2000 and then the room was completely closed out by shutting door and windows, as you can see **test5** shows steady decay after 2000.

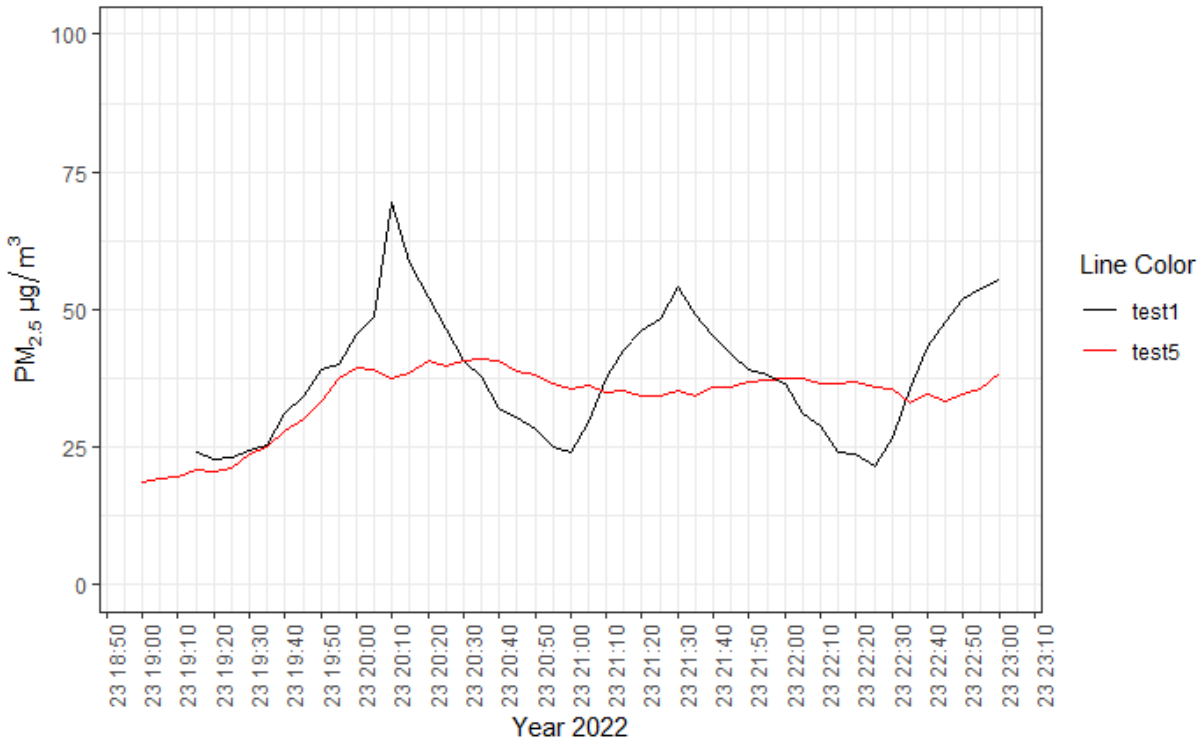

Figure B.8 Time series plot for testing our indoor air purifier in KG122.

CR box filter was also tested inside KG122, the results illustrated that the box filter can bring the overall indoor $PM_{2.5}$ concentration lower than 10 µg/m^3 which is better than the indoor air purifier, however based on the decibel readings the CR box filter is louder compared to the commercialized indoor air purifier, **figure B.9** shows the result for box filter performance. During the normal weekday with the room under normal operations we noticed that the indoor concentrations were elevated and higher than outdoor concentrations due to indoor activities. And the elevated CO_2 concentrations also indicated that the room might have incense burning during the day. **Figure B.10** shows high CO_2 indoor readings inside sleeping room in the early afternoon likely during the napping period for kids. And during the day the CO_2 level is consistently higher than 2500 ppm which is higher than the recommended indoor CO_2 concentrations for kids.

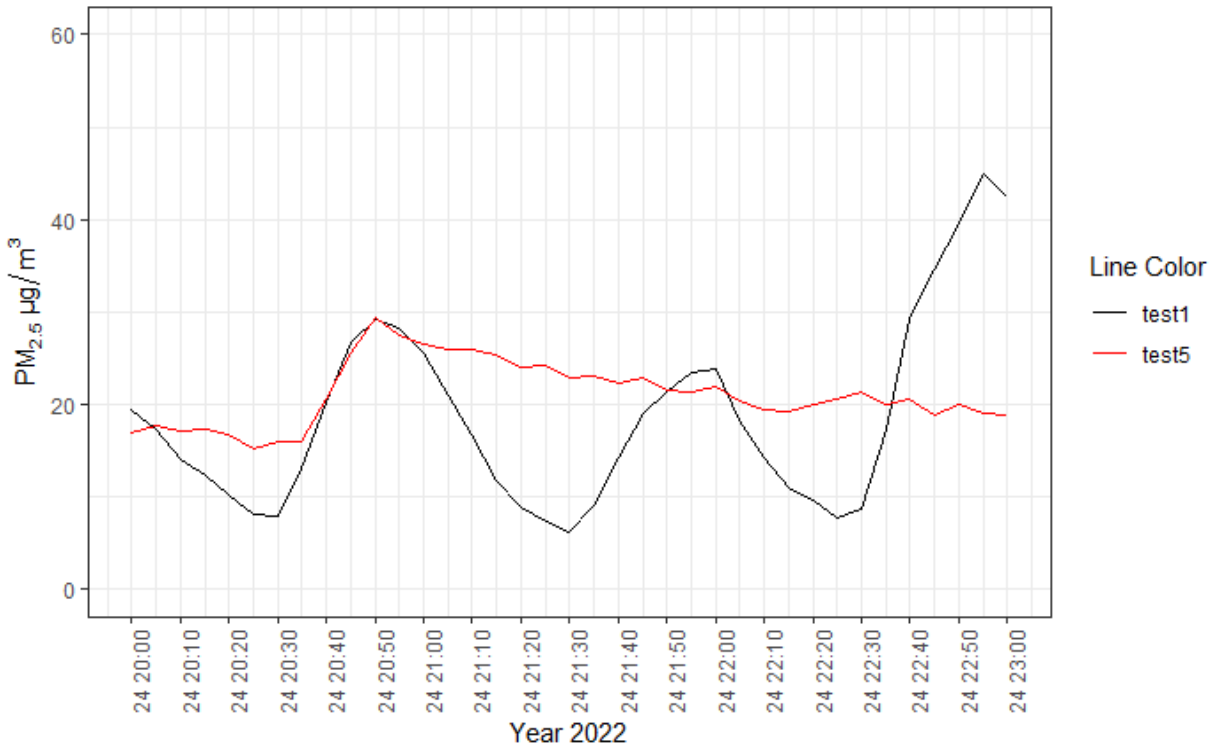

Figure B.9 Time series plot for testing out CR box filter in KG122.

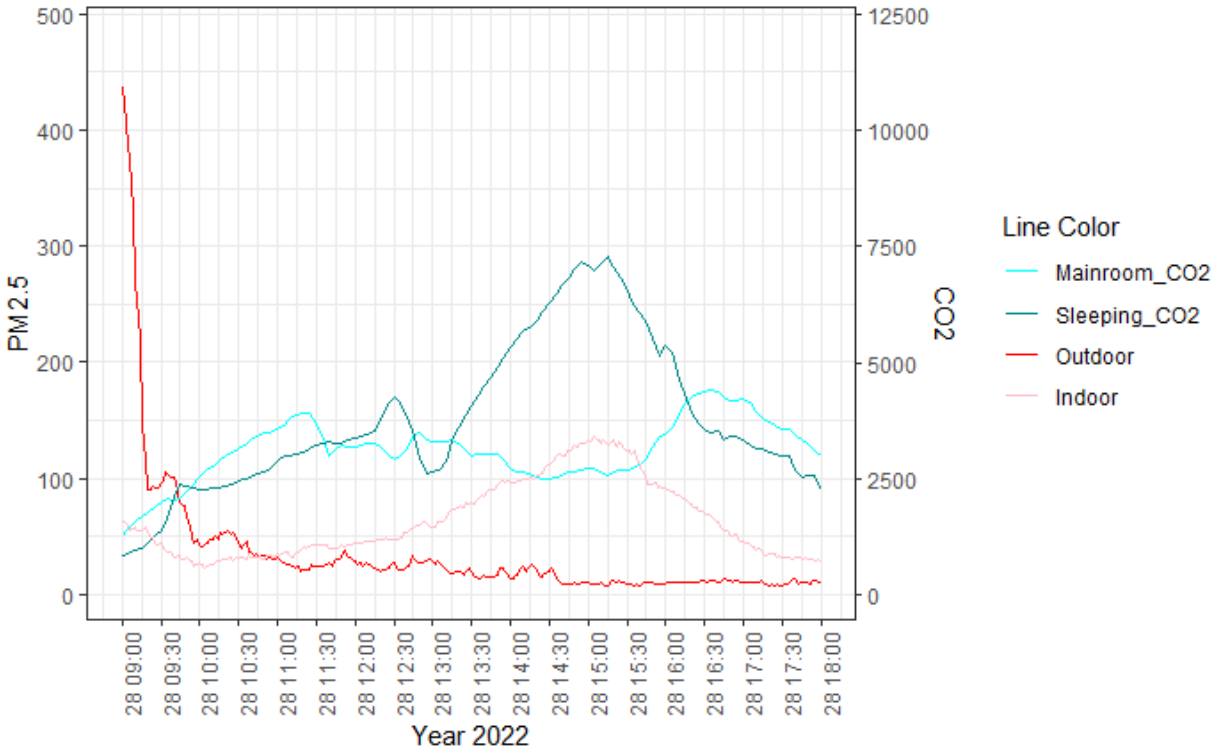

Figure B.10 On a school day indoor $PM_{2.5}$ concentration higher than outdoor, and elevated CO_2 indicates room operation.

Recommendations based on special study:

1. During the winter heating season, the outdoor concentration could be five times higher than indoor, if opening windows is needed to vent out room CO_2 concentration, try to do that when you see a relatively low outdoor concentration.
2. Indoor air purifier or DIY built filter box will effectively help improving the indoor air quality, this could be a useful short-term solution for most of the kindergartens, however, they need to have air purifier in each room and with long lasting filter replacement in order to keep the purifier effective.
3. Based on kindergarten survey the kindergarten teacher usually keeps the air purifier running for 10 to 15 minutes at a time and based on our special study the runtime must be

longer than one hour to improving the indoor air quality during a testing period, which means during normal operation the time will be much longer to keep indoor $PM_{2.5}$ concentration relatively low. We recommend keeping the air purifier always on at low speed during the day normal operation hours.

4. Don't burn incense.

Final Conclusions and Recommendations:

The summer special study shows while the outdoor $PM_{2.5}$ is low the indoor activities can still contribute to the increasing indoor $PM_{2.5}$ levels. This suggests that it might still be useful to operate the air purifier in the summer.

For those kindergartens with higher CO_2 levels, it is important to open the window and exchange the outdoor air indoor to lower CO_2 level, this can only be done in the summer while outdoor $PM_{2.5}$ levels are low.

The winter special study suggests the CR box fan can improve indoor air quality for kindergartens. However, during winter heating season when outdoor $PM_{2.5}$ levels are high the air purifier needs to be always plugged in to clean the maintain the indoor $PM_{2.5}$ at a lower level. Teacher survey shows most teaches turned on their air purifier for 10 to 20 minutes which is not enough to clean the room.